ABSTRACT

ROCHE, MEGHAN CATHREEN. Gene Editing-Assisted Generation of Delayed Bolting Lettuce (*Lactuca sativa* L.) for High Temperature Conditions. (Under the direction of Dr. Ricardo Hernández and Dr. Wusheng Liu).

Lettuce (*Lactuca sativa* L.) is a popular crop for cultivation and consumption, with the farming of lettuce increasing in popularity in recent years. With increased interest in this crop, growers are expanding from fields into new cultivation systems, including indoor controlled-environment methods, such as greenhouses and vertical farms. Lettuce cultivation does not come without challenges, however, as increasing global temperatures push demand for cultivars with improved stress adaptations, and yield demands in indoor cultivation favor enhanced growing temperatures, in spite of the threat of premature bolting. Bolting, the transition from vegetative to reproductive growth, reduces quality and makes the lettuce head unsalable, causing economic loss to growers. Thus, while climate change necessitates the development of crops adapted to warmer temperatures for field cultivation, so too can the breeding of crops for controlled-environment cultivation. Towards this aim, the primary objective of this work was to knockout floral promotion genes in lettuce to delay the onset of heat-induced bolting. To achieve this objective, two goals had to first be achieved; optimization of a lettuce transformation protocol in the cultivars of interest, and identifying the genes to target for knockout in lettuce via thorough literature review.

In spite of the achievements in lettuce transformation and regeneration, there remains a genotype dependence upon the ability to efficiently transform and regenerate lettuce plants. In this work, an optimized *Agrobacterium*-mediated transformation protocol was successfully developed for elite lettuce cultivars of the romaine, leaf, and butterhead cultivar types. A plant growth regulator combination of 1-naphthaleneacetic acid (NAA; 0.10 mg/L) and 6-

benzyladenine (BA; 0.25 mg/L), the use of cotyledons and the first true leaf as explants, and the use of hygromycin (15 mg/L) for transgenic plant selection worked well for seven out of the eleven tested cultivars, achieving a 24.3% – 100% transformation efficiency. These seven cultivars include two romaine-types, three leaf-types, and two butterhead-types, and marks the first successful genetic transformation of the romaine cvs. 'Kahu' and 'Rosalita', the leaf lettuces 'Red Sails' and 'Royal Oak Leaf', and the butterhead 'Lollo Biondo'. While this optimized protocol did not successfully regenerate plants in the remaining four cultivars, successive use of kanamycin selection (40 mg/L) with the same plant growth regulators enabled transformation in the butterhead-type 'Mariska'.

Flowering regulation in the model species *Arabidopsis thaliana* involves five defined floral induction pathways; autonomous, vernalization, photoperiod, gibberellin, and thermosensory. In the complex regulation of floral timing, no pathway exists exclusively of another, as components are frequently observed to overlap and/or exhibit functionality in multiple pathways at once. While the genes of the autonomous pathway were once thought to contribute to flowering regardless of environmental conditions, convergence between autonomous pathway factors and temperature-based flowering led to the identification of the thermosensory pathway. Accordingly, the key autonomous pathway genes serve crossover function in both pathways. In the thermosensory pathway, warm temperatures trigger the acceleration of flowering, and autonomous pathway genes are central in coordinating these environmental responses. From this deep dive into *Arabidopsis* flowering pathways, and study of their conserved function in Asteraceae, three candidate genes were identified for knockout in lettuce, *FLOWERING LOCUS T* (*FT*), *FLOWERING LOCUS CA* (*FCA*), and *FLOWERING*

LOCUS D (*FLD*), all identified to play integral roles in the warm temperature induced initiation of flowering.

CRISPR/Cas9 was utilized to target the endogenous lettuce genes, *LsFT, LsFCA* and *LsFLD* for editing, with the goal of delaying bolting in warm environments. While bona fide editing of the target genes could not be confirmed, this effort produced lines with marked delays in lettuce bolting when cultivated under increased ambient temperatures, demonstrating its potential in future grower and breeder applications.

Gene Editing-Assisted Generation of Delayed Bolting Lettuce (*Lactuca sativa* L.) for High Temperature Conditions

by
Meghan Cathreen Roche

A dissertation submitted to the Graduate Faculty of
North Carolina State University
in partial fulfillment of the
requirements for the degree of
Doctor of Philosophy

Horticultural Science

Raleigh, North Carolina
2024

APPROVED BY:

_____	_____
Dr. Ricardo Hernández Committee Co-Chair	Dr. Wusheng Liu Committee Co-Chair
_____	_____
Dr. José Alonso	Dr. Ralph Dewey

BIOGRAPHY

Meghan Roche is doctoral candidate in the Department of Horticultural Sciences from North Carolina State University (NCSU), minoring in Biotechnology. She works as a research assistant in the translational genomics and the controlled-environment horticulture labs. Before joining NCSU, Meghan completed a B.S. in Plant Sciences from Cornell University in 2004, and an M.S. in Plant Breeding from Texas A&M University in 2007.

Meghan is researcher and scientist in horticulture and biotechnology with an emphasis on tissue culture, genetic transformation and gene editing. She has an extensive background in tissue culture, molecular biology bench work, microscopy, seed quality, and crop breeding. Her current research is focused on gene-editing in lettuce to develop cultivars resistant to bolting under high temperature conditions.

ACKNOWLEDGMENTS

First and foremost, I would like to thank my parents, Colleen and Terrence Roche, for whom, without your determined support, in every sense of the word, I would not have achieved this seemingly insurmountable ambition. Your continued encouragement, kindness, and help is the singular reason for my success, that and dogged determination. I will never forget everything you've done for me. To my sister as well, Caelynn Prylo, and her brood, whom while enduring too much time out-of-contact, while my nose was to the figurative grindstone, also supported me from afar. I love you and thank you, sincerely.

I would also like to thank my friends; Bree Helms, Kristen Borgna, Amberly Rowles-Lawson, Crystal Johnson-Deaton, and Deidre Newport. Thank you for putting up with me when I was grumpy or tired. Thank you for being patient when I had to work and couldn't visit with you. Thank you for being a kind ear and a shoulder to cry on. Your support means the world to me. I would also like to thank my teammates. The welcome diversion of practicing and playing with you all has made the years upon years of graduate school *almost* tolerable.

I would also like to thank my lab-mate Dr. Debao Huang. Your guidance through the duration of my tenure has helped me immensely and I oftentimes would have been lost without you. Your knowledge, work ethic, and the joy to bring to the lab, continue to impress me daily. Last but not least, thank you to Cristian Collado and Partin Thompson, who helped me immensely in getting my screening trials up and running, and in keeping them running.

TABLE OF CONTENTS

LIST OF TABLES

LIST OF FIGURES

CHAPTER 1

THE AUTONOMOUS AND THERMOSENSORY FLOWERING PATHWAYS IN THE DECISION TO FLOWER: THE PUSH AND PULL OF GENETICS AND ENVIRONMENT

Flowering regulation in the model species *Arabidopsis thaliana* involves five defined primary floral induction pathways; autonomous, vernalization, photoperiod, gibberellin, and thermosensory (Capovilla et al., 2014). In the complex regulation of floral timing, no pathway exists exclusively of another, as components are frequently observed to overlap and/or exhibit functionality in multiple pathways at once. While the genes of the autonomous pathway were once thought to contribute to flowering regardless of environmental conditions, convergence with autonomous pathway factors and temperature-based flowering led to the identification of the thermosensory pathway (Blázquez et al., 2003; Balasubramanian et al., 2006). Accordingly, the key autonomous pathway genes serve crossover function in both pathways. In the thermosensory pathway, warm temperatures trigger the acceleration of flowering, while cool ambient temperatures serve to delay flowering, and autonomous pathway genes are central in coordinating these environmental responses (Blázquez et al., 2003; Lee et al., 2007; Kumar et al., 2012; Jung et al., 2012; Capovilla et al., 2014).

FLOWERING LOCUS C (FLC), a potent floral repressor

The MADS-box gene *FLC* is a potent floral repressor in the autonomous, vernalization, and thermosensory pathways regulating flowering (Michaels and Amasino, 1999; He et al., 2003). FLC represses the expression of the downstream floral activators *FLOWERING LOCUS T* (*FT*) and *SUPPRESSOR OF OVEREXPRESSION OF CONSTANS 1* (*SOC1*) (Michaels and Amasino, 1999; He et al., 2003; **Figure 1**) by binding the CArG boxes in the first intron and promoter of

FT and *SOC1*, respectively (Helliwell, et al., 2006; Lee et al., 2007). Genes of the autonomous pathway promote flowering via repression of *FLC* expression. These genes include *FLOWERING CONTROL LOCUS A* (*FCA*), *FLOWERING LOCUS Y* (*FY*), *FLOWERING LOCUS D* (*FLD*), *FLOWERING LOCUS VE* (*FVE*), *FLOWERING LOCUS PA* (*FPA*), *FLOWERING LOCUS K* (*FLK*), and *LUMINIDEPENDENS* (*LD*) (He et al., 2003). Null mutations in autonomous pathway genes show late flowering under both long and short photoperiods, but remain responsive to vernalization (in lines with functional *FRIGIDA (FRI)*) and gibberellin (Lee et al., 1994).

Autonomous pathway members act in the repression of *FLC* at all stages of expression in complex, interconnected phases, with fail-safes at every stage to ensure successful flowering. The H2A.Z histone variant acts in the perception of ambient temperature (Kumar and Wigge, 2010). H2A.Z serves both a repressive and promotive function, depending upon its location in the genome and gene body (Xue et al., 2021), and its presence in the +1 nucleosome position of *FLC* is associated with active transcription and decreased RNA Pol II stalling (Weber et al., 2014). The Swi2/Snf2-related (SWR1) complex members ACTIN-RELATED PROTEIN 6 (ARP6), PERIOD-INDEPENDENT EARLY FLOWERING 1 (PIE1), SWR1C SUBUNIT 6 (SWC6), and SET DOMAIN GROUP 7 (SDG7) facilitate the deposition of H2A.Z at *FLC*, activating its transcription (Deal et al., 2007; Ji et al., 2023; Woude et al., 2019; Potok et al., 2019; Kumar et al., 2012), and mutants of *arp6* and *pie1* have a constitutive warm ambient temperature phenotype and flower early because they are unable to incorporate H2A.Z (Kumar and Wigge, 2010; Deal et al., 2007). H2A.Z is present in nucleosomes at cooler temperatures but is evicted from most thermoresponsive genes at increased temperatures (Kumar and Wigge, 2010; Xue et al., 2021), and while H2A.Z remains present in *FLC* chromatin after flowering,

FLC has been deactivated by H3K27me3 deposition (Kumar and Wigge, 2010; Deal et al., 2007).

SWITCH/SUCROSE NONFERMENTING (SWI/SNF) complexes remodel histone-chromatin contacts, and subunits of the complex act on both floral repressors and floral promoters to regulate flowering (Jégu et al., 2014). Identified SWI/SNF complex subunits in *Arabidopsis* include BRAHMA (BRM), BUSHY(BSH), SWI3A, SWI3B, and SWI3C (Sarnowski et al., 2002). BRM is a key component of the thermosensory pathway, acting to repress *FLC* by opposing transcriptional activation by H2A.Z (Farrona et al., 2011; Li et al., 2015; Torres and Deal, 2019). BRM accomplishes this repression by destabilizing the *FLC* +1 nucleosome (Torres and Deal, 2019), necessitating H2A.Z deposition to reverse the repressed state (Farrona et al., 2011). BRM is upregulated in response to heat treatment, and increased *FLC* expression is observed in *brm* mutants, along with increased H3K4me3 and reduced H3K27me3, indicating that BRM carries out its repression of *FLC* specifically under warmer temperatures (Buszewicz et al., 2016; Farrona et al., 2011; Li et al., 2015). In *Drosophila*, SWI/SNF complex homologs function as a fail-safe, meant to suppress mutations in Polycomb-group genes, like CURLY LEAF (CLF) (Kennison and Tamkun, 1988). This function is preserved in plants, whereby the presence of SWI/SNF components in *FLC* chromatin in warm ambient temperatures not only prevents H2A.Z occupation, but also enables CLF-PRC2-mediated H3K27me3 to act in *FLC* suppression (Hurtado et al., 2006). The SWI/SNF subunits BSH, SWI3B, and SWI3C interact with FCA via its C-terminus, (Sarnowski et al., 2002; Sarnowski et al., 2005) and BRM interacts with SWI3B and SWI3C towards the regulation of temperature-dependent flowering (Hurtado et al., 2006), indicating that FCA may also function via the SWI/SNF complex.

In transcriptional *FLC* repression, MUT9-LIKE KINASE 4 (MLK4) phosphorylates *FLC* histone 3 at threonine 3 (H3T3) to limit recruitment of transcription machinery to the *FLC* transcription start site (TSS) (Wang et al., 2021; Xing et al., 2008b) while TATA-binding protein-associated factor 15b (TAF15b) and C-TERMINAL DOMAIN PHOSPHATASE-LIKE 1 (CPL1) bind to the TSS to reduce transcript elongation at *FLC* by dephosphorylating RNA Pol II Ser5p (Eom and Lee, 2018; Kyung et al., 2023). To facilitate this action, the prion-like domain (PrD) of TAF15b complexes with DECAPPING 1 (DCP1) by liquid-liquid phase separating (LLPS) into the membraneless organelles, mRNA processing bodies (p-bodies) (Chakrabortee et al., 2016; Dong et al., 2016). The formation of p-bodies is correlated with environmental conditions unfavorable to flowering, such as cold and heat, indicating that their formation is temperature-mediated, is required for TAF15b's suppressive activity on *FLC*, and that these foci are where the interaction with Pol II occurs (**Figure 1**; Eom et al., 2018; Eom and Lee, 2018).

During *FLC* transcript elongation, FPA-enriched Ser2p Pol II pauses and accumulate near the transcription end site of *FLC*, facilitated by the negative transcription factor BORDER (BDR), and the transcription complex component MEDIATOR SUBUNIT 8 (MED8), with MED8 binding directly to *FLC* (Parker et al., 2021; Yu et al., 2021; Yuan et al., 2023). The APOPTOSIS AND SPLICING ASSOCIATED-PROTEIN (ASAP) complex component and splicing regulator SERINE/ARGININE RICH 45 (SR45) and hnRNP R-LIKE PROTEIN (HRLP) also phase separate via LLPS to enable HRLP's restriction of cotranscriptional *FLC* splicing, with SR45 promoting proper splicing of *FPA* pre-mRNA (Ali et al., 2007; Zhang et al., 2022; Zhang et al., 2017). Together, these actions lead to the formation of an RNA-DNA heteroduplex (R-loop) near *FLC* intron 1, leading to reduced Pol II presence and suppression of

transcriptional elongation of *FLC* (Ali et al., 2007; Zhang et al., 2022; Parker et al., 2021; Yu et al., 2021; Yuan et al., 2023).

The sense *FLC* transcript is alternatively spliced and four isoforms have been identified, with *FLC.1* being the only functional variant (Feng et al., 2011; Schon et al., 2021). *FLC.1* utilizes distal polyadenylation, while the three non-functional isoforms utilize proximal poly(A) sites (Feng et al., 2011; Schon et al., 2021). The mRNA N^6-methyladenosine (m^6A) methyltransferase writer FIONA 1 (FIO1) is required for proper *FLC* transcript splicing, with mutants of *fio1* have vastly reduced levels of the functional *FLC.1* transcript isoform (Cai et al., 2023). The *FLC* activator FRI also promotes distal polyadenylation, while the primary autonomous pathway components FCA, FY and FLK promote proximal polyadenylation of *FLC* (Schon et al., 2021; Feng et al., 2011; Amara et al., 2023). FLK is also and m^6A reader and, along with KH domain-containing proteins KHZ1 and KHZ2, binds nascent *FLC* and acts to suppress the splicing of functional *FLC* isoforms, in addition to reducing the stability of *FLC* transcripts (Lim et al., 2004; Ripoll et al., 2009; Amara et al., 2023; Yan et al., 2017; Yan et al., 2019). The FLK paralog PEPPER (PEP) antagonizes FLK's repressive action on *FLC*, in both transcriptional activation of and generation of correctly spliced transcripts of *FLC*, and FLK represses this action (Ripoll et al., 2009).

FLC is also transcribed into multiple non-coding antisense transcripts, named *Cold induced long antisense intragenic RNA* (*COOLAIR*) (Swiezewski et al., 2009). *COOLAIR* is transcribed in response to cold ambient temperatures in a manner predominantly independent of vernalization and is associated with reduced *FLC* sense expression (Swiezewski et al., 2009). Mutated *Arabidopsis* lines unable to transcribe *COOLAIR* also showed elevated *FLC* expression (Marquardt et al., 2014; Tian et al., 2019). Adding additional layers to floral timing, the ability to

repress *FLC* via *COOLAIR* has been demonstrated as a safeguard in case of the loss of *FT* function (Luo et al., 2019).

COOLAIR is transcribed from a start site just 3' of the sense *FLC* polyadenylation site (Marquardt et al., 2014), with transcript elongation regulated by FPA and the transcription elongation factor b (P-TEFb) component, CDKC;2, via Pol II Ser2p (Wang et al., 2014; Parker et al., 2021), and counteracted by TAF15b (Eom et al., 2018; Kyung et al., 2023). During *COOLAIR* transcript elongation, Pol II pauses and accumulates, facilitated by the negative transcription factor BDR and FPA (**Figure 1**; Yu et al., 2021), creating an R-loop between the nascent *COOLAIR* transcript and the *FLC* chromatin, which is stabilized by NODULIN HOMEOBOX (NDX) (Sun et al., 2013; Baxter et al., 2021). NDX is then bound by the POLYCOMB REPRESSIVE COMPLEX 2 (PRC2) component VIVIPAROUS 1/ABI 3-LIKE (VAL1), which assists in the recruitment of the PRC1 to monoubiquitinate H2A on *FLC* chromatin, reducing chromatin accessibility (Mikulski et al., 2022; Yin et al., 2021). Stalling of the replisome also enables the temporal recruitment of polyadenylation and chromatin remodeling complexes (Sun et al., 2013; Fang et al., 2020; Baxter et al., 2021; Qi et al., 2022).

COOLAIR is also alternatively spliced, with polyadenylation occurring distal to the *FLC* promoter or proximally within the sixth intron (Hornyik et al., 2010; Marquardt et al., 2014). Proximally polyadenylated *COOLAIR* enables repression of *FLC*, while distal polyadenylation hinders *FLC* suppression (Marquardt et al., 2014; Tian et al., 2019).

FCA and FY, promotion of proximal polyadenylation of COOLAIR

FCA and FY work together with FPA to function in the proximal 3'-end processing of *COOLAIR* by associating with *FLC* chromatin at the proximal poly(A) site, resulting in *FLC*

repression (**Figure 1**; Liu et al., 2010; Hornyik et al., 2010; Duc et al., 2013; Parker et al., 2021; Quesada et al., 2003; Liu et al., 2007; Fang et al., 2020). The m^6A methyltransferase writer complex component, FLX-LIKE 2 (FLL2), orchestrates LLPS with the polyadenylation factors FCA and FY, along with m^6A members FPA, mRNA m^6A methyltransferase (MTA), and CLEAVAGE STIMULATING FACTOR 64 (CstF64) via their prion-like domains (Xu et al., 2021a; Chakrabortee et al., 2016; Fang et al., 2019). With Factor Interacting with Poly(A) polymerase 1 (FIP1) binding the *COOLAIR* RNA, Pre-mRNA processing factor 8 (PRP8), CstF77, and CstF64 join the complex, with CstF64 tethering the LLPS proteins and enabling their interaction (Forbes et al., 2006; Hunt and Addepalli, 2008; Sonmez et al., 2011; Fang et al., 2019). This complexing supports *COOLAIR* polyadenylation by FCA, FY, CstF64 and CstF77, thus clearing the R-loop (Sun et al., 2013; Xu et al., 2021a; Baxter et al., 2021; Liu et al., 2010).

FCA encodes an RNA-binding protein and functions in pre-mRNA 3'-end processing (Quesada et al., 2003). FCA is comprised of two 5'-end RRMs, a proline/glycine rich motif, and a WW protein binding domain, surrounded by polyglutamine tracts (Macknight et al., 1997). FY is related to the fungal Pfs2p end-processing factor and the mammalian cleavage and polyadenylation specificity factor WDR33, and contains a series of seven WD40 repeats and two PPLPP (Pro-Pro-Leu-Pro-Pro) repeat regions (Henderson et al., 2005; Yu et al., 2019). Mutations in *fy* disrupt canonical polyadenylation signal recognition, and distal or proximal *FLC* polyadenylation is dependent upon the location of the mutations. Mutations in the WD40 repeat region of FY lead to reduced A-rich signal recognition, and thus, proximal polyadenylation. Mutations in the PPLPP repeat region lead to enhanced A-rich signal recognition, and thus distal polyadenylation. The WD40 repeat is the dominant domain in polyadenylation signal recognition and the PPLPP mutation-related phenotype is due to reduced binding to the WW domain of FCA

(Simpson et al., 2003; Henderson et al., 2005; Yu et al., 2019: Quesada et al., 2003; Adams et al., 2009).

FCA expression is auto-regulated, and it is transcribed into four isoforms via the utilization of different poly(A) sites within its pre-mRNA (Macknight et al., 1997). The *FCA-α, δ,* and *γ* isoforms are produced by the distal poly(A) site selection in the 3' UTR, while *FCA-β* is produced by proximal poly(A) site selection within the third intron (Macknight et al., 1997). *FCA-γ* is the only isoform encoding the functional full-length FCA protein, and its production is regulated in a spatial, temporal, and temperature-dependent manner (Macknight et al., 1997; Simpson et al., 2003; Quesada et al., 2003). When an *FCA* intronless isoform is overexpressed in wild-type *Arabidopsis*, the non-functional *FCA-β* isoform is exclusively produced (Quesada et al., 2003), while intronless *FCA* overexpression in *fca* mutants leads to production of *FCA*-γ and early flowering (Macknight et al., 2002). This auto-regulation of *FCA* occurs via an interaction with FY (Simpson et al., 2003; Quesada et al., 2003) and is dependent upon ambient temperature, as an increase in the *FCA-β* isoform was observed when *Arabidopsis* plants were transferred from 23 ℃ to 27 ℃ (Balasubramanian et al., 2006).

FCA expression is positively regulated by the pre-mRNA 3'-end processing factor hnRNP A1-like protein 1 (HLP1), which directly binds the 3'-UTR and the third intron in the *FCA* pre-mRNA (Zhang et al., 2015). Mutants of *hlp1* exhibited a poly(A) site shift from the distal to the proximal site in *FCA* transcripts, leading to upregulation of the non-functional *FCA-β* and delayed flowering (Zhang et al., 2015). DCL4 also acts in transcript termination of *FCA*, promoting cleavage of the nascent transcript downstream of the polyadenylation site in an effort to promote RNA expression (Liu et al, 2012). Mutants of *dcl4* have transcriptional read-through at *FCA*, with transcripts being targeted by endogenous RNAi machinery (Liu et al, 2012).

Suppressive *FCA* alternative polyadenylation is facilitated by the *Arabidopsis* homolog of Protein 1 of Cleavage Factor 1 (Pcf11p)-similar protein 4 (PCFS4), a yeast polyadenylation component homolog (Xing et al., 2008a). Via complexing with FY and the polyadenylation factor CLPS3, PCFS4 promotes FCA polyadenylation within the third intron, yielding *FCA-β* transcripts (Xing et al., 2008a).

FCA acts in both basal and acquired thermotolerance, and *FCA* expression is induced by warm temperatures (37 ℃) and suppressed by cold (4 ℃) (Lee et al., 2015). Overexpression of *FCA* leads to increased heat tolerance, while lesions in *fca* lead to reduced tolerance to heat stress (45 ℃) (Lee et al., 2015). This occurs due to the action of FCA in inducing the expression of and maintaining protein stability of the antioxidant *protochloropyllide oxidoreductases* (*POR*) genes *PORA* and *PORB,* and its interaction with ABA-INSENSITIVE 5 (ABI5) in the activation of the antioxidant *1-CYSTEINE PEROXIREDOXIN 1* (*PER1*) under warm ambient temperatures (28 ℃ - 45 ℃) (Ha et al., 2017; Lee et al., 2015). FCA also acts in processing of the thermotolerance-associated mRNA *miR398,* and increased expression of *miR398* is observed in increased ambient temperatures (23 ℃ vs. 16 ℃) (Guan et al., 2013; Lee et al., 2010). In addition, FCA acts in the processing of the pri-miRNAs of the floral promoting microRNAs *miR172a*, *miR172b*, and *miR172d*, binding the sequence flanking the stem-loop in *pri-miR172* via its RRMs (Jung et al., 2012; Lee et al., 2010). Mutants of *fca* have reduced *miR172* expression, contributing to the delayed flowering phenotype (Jung et al., 2012; Lee et al., 2010). Both *FCA* and mature *miR172* are observed to increase in expression under increased ambient temperature (23 ℃ vs. 16 ℃), indicating that processing of *pri-miR172* by FCA is amplified at higher temperatures (**Figure 2**; Jung et al., 2012; Lee et al., 2010). The temperature-dependent function of FCA is also modulated through suppression of *SHORT VEGETATIVE PHASE* (*SVP)*

(Li et al., 2008), and *fca* mutants flower at the same time regardless if the environment is 16 ℃ or 23 ℃ (Blázquez et al. 2003).

FLD and FVE, epigenetic regulation of FLC expression

Much of the activation and repression of *FLC* expression occurs epigenetically via chromatin modifications (He, 2009). *COOLAIR* replisome slowing and R-loop resolution enables the temporal recruitment of the autonomous pathway chromatin remodeling complex (AuPC) to *FLC* chromatin (**Figure 1**; Baxter et al., 2021; Fang et al., 2020; Qi et al., 2022), with FLD, FY, SDG26, LD, ELF4-Like 2 (EFL2), EFL4, and ANTHESIS PROMOTING FACTOR 1 (APRF1) forming the complex (Baxter et al., 2021; Fang et al., 2020; Qi et al., 2022). In the AuPC, LD is the scaffold supporting other proteins of the complex, with the FLD C-terminal domain binding to the LD N-terminal homeodomain (Qi et al., 2022). LD also binds EFL2 and EFL4 by its TFIIS domain, and APRF1 by its C-terminal region. SDG26 interacts via EFL2 and EFL4, with SDG26 binding directly to *FLC*, and additionally interacting with FY (Fang et al., 2020; Qi et al., 2022). While FLD, SDG26, and LD facilitate methylase activity, halting accumulation of H3K4me1 and H3K36me3 at the *FLC* chromatin, EFL2 and EFL4 recruit members of the histone deacetylase complex, including HISTONE DEACETYLASE 19 (HDA19) and HDA6 (Qi et al., 2022). Mutants of *sdg26* exhibit temperature-insensitive flowering, indicating the thermoresponsive nature of the AuPC complex (Pajoro et al., 2017). The PRC2-components VAL1 and VAL2 also recruit the POLYCOMB REPRESSIVE COMPLEX 1 (PRC1) and the ASAP complex to *FLC* chromatin (Mikulski et al., 2022; Qüesta et al., 2016). While the PRC1 affects *FLC* transcription by monoubiquitinating H2A, thus altering chromatin accessibility (Qüesta et al., 2016; Baile et al., 2021; Mikulski et al., 2022), the ASAP complex indirectly

suppresses *FLC* expression in warm conditions via deacetylation (Mikulski et al., 2022; Chen et al., 2019). VAL1 recruits the ASAP complex components SR45, ACINUS and SIN3-associated protein 18 (SAP18) (Mikulski et al., 2022; Chen et al., 2019), and while SR45 is a positive splicing factor for *ACINUS* and *SAP18*, SAP18 functions in the recruitment of the histone deacetylase complex to *FLC* chromatin (Chen et al., 2019; Qüesta et al., 2016; Baile et al., 2021). VAL1/2 also recruit HDA6 and HDA9 to *FLC* chromatin directly (Chhun et al., 2016; Zeng et al., 2020). Together, the action of the AuPC and ASAP complexes affects FLC deacetylation, furthering the clearing of impediments to H3K27me3 deposition for *FLC* suppression (Liu et al., 2010; Fang et al., 2020; Xu et al., 2008; Zeng et al., 2020).

FLD works together with FVE, MULTICOPY SUPPRESSOR OF IRA 5 (MSI5), HISTONE DEACETYLASE5 (HDA5), HDA6, and HDA9 to form a histone deacetylase complex acting on *FLC* chromatin to remove active H2/H3 acetylation marks, leading to repression of *FLC* expression (**Figure 1**; Gu et al., 2011; Yu et al., 2011; Luo et al., 2015; Zeng et al., 2020). *Arabidopsis* FLD is a homolog to the human histone deacetylase LYSINE-SPECIFIC HISTONE DEMETHYLASE 1 (KIAA0601/LSD1), and contains a SWIRM domain, polyamine oxidase domain, and c-terminal domain (He et al., 2003). FLD complexes with HDA6 via its SWIRM domain, while HDA5 and HDA6 bind to FVE and to *FLC* chromatin (Qi et al., 2022; Yu et al., 2011; Yu et al., 2016; Luo et al., 2015). MSI5 also joins the complex, and together they function to deacetylate *FLC* histone H2/H3 (Gu et al., 2011; Yu et al., 2016; Luo et al., 2015; Wu et al., 2008; Yu et al., 2011). Mutants of *fld* show hyperacetylation at histones H3 and H4 of *FLC*, proximal to the transcription start site (TSS), as well as increased H3K4 dimethylation and trimethylation (Yu et al., 2011; He et al., 2003; Liu et al., 2007), leading to increased expression of *FLC* and delayed flowering (He et al., 2003). FLD also represses *FLC*

expression in a partially redundant manner with the FLD homologs Lysine-Specific Demethylase 1-Like (LSD1-LIKE1; LDL1) and LDL2 (Jiang et al., 2007). LDL1 and SUVR5 (SU(VAR) 3-9-RELATED PROTEIN 5) interact with one another and have also been implicated in repressing *FLC* expression via the autonomous pathway. Loss of either protein results in reduced H3K9me2 and H3K27me2 in addition to increased H4ac of *FLC* chromatin and enhanced *FLC* expression (Krichevsky et al., 2007).

FVE is a homolog of human Retinoblastoma-Associated Protein 46/48, functioning in histone-binding. FVE contains a nuclear localization signal (NLS) and six WD repeats, with the fourth WD domain containing the retinoblastoma-binding motif that enables its histone deacetylase and HDAC-binding activity (Gu et al., 2011; Ausín et al., 2004). Similar to *fld, fve* mutants also exhibit increased acetylation on *FLC* chromatin (He et al., 2003; Ausín et al., 2004). Working with FVE and MSI5, LIKE HETEROCHROMATIN PROTEIN 1 (LHP1), PWWP DOMAIN PROTEIN 1 (PDP1), PDP2 and PDP3 act in recruiting the POLYCOMB REPRESSIVE COMPLEX 2 (PRC2) to *FLC* chromatin to suppress *FLC* expression via the deposition of repressive H3K27me3 under normal conditions (**Figure 1**; Jiang et al., 2008; Zhou et al., 2018). The PRC2 component MSI1 also complexes with HDA6 in the deacetylation of H3K9, possibly acting as a bridge between the histone deacetylase complex and PRC2, as removal of H3 acetylation enables subsequent deposition of repressive H3K27me3 (Xu et al., 2021b).

FVE also acts with the CULLIN 4 (CUL4) ubiquitin ligase and DNA DAMAGE-BINDING PROTEIN 1 (DDB1A/B) via the PRC2 to repress *FLC* (Pazhouhandeh et al., 2011). EMBRYO DEFECTIVE 1579 (EMB1579) enables the interaction of the CUL4/DDB1A/B^{FVE} complex with the PRC2-component CLF, a methyltransferase, via LLPS. CLF acts specifically

in H3K27me3 deposition on *FLC* chromatin to repress it and promote flowering (Jiang et al., 2008). EMB1579 is thought to orchestrate condensation of the complex and reduced H3K27me3 is observed on *FLC* chromatin in *emb1579* mutants, with a complementary delay in flowering observed (Zhang et al, 2020).

FVE also functions in delaying flowering in unfavorable conditions. FVE negatively regulates the Cold-responsive Binding Factor/Dehydration Responsive Element Binding protein (CBF/DREB) pathway under intermittent cold stress (Kim et al., 2004). Specifically, FVE binds to the chromatin of the CBF/DREB pathway target *COR15A*, as well as *FLC*, in the formation of a multiprotein complex to delay flowering in cold, deacetylating gene targets (Jeon and Kim, 2011). The temperature-dependent function of FVE is also modulated through suppression of the floral repressor *SVP* (Li et al., 2008), and *fve* mutants flower synchronically at 16 ℃ or 23 ℃ (**Figure 2**; Blázquez et al. 2003).

FT, a key floral activator

FT encodes a phosphatidylcholine-binding protein, containing a 5' CArG box that enables binding by FLC, and a central matrix-attachment region (MAR) surrounded by a Phosphatidylethanolamine-Binding Protein (PEBP) domain, enabling FT mobile transport (Searle et al., 2006; Helliwell et al., 2006; Yun et al., 2012; Kardailsky et al., 1999). *FT* expression is promoted by the transcription factor CONSTANS (CO) in the photoperiod pathway, and FT promotes the expression of *SOC1*, which then activates floral meristem identity genes (Samach et al., 2000). CO activates *FT* via a conserved motif in the promoter, and the ability to bind and activate *FT* is dependent upon the absence of H3K27me3 (Adrian et al.,

2010). CO cannot promote *SOC1* expression in the absence of *FT* expression, and thus floral promotion is delayed (Yoo et al., 2005).

FT is a mobile protein, produced in leaves and transported to shoot apical meristem (SAM) to act in the promotion of flowering (Nakamura et al., 2019; Susila et al., 2021). Transport of the mobile FT protein from leaf to shoot apex is temperature-dependent, and temperature-insensitivity is observed in the strong *Arabidopsis ft-10* mutant (Balasubramanian et al., 2006). FT binds to phosphatidylglycerol at the lipid membrane of phloem companion cells, and low temperatures (16 ℃) induce sequestration of FT, inhibiting its transport. The sequestration is released at warm temperatures (23 ℃), enabling the transport of mobile FT to shoot apex to act in the induction of flowering (**Figure 2**; Liu et al., 2020; Susila et al., 2021). In *Arabidopsis*, the amino acid residues responsible for phosphatidylcholine binding have been identified to be Arg-13, Asp-17 and Arg-83, as directed mutations of these residues led to delayed flowering (Nakamura et al., 2019).

The expression of *FT* is also epigenetically regulated. The PRC2 components CLF and FIE act in the repression of *FT* expression by depositing H3K27me3 on *FT* chromatin to prevent precocious flowering during vegetative development (Jiang et al., 2008). The suppression of *FT* by CLF is relieved by a complex of Nuclear-Factor-Y Subunit C (NF-YC) and CO, which antagonize the ability of CLF to bind and deposit H3K27me3 on *FT* chromatin as plants mature (**Figure 2**; Liu et al., 2018; Luo et al., 2018). In addition, the chromatin-remodeler PICKLE (PKL) and the methyltransferase *ARABIDOPSIS* HOMOLOG OF TRITHORAX 1 (ATX1) act coordinately to facilitate H3K4me3 at *FT* to activate its expression, antagonizing the action of CLF and the Polycomb-group proteins (Jing et al., 2019), and mutants of *pkl* have reduced *FT* expression and are delayed in flowering (Carter et al., 2018). *FT* is also regulated in a

photoperiod and temperature-dependent manner by the H3K27me3 demethylase JUMONJI 13 (JMJ13), to suppress flowering under both long and short days in warm ambient conditions (Zheng et al., 2019). The MAR-binding factor/AT-hook protein AT-hook motif nuclear localized 22 (AHL22) binds to the *FT* chromatin via the ATR motif within its MAR. AHL22 recruits histone deacetylases HDA19, HDA6 and HDA9, promoting H3 deacetylation and H3K9me2 dimethylation to suppress *FT* expression (Yun et al., 2012). This suppression occurs preferentially at cooler ambient temperatures (**Figure 2**; Shen et al., 2019).

In the regulation of *FT*, the SWR1 component SWR1C SUBUNIT 4 (SWC4) recruits PIE1 to *FT* chromatin for H2A.Z deposition (Gómez-Zambrano et al., 2018). PIE1 also interacts with PKL to promote deposition of H3K27me3. PKL, PIE1 and CLF work coordinately in the same pathway to facilitate global H3K27me3, and, interestingly, 90% of H3K27me3 is colocalized with H2A.Z (**Figure 2**; Carter et al., 2018). H2A.Z exhibits a repressive effect on *FT* at cooler temperatures, and H2A.Z deposition at *FT* is high at 17 ℃, but greatly decreased at 27 ℃. Accordingly, low *FT* expression is observed at 17 ℃, but higher expression is observed at higher temperatures (27 ℃) (Kumar and Wigge, 2010). Genome-wide, a high correlation is observed between genes enriched in H3K27me3 and those enriched in H2A.Z, and thus, those having reduced H3K27me3 correlatively have reduced H2A.Z, and this correlation holds true for *FT* (Carter et al., 2018).

FT expression is positively regulated by *PHYTOCHOCHROME INTERACTING FACTOR 4* (*PIF4*), whose expression is activated by warm temperatures (Kumar et al., 2012; Fernández et al., 2016). PIF4 binds to the *FT* promoter near the TSS site to promote *FT* expression in a temperature-dependent manner, with preferential binding at higher temperatures (27 ℃) versus lower temperatures (12 ℃). This binding is enabled by eviction of the H2A.Z

histone variant from the PIF4 binding site in *FT*, which also occurs at higher temperatures (**Figure 2**; Kumar et al., 2012). Mutants of *pif4* are insensitive to increased temperatures (27 ℃) and are late-flowering due to a reduction in *FT* expression, while the *PIF4* overexpression lines have enhanced *FT* expression, leading to precocious flowering (Kumar et al., 2012; Fernández et al., 2016). Thermosensory flowering also occurs by sequestration of the circadian evening complex (EC) component and floral repressor EARLY FLOWERING 3 (ELF3) (Jung et al., 2020). ELF3 acts in repression of *PIF4* under cool temperatures, and this repression is relieved upon warming, enabling the thermosensitivity of PIF4 and its downstream partners, like *FT* (Box et al., 2015; Press et al., 2016; Kumar et al., 2012). The ELF3 protein has a largely disordered poly-glutamine (poly-Q) tract within a PrD, which functions in temperature-sensing. A reduction in binding of ELF3 to gene targets is observed as temperatures increase, and a concurrent increase in the formation of LLPS nuclear bodies is observed, with sequestration of ELF3 into nuclear bodies relieving transcriptional repression of target genes (Jung et al., 2020). ELF3 and the EC also act with the SWR1 complex in the suppressive deposition of H2A.Z at target genes in thermally-sensitive circadian regulation (Tong et al., 2020).

The MADS-box transcription factor and floral repressor *SVP*, is also a central regulator of the thermosensory pathway, serving its function individually and via complexing with FLM-β (Posé et al., 2013; Li et al., 2008). SVP acts downstream of the autonomous pathway genes, binding to the *FT* promoter at the vCArG III motif, and *SOC1* near the 5’ UTR, repressing their expression, and mutants of *svp* are insensitive to temperature (**Figure 2**; Li et al., 2008; Tao et al., 2012; Lee et al., 2007). The action of the SWI/SNF chromatin remodeler BRM also enables SVP to carry out its function under cool temperatures, with binding of BRM to *SVP* preventing binding and repressive methylation by the CLF-PRC2 complex, thus enabling SVP to suppress

FT (Li et al., 2015). SVP also promotes the expression of the *FT* repressors *TEMPRANILLO 1* (*TEM1*) and *TEM2*. SVP activates *TEM2* expression under cool temperatures (16 ℃) and both *TEM1* and *TEM2* under warm temperatures (22 ℃) (Marín-González et al., 2015), with TEM1 binding to the *FT* 5'-UTR and recruiting the PRC2 to deposit H3K27me3 (Hu et al., 2021). SVP also promotes the expression of the MYB transcription factor *EARLY FLOWERING MYB PROTEIN* (*EFM*) and the H3K36me2 demethylase *JUMONJI 30* (*JMJ30*) to repress *FT* expression under reduced temperatures (16 ℃) and long day photoperiods (Yan et al., 2014).

The FLC homolog FLOWERING LOCUS M / MADS AFFECTING FLOWERING 1 (FLM/MAF1) is a primary regulator in the ambient temperature pathway. The *FLM* transcript undergoes alternative splicing in response to ambient temperature, forming α, β, γ, and δ isoforms (Scortecci et al., 2001; Lee et al., 2020). The functional FLM-β isoform complexes with SVP, enabling its translocation to the nucleus, delaying flowering in undesirable conditions by repressing downstream floral activators such as *FT*, *SOC1*, *SCHLAFMUTZE* (*SMZ*), *Arabidopsis thaliana CENTRORADIALIS homologue* (*ATC*), and *SEPALLATA 3* (*SEP3*) (Lee et al., 2013; Jin et al., 2022; Posé et al., 2013). At low ambient temperatures (16 ℃), Splicing Factor 1 (SF1), Glycine-rich RNA-binding protein 7 (GRP7), GRP8, Cyclin-dependent kinase G2 (CDKG2) and the cognate cyclin, ARGININE-RICH CYCLYN L1 (CYCL1) promote maturation of the functional *FLM-β* isoform (Scortecci et al., 2001; Lee et al., 2020; Lee et al., 2022; Steffen et al., 2019; Nibau et al., 2020). Interestingly, in addition to reduced accumulation of *FLM-β* in *cdkg2* mutant lines, reduced expression of *SVP* was also observed (Nibau et al., 2020). Upon temperature increase (27 ℃), however, SF1, pre-mRNA processing factor 39a (PRP39a) and RNA-binding protein 45d (RBP45d) generate the *FLM-δ* splice isoform (Lee et al., 2020; Wang et al., 2007; Chang et al., 2022; Huang et al., 2022), which is unable to suppress downstream

floral activators (Capovilla et al., 2017). Also, while a slight increase in *SVP* mRNA expression is observed under increased temperatures, proteasome-mediated degradation and reduced nuclear localization of SVP reduce the pool of available SVP protein for binding to extant FLM-β, enabling the promotion of flowering (**Figure 2**; Posé et al., 2013; Lee et al., 2013; Lee et al., 2014; Fernández et al., 2016; Jin et al., 2022).

FT expression is also regulated in a temperature-dependent manner by microRNAs. *miR172* is active in promoting *FT* expression, while suppressing the *FT* repressors *APETALA 2* (*AP2*), *TARGET OF EAT 1* (*TOE1*), *TOE2*, *TOE3*, *SCHNARCHZAPFEN* (*SNZ*) and *SMZ* (**Figure 2**; Jung et al., 2012). This action is counteracted by SVP, which preferentially binds *miR172a* at lower temperatures (16 ℃), as well as TEM1 and TEM2 (Cho et al., 2012; Tao et al., 2012; Aguilar-Jaramillo et al., 2019). Mutants of *svp* have increased *miR172* expression and *miR172* overexpressors flowered early, regardless of the ambient temperature, with a concurrent increase in *FT* expression observed (Lee et al., 2010). The microRNA *miR169* acts to suppress the floral promoters *Nuclear Factor-YA2* (*NF-YA2*) and *JAZ4*, under cool ambient temperatures. Under warm ambient temperatures, however, the NF-Y complex with NF-YA2 promotes expression of *FT,* while JAZ4 acts to repress *TOE1* and *TOE2* **(Figure 2**; Gyula et al., 2018). The microRNA *miR156* forms a module with SQUAMOSA PROMOTER BINDING-LIKE 3 (SPL3) to regulate *FT* expression in an ambient temperature-dependent manner. While SPL3 promotes *FT* expression, *miR156* acts in the degradation of *SPL3* transcripts under cool (16 ℃) ambient temperatures, thus delaying flowering (**Figure 2**; Kim et al., 2012). The PRC1 component B LYMPHOMA MOLONEY MURINE LEUKEMIA VIRUS INSERTION REGION 1 HOMOLOG 1 (BMI1) acts to suppress *miR156* via PRC2-mediated H3K27me3, and this suppression is aided by VAL1/2, enabling upregulation of *FT* and the transition to flowering

(Picó et al., 2015). Conversely, *miR156* is promoted by BRM, thus aiding in suppressing the floral transition (Xu et al., 2016). Also a PRC1 component, EMBRYONIC FLOWER 1 (EMF1) acts to suppress the flowering promoters *miR172* and *SPL3*, in partial coordination of the action of *miR156* (Picó et al., 2015; Kim et al., 2012).

The complexity of the pathways leading to floral induction cannot be understated. The comprehensive dissection of a mere two pathways; autonomous and thermosensory, alights to that. Elegant, interrelated systems have been characterized, with their exposition growing in detail by-the-year. The finely calibrated responses to ambient conditions serve to reveal the profound level of care plants put into the decision to flower, with overlapping gene functionality and fail-safes ensuring the passage of genetic material to the subsequent generation.

References

Adams S, Allen T, Whitelam GC (2009) Interaction between the light quality and flowering time pathways in *Arabidopsis*. Plant J **60**: 257–267

Adrian J, Farrona S, Reimer JJ, Albani MC, Coupland G, Turck F (2010) *Cis*-regulatory elements and chromatin state coordinately control temporal and spatial expression of *FLOWERING LOCUS T* in *Arabidopsis*. Plant Cell **22**: 1425–1440

Aguilar-Jaramillo AE, Marín-González E, Matías-Hernández L, Osnato M, Pelaz S, Suárez-López P (2019) TEMPRANILLO is a direct repressor of the microRNA miR172. Plant J **100**: 522–535

Ali GS, Palusa SG, Golovkin M, Prasad J, Manley JL, Reddy ASN (2007) Regulation of plant developmental processes by a novel splicing factor. PLoS ONE **2**: e471

Amara U, Hu J, Cai J, Kang H (2023) FLK is an mRNA m6A reader that regulates floral transition by modulating the stability and splicing of *FLC* in *Arabidopsis*. Mol Plant **16**: 919–929

Ausín I, Alonso-Blanco C, Jarillo JA, Ruiz-García L, Martínez-Zapater JM (2004) Regulation of flowering time by FVE, a retinoblastoma-associated protein. Nat Genet **36**: 162–166

Baile F, Merini W, Hidalgo I, Calonje M (2021) EAR domain-containing transcription factors trigger PRC2-mediated chromatin marking in *Arabidopsis*. Plant Cell **33**: 2701–2715

Balasubramanian S, Sureshkumar S, Lempe J, Weigel D (2006) Potent induction of *Arabidopsis thaliana* flowering by elevated growth temperature. PLoS Genet **2**: e106

Baxter CL, Šviković S, Sale JE, Dean C, Costa S (2021) The intersection of DNA replication with antisense 3’ RNA processing in *Arabidopsis* FLC chromatin silencing. Proc Natl Acad Sci USA **118**: e2107483118

Blázquez MA, Ahn JH, Weigel D (2003) A thermosensory pathway controlling flowering time in *Arabidopsis thaliana*. Nat Genet **33**: 168–171

Box MS, Huang BE, Domijan M, Jaeger KE, Khattak AK, Yoo SJ, Sedivy EL, Jones DM, Hearn TJ, Webb AAR, et al (2015) ELF3 controls thermoresponsive growth in *Arabidopsis*. Curr Biol **25**: 194–199

Buszewicz D, Archacki R, Palusiński A, Kotliński M, Fogtman A, Iwanicka-Nowicka R, Sosnowska K, Kuciński J, Pupel P, Olędzki J, et al (2016) HD2C histone deacetylase and a SWI/SNF chromatin remodeling complex interact and both are involved in mediating the heat stress response in *Arabidopsis*. Plant Cell Environ **39**: 2108–2122

Cai J, Hu J, Amara U, Park SJ, Li Y, Jeong D, Lee I, Xu T, Kang H (2023) *Arabidopsis* N6-methyladenosine methyltransferase FIONA1 regulates floral transition by affecting the splicing of *FLC* and the stability of floral activators SPL3 and SEP3. J Exp Bot **74**: 864–877

Capovilla G, Schmid M, Posé D (2014) Control of flowering by ambient temperature. J Exp Bot 66: 59–69

Capovilla, Giovanna, Efthymia Symeonidi, Rui Wu MS (2017) Contribution of major FLM isoforms to temperature-dependent flowering in *Arabidopsis thaliana*. J Exp Bot **68**: 5117–5127

Carter B, Bishop B, Ho KK, Huang R, Jia W, Zhang H, Pascuzzi PE, Deal RB, Ogas J (2018) The chromatin remodelers PKL and PIE1 act in an epigenetic pathway that determines H3K27me3 homeostasis in *Arabidopsis*. Plant Cell **30**: 1337–1352

Chakrabortee S, Kayatekin C, Newby GA, Mendillo ML, Lancaster A, Lindquist S (2016) Luminidependens (LD) is an *Arabidopsis* protein with prion behavior. Proc Natl Acad Sci USA **113**: 6065–6070

Chang P, Hsieh HY, Tu SL (2022) The U1 snRNP component RBP45d regulates temperature-responsive flowering in *Arabidopsis*. Plant Cell **34**: 834–851

Chen SL, Rooney TJ, Hu AR, Beard HS, Garrett WM, Mangalath LM, Powers JJ, Cooper B, Zhang XN (2019) Quantitative proteomics reveals a role for SERINE/ARGININE-Rich 45 in regulating RNA metabolism and modulating transcriptional suppression via the ASAP complex in *Arabidopsis thaliana*. Front Plant Sci **10**: 460337

Chhun T, Chong SY, Park BS, Wong ECC, Yin JL, Kim M, Chua NH (2016) HSI2 Repressor recruits MED13 and HDA6 to down-regulate seed maturation gene expression directly during Arabidopsis early seedling growth. Plant Cell Physiol **57**: 1689–1706

Cho HJ, Kim JJ, Lee JH, Kim W, Jung JH, Park CM, Ahn JH (2012) SHORT VEGETATIVE PHASE (SVP) protein negatively regulates *miR172* transcription via direct binding to the *pri-miR172a* promoter in *Arabidopsis*. FEBS Lett **586**: 2332–2337

Deal RB, Topp CN, McKinney EC, Meagher RB (2007) Repression of flowering in *Arabidopsis* requires activation of *FLOWERING LOCUS C* expression by the histone variant H2A.Z. Plant Cell **19**: 74–83

Dong OX, Meteignier L-V, Plourde MB, Ahmed B, Wang M, Jensen C, Jin H, Moffett P, Li X, Germain H (2016) *Arabidopsis* TAF15b localizes to RNA processing bodies and contributes to snc1-mediated autoimmunity. Mol Plant-Microbe Interact **29**: 247–257

Duc C, Sherstnev A, Cole C, Barton GJ, Simpson GG (2013) Transcription termination and chimeric RNA formation controlled by *Arabidopsis thaliana* FPA. PLoS Genet **9**: e1003867

Eom H, Lee I (2018) Role of TAF15b in transcriptional regulation of autonomous pathway for flowering. Plant Signal Behav **13**: e1471300

Eom H, Park SJ, Kim MK, Kim H, Kang H, Lee I (2018) TAF15b, involved in the autonomous pathway for flowering, represses transcription of *FLOWERING LOCUS C*. Plant J **93**: 79–91

Fang X, Wang L, Ishikawa R, Li Y, Fiedler M, Liu F, Calder G, Rowan B, Weigel D, Li P, et al (2019) *Arabidopsis* FLL2 promotes liquid–liquid phase separation of polyadenylation complexes. Nature **569**: 265–269

Fang X, Wu Z, Raitskin O, Webb K, Voigt P, Lu T, Howard M, Dean C (2020) The 3' processing of antisense RNAs physically links to chromatin-based transcriptional control. Proc Natl Acad Sci USA **117**: 15316–15321

Farrona S, Hurtado L, March-Díaz R, Schmitz RJ, Florencio FJ, Turck F, Amasino RM, Reyes JC (2011) Brahma is required for proper expression of the floral repressor *FLC* in *Arabidopsis*. PLoS ONE **6**: e17997

Feng, Wei, Yannick Jacob, Kira M. Veley, Lei Ding, Xuhong Yu, Goh Choe SDM (2011) Hypomorphic alleles reveal FCA-independent roles for FY in the regulation of *FLOWERING LOCUS C*. Plant Physiol **155**: 1425–1434

Fernández V, Takahashi Y, Le Gourrierec J, Coupland G (2016) Photoperiodic and thermosensory pathways interact through CONSTANS to promote flowering at high temperature under short days. Plant J **86**: 426–440

Forbes KP, Addepalli B, Hunt AG (2006) An *Arabidopsis* Fip1 homolog interacts with RNA and provides conceptual links with a number of other polyadenylation factor subunits. J Biol Chem **281**: 176–186

Gómez-Zambrano Á, Crevillén P, Franco-Zorrilla JM, López JA, Moreno-Romero J, Roszak P, Santos-González J, Jurado S, Vázquez J, Köhler C, et al (2018) *Arabidopsis* SWC4 binds DNA and recruits the SWR1 complex to modulate histone H2A.Z deposition at key regulatory genes. Mol Plant **11**: 815–832

Gu X, Jiang D, Yang W, Jacob Y, Michaels SD, He Y (2011) *Arabidopsis* homologs of retinoblastoma-associated protein 46/48 associate with a histone deacetylase to act redundantly in chromatin silencing. PLoS Genet **7**: e1002366

Guan Q, Lu X, Zeng H, Zhang Y, Zhu J (2013) Heat stress induction of *miR398* triggers a regulatory loop that is critical for thermotolerance in *Arabidopsis*. Plant J **74**: 840–851

Gyula P, Baksa I, Tóth T, Mohorianu I, Dalmay T, Szittya G (2018) Ambient temperature regulates the expression of a small set of sRNAs influencing plant development through NF-YA2 and YUC2. Plant Cell Environ **41**: 2404–2417

Ha JH, Lee HJ, Jung JH, Park CM (2017) Thermo-induced maintenance of photo-oxidoreductases underlies plant autotrophic development. Dev Cell **41**: 170-179.e4

He Y (2009) Control of the transition to flowering by chromatin modifications. Mol Plant **2**: 554–564

He Y, Michaels SD, Amasino RM (2003) Regulation of flowering time by histone acetylation in *Arabidopsis*. Science **302**: 1751–1754

Helliwell CA, Wood CC, Robertson M, James Peacock W, Dennis ES (2006) The *Arabidopsis* FLC protein interacts directly in vivo with SOC1 and FT chromatin and is part of a high-molecular-weight protein complex. Plant J **46**: 183–192

Henderson IR, Liu F, Drea S, Simpson GG, Dean C (2005) An allelic series reveals essential roles for FY in plant development in addition to flowering-time control. Development **132**: 3597–3607

Hornyik C, Terzi LC, Simpson GG (2010) The Spen family protein FPA controls alternative cleavage and polyadenylation of RNA. Dev Cell **18**: 203–213

Hu H, Tian S, Xie G, Liu R, Wang N, Li S, He Y, Du J (2021) TEM1 combinatorially binds to FLOWERING LOCUS T and recruits a Polycomb factor to repress the floral transition in *Arabidopsis*. Proc Natl Acad Sci USA **118**: e2103895118

Huang W, Zhang L, Zhu Y, Chen J, Zhu Y, Lin F, Chen X, Huang J (2022) A genetic screen in *Arabidopsis* reveals the identical roles for RBP45d and PRP39a in 5' cryptic splice site selection. Front Plant Sci **13**: 1086506

Hunt A, Addepalli B (2008) The interaction between two *Arabidopsis* polyadenylation factor subunits involves an evolutionarily-conserved motif and has implications for the Assembly and function of the polyadenylation complex. Protein Pept Lett **15**: 76–88

Hurtado L, Farrona S, Reyes JC (2006) The putative SWI/SNF complex subunit BRAHMA activates flower homeotic genes in *Arabidopsis thaliana*. Plant Mol Biol **62**: 291–304

Jégu T, Latrasse D, Delarue M, Hirt H, Domenichini S, Ariel F, Crespi M, Bergounioux C, Raynaud C, Benhamed M (2014) The BAF60 subunit of the SWI/SNF chromatin-remodeling complex directly controls the formation of a gene loop at *FLOWERING LOCUS C* in *Arabidopsis*. Plant Cell **26**: 538–551

Jeon J, Kim J (2011) FVE, an *Arabidopsis* homologue of the retinoblastoma-associated protein that regulates flowering time and cold response, binds to chromatin as a large multiprotein complex. Mol Cells **32**: 227–234

Ji X, Liu W, Zhang F, Su Y, Ding Y, Li H (2023) H3K36me3 and H2A.Z coordinately modulate flowering time in *Arabidopsis*. J Genet Genomics. doi: 10.1016/J.JGG.2023.05.012

Jiang D, Yang W, He Y, Amasino RM (2007) *Arabidopsis* relatives of the human lysine-specific demethylase1 repress the expression of *FWA* and *FLOWERING LOCUS C* and thus promote the floral transition. Plant Cell **19**: 2975–2987

Jiang D, Wang Y, Wang Y, He Y (2008) Repression of *FLOWERING LOCUS C* and *FLOWERING LOCUS T* by the *Arabidopsis* Polycomb repressive complex 2 components. PLoS ONE **3**: e3404

Jin S, Kim SY, Susila H, Nasim Z, Youn G, Ahn JH (2022) FLOWERING LOCUS M isoforms differentially affect the subcellular localization and stability of SHORT VEGETATIVE PHASE to regulate temperature-responsive flowering in *Arabidopsis*. Mol Plant **15**: 1696–1709

Jing Y, Guo Q, Lin R (2019) The chromatin-remodeling factor PICKLE antagonizes Polycomb repression of FT to promote flowering. Plant Physiol **181**: 656–668

Jung JH, Seo PJ, Ahn JH, Park CM (2012) *Arabidopsis* RNA-binding protein FCA regulates microRNA172 processing in thermosensory flowering. J Biol Chem **287**: 16007–16016

Jung JH, Barbosa AD, Hutin S, Kumita JR, Gao M, Derwort D, Silva CS, Lai X, Pierre E, Geng F, et al (2020) A prion-like domain in ELF3 functions as a thermosensor in *Arabidopsis*. Nature **585**: 256–260

Kardailsky I, Shukla VK, Ahn JH, Dagenais N, Christensen SK, Nguyen JT, Chory J, Harrison MJ, Weigel D (1999) Activation tagging of the floral inducer FT. Science **286**: 1962–1965

Kennison JA, Tamkun JW (1988) Dosage-dependent modifiers of Polycomb and antennapedia mutations in Drosophila. Proc Natl Acad Sci USA **85**: 8136–8140

Kim HJ, Hyun Y, Park JY, Park MJ, Park MK, Kim MD, Kim HJ, Lee MH, Moon J, Lee I, et al (2004) A genetic link between cold responses and flowering time through FVE in *Arabidopsis thaliana.* Nat Genet 36: 167–171

Kim JJ, Lee JH, Kim W, Jung HS, Huijser P, Ahn JH (2012) The microRNA156-SQUAMOSA PROMOTER BINDING PROTEIN-LIKE3 module regulates ambient temperature-responsive flowering via FLOWERING LOCUS T in *Arabidopsis*. Plant Physiol **159**: 461–478

Krichevsky A, Gutgarts H, Kozlovsky S V., Tzfira T, Sutton A, Sternglanz R, Mandel G, Citovsky V (2007) C2H2 zinc finger-SET histone methyltransferase is a plant-specific chromatin modifier. Dev Biol **303**: 259–269

Kumar SV, Wigge PA (2010) H2A.Z-containing nucleosomes mediate the thermosensory response in *Arabidopsis*. Cell **140**: 136–147

Kumar SV, Lucyshyn D, Jaeger KE, Alós E, Alvey E, Harberd NP, Wigge PA (2012) Transcription factor PIF4 controls the thermosensory activation of flowering. Nature **484**: 242–245

Kyung J, Jeong D, Kim J, Kim J-S (2023) C-terminal domain phosphatase-Like 1 protein promotes flowering with TAF15b by repressing the floral repressor gene flowering locus C. Res Sq. doi: 10.21203/RS.3.RS-2457236/V1

Lee I, Aukerman MJ, Gore SL, Lohman KN, Michaels SD, Weaver LM, John MC, Feldmann KA, Amasino RM (1994) Isolation of *LUMINIDEPENDENS*: A gene involved in the control of flowering time in *Arabidopsis*. Plant Cell **6**: 75–83

Lee JH, Yoo SJ, Park SH, Hwang I, Lee JS, Ahn JH (2007) Role of SVP in the control of flowering time by ambient temperature in *Arabidopsis*. Genes Dev **21**: 397–402

Lee H, Yoo SJSK, Lee JH, Kim W, Yoo SJSK, Fitzgerald H, Carrington JC, Ahn JH (2010) Genetic framework for flowering-time regulation by ambient temperature-responsive miRNAs in *Arabidopsis*. Nucleic Acids Res **38**: 3081–3093

Lee JH, Ryu HS, Chung KS, Posé D, Kim S, Schmid M, Ahn JH (2013) Regulation of temperature-responsive flowering by MADS-box transcription factor repressors. Science **342**: 628–632

Lee HJ, Chung KS, Kim SK, Ahn JH. (2014) Post-translational regulation of SHORT VEGETATIVE PHASE as a major mechanism for thermoregulation of flowering. Plant Signal Behav **9**: e28193

Lee S, Lee HJ, Jung JH, Park CM (2015) The *Arabidopsis thaliana* RNA-binding protein FCA regulates thermotolerance by modulating the detoxification of reactive oxygen species. New Phytol **205**: 555–569

Lee KC, Chung KS, Lee HT, Park JH, Lee JH, Kim JK (2020) Role of *Arabidopsis* splicing factor SF1 in temperature-responsive alternative splicing of FLM pre-mRNA. Front Plant Sci **11**: 596354

Lee KC, Lee HT, Jeong HH, Park JH, Kim YC, Lee JH, Kim JK (2022) The splicing factor 1–FLOWERING LOCUS M module spatially regulates temperature-dependent flowering by modulating *FLOWERING LOCUS T* and *LEAFY* expression. Plant Cell Rep **41**: 1603–1612

Li, Dan; Liu, Chang; Shen, Lisha; Wu, Yang; Chen, Hongyan; Robertson, Masumi; Helliwell, Chris A; Ito, Toshiro; Meyerowitz, Elliot; Yu H (2008) A repressor complex governs the integration of flowering signals in *Arabidopsis*. Dev Cell **15**: 110–120

Li C, Chen C, Gao L, Yang S, Nguyen V, Shi X, Siminovitch K, Kohalmi SE, Huang S, Wu K, et al (2015) The *Arabidopsis* SWI2/SNF2 chromatin remodeler BRAHMA regulates Polycomb function during vegetative development and directly activates the flowering repressor gene SVP. PLoS Genet **11**: e1004944

Lim MH, Kim J, Kim YS, Chung KS, Seo YH, Lee I, Kim J, Hong CB, Kim HJ, Park CM (2004) A new *Arabidopsis* gene, FLK, encodes an RNA binding protein with K homology motifs and regulates flowering time via Flowering Locus C. Plant Cell **16**: 731–740

Liu F, Quesada V, Crevillé P, Bä Urle I, Swiezewski S, Dean C (2007) The *Arabidopsis* RNA-binding protein FCA requires a lysine-specific demethylase 1 homolog to downregulate FLC. Mol Cell **28**: 398–407

Liu F, Marquardt S, Lister C, Swiezewski S, Dean C (2010) Targeted 3' processing of antisense transcripts triggers *Arabidopsis* FLC chromatin silencing. Science **327**: 94–97

Liu F, Bakht S, Dean C (2012) Cotranscriptional role for *Arabidopsis* DICER-LIKE 4 in transcription termination. Science **335**: 1621–1623

Liu X, Yang Y, Hu Y, Zhou L, Li Y, Hou X (2018) Temporal-specific interaction of NF-YC and CURLY LEAF during the floral transition regulates flowering. Plant Physiol **177**: 105–114

Liu L, Zhang Y, Yu H (2020) Florigen trafficking integrates photoperiod and temperature signals in *Arabidopsis*. J Integr Plant Biol **62**: 1385–1398

Luo M, Tai R, Yu CW, Yang S, Chen CY, Lin WD, Schmidt W, Wu K (2015) Regulation of flowering time by the histone deacetylase HDA5 in *Arabidopsis*. Plant J **82**: 925–936

Luo X, Gao Z, Wang Y, Chen Z, Zhang W, Huang J, Yu H, He Y (2018) The NUCLEAR FACTOR-CONSTANS complex antagonizes Polycomb repression to de-repress *FLOWERING LOCUS T* expression in response to inductive long days in *Arabidopsis*. Plant J **95**: 17–29

Luo X, Chen T, Zeng X, He D, He Y (2019) Feedback regulation of *FLC* by FLOWERING LOCUS T (FT) and FD through a 5' *FLC* promoter region in *Arabidopsis*. Mol Plant **12**: 285–288

Macknight R, Bancroft I, Page T, Lister C, Schmidt R, Love K, Westphal L, Murphy G, Sherson S, Cobbett C, et al (1997) *FCA*, a gene controlling flowering time in *Arabidopsis*, encodes a protein containing RNA-binding domains. Cell **89**: 737–745

Macknight R, Duroux M, Laurie R, Dijkwel P, Simpson G, Dean C (2002) Functional significance of the alternative transcript processing of the *Arabidopsis* floral promoter *FCA*. Plant Cell **14**: 877–888

Marín-González E, Matías-Hernández L, Aguilar-Jaramillo AE, Lee JH, Ahn JH, Suárez-López P, Pelaz S (2015) SHORT VEGETATIVE PHASE up-regulates *TEMPRANILLO2* floral repressor at low ambient temperatures. Plant Physiol **169**: 1214–1224

Marquardt S, Raitskin O, Wu Z, Liu F, Sun Q, Dean C (2014) Functional consequences of splicing of the antisense transcript *COOLAIR* on *FLC* transcription. Mol Cell **54**: 156

Michaels SD, Amasino RM (1999) FLOWERING LOCUS C encodes a novel MADS domain protein that acts as a repressor of flowering. Plant Cell **11**: 949–956

Mikulski P, Wolff P, Lu T, Nielsen M, Echevarria EF, Zhu D, Questa JI, Saalbach G, Martins C, Dean C (2022) VAL1 acts as an assembly platform co-ordinating co-transcriptional repression and chromatin regulation at Arabidopsis FLC. Nat Commun **13**: 1–12

Nakamura Y, Lin YC, Watanabe S, Liu Y chi, Katsuyama K, Kanehara K, Inaba K (2019) High-resolution crystal structure of *Arabidopsis* FLOWERING LOCUS T illuminates its phospholipid-binding site in flowering. iScience **21**: 577–586

Nibau C, Gallemí M, Dadarou D, Doonan JH, Cavallari N (2020) Thermo-sensitive alternative splicing of *FLOWERING LOCUS M* is modulated by cyclin-dependent kinase G2. Front Plant Sci **10**: 1–14

Pajoro A, Severing E, Angenent GC, Immink RGH (2017) Histone H3 lysine 36 methylation affects temperature-induced alternative splicing and flowering in plants. Genome Biol **18**: 1–12

Parker MT, Knop K, Zacharaki V, Sherwood A V., Tomé D, Yu X, Martin PGP, Beynon J, Michaels SD, Barton GJ, et al (2021) Widespread premature transcription termination of *Arabidopsis thaliana NLR* genes by the spen protein FPA. Elife **10**: 1–36

Pazhouhandeh M, Molinier J, Berr A, Genschik P (2011) MSI4/FVE interacts with CUL4-DDB1 and a PRC2-like complex to control epigenetic regulation of flowering time in *Arabidopsis*. Proc Natl Acad Sci USA **108**: 3430–3435

Picó S, Ortiz-Marchena MI, Merini W, Calonje M (2015) Deciphering the role of POLYCOMB REPRESSIVE COMPLEX1 variants in regulating the acquisition of flowering competence in *Arabidopsis*. Plant Physiol **168**: 1286–1297

Posé D, Verhage L, Ott F, Yant L, Mathieu J, Angenent GC, Immink RGH, Schmid M (2013) Temperature-dependent regulation of flowering by antagonistic FLM variants. Nature **503**: 414–417

Potok ME, Wang Y, Xu L, Zhong Z, Liu W, Feng S, Naranbaatar B, Rayatpisheh S, Wang Z, Wohlschlegel JA, et al (2019) *Arabidopsis* SWR1-associated protein methyl-CpG-binding domain 9 is required for histone H2A.Z deposition. Nat Commun **10**: 1–14

Press MO, Lanctot A, Queitsch C (2016) PIF4 and ELF3 act independently in *Arabidopsis thaliana* thermoresponsive flowering. PLoS ONE **11**: e0161791

Quesada, Victor, Richard Macknight, Caroline Dean, Gordon G. Simpson (2003) Autoregulation of FCA pre-mRNA processing controls *Arabidopsis* flowering time. EMBO J **22**: 3142–3152

Qi PL, Zhou HR, Zhao QQ, Feng C, Ning YQ, Su YN, Cai XW, Yuan DY, Zhang ZC, Su XM, et al (2022) Characterization of an autonomous pathway complex that promotes flowering in *Arabidopsis*. Nucleic Acids Res **50**: 7380–7395

Qüesta JI, Song J, Geraldo N, An H, Dean C (2016) *Arabidopsis* transcriptional repressor VAL1 triggers Polycomb silencing at *FLC* during vernalization. Science **353**: 485–488

Ripoll JJ, Rodríguez-Cazorla E, González-Reig S, Andújar A, Alonso-Cantabrana H, Perez-Amador MA, Carbonell J, Martínez-Laborda A, Vera A (2009) Antagonistic interactions between *Arabidopsis* K-homology domain genes uncover PEPPER as a positive regulator of the central floral repressor *FLOWERING LOCUS C*. Dev Biol **333**: 251–262

Samach A, Onouchi H, Gold SE, Ditta GS, Schwarz-Sommer Z, Yanofsky MF, Coupland G (2000) Distinct roles of constans target genes in reproductive development of *Arabidopsis*. Science **288**: 1613–1616

Sarnowski TJ, Świezewski S, Pawlikowska K, Kaczanowski S, Jerzmanowski A (2002) AtSWI3B, an *Arabidopsis* homolog of SWI3, a core subunit of yeast Swi/Snf chromatin remodeling complex, interacts with FCA, a regulator of flowering time. Nucleic Acids Res **30**: 3412–3421

Sarnowski TJ, Rios G, Jásik J, Świezewski S, Kaczanowski S, Li Y, Kwiatkowska A, Pawlikowska K, Koźbiał M, Koźbiał P, et al (2005) SWI3 subunits of putative SWI/SNF chromatin-remodeling complexes play distinct roles during *Arabidopsis* development. Plant Cell **17**: 2454–2472

Schon M, Baxter C, Xu C, Enugutti B, Nodine MD, Dean C (2021) Antagonistic activities of cotranscriptional regulators within an early developmental window set *FLC* expression level. Proc Natl Acad Sci USA **118**: e2102753118

Scortecci KC, Michaels SD, Amasino RM (2001) Identification of a MADS-box gene, *FLOWERING LOCUS M*, that represses flowering. Plant J **26**: 229–236

Searle I, He Y, Turck F, Vincent C, Fornara F, Kröber S, Amasino RA, Coupland G (2006) The transcription factor FLC confers a flowering response to vernalization by repressing meristem competence and systemic signaling in Arabidopsis. Genes Dev **20**: 898–912

Shen Y, Lei T, Cui X, Liu X, Zhou S, Zheng Y, Guérard F, Issakidis-Bourguet E, Zhou D (2019) *Arabidopsis* histone deacetylase HDA15 directly represses plant response to elevated ambient temperature. Plant J **100**: 991–1006

Simpson GG, Dijkwel PP, Quesada V, Henderson I, Dean C (2003) FY is an RNA 3′ end-processing factor that interacts with FCA to control the *Arabidopsis* floral transition. Cell **113**: 777–787

Sonmez C, Bäurle I, Magusin A, Dreos R, Laubinger S, Weigel D, Dean C (2011) RNA 3′ processing functions of *Arabidopsis* FCA and FPA limit intergenic transcription. Proc Natl Acad Sci USA **108**: 8508–8513

Steffen A, Elgner M, Staiger D (2019) Regulation of flowering time by the RNA-binding proteins AtGRP7 and AtGRP8. Plant Cell Physiol **60**: 2040–2050

Sun Q, Csorba T, Skourti-Stathaki K, Proudfoot NJ, Dean C (2013) R-loop stabilization represses antisense transcription at the *Arabidopsis FLC* locus. Science **340**: 619–621

Susila H, Jurić S, Liu L, Gawarecka K, Chung KS, Jin S, Kim S-J, Nasim Z, Youn G, Suh MC, et al (2021) Florigen sequestration in cellular membranes modulates temperature-responsive flowering. Science **373**: 1137–1142

Swiezewski S, Liu F, Magusin A, Dean C (2009) Cold-induced silencing by long antisense transcripts of an *Arabidopsis* Polycomb target. Nature **462**: 799–802

Tao Z, Shen L, Liu C, Liu L, Yan Y, Yu H (2012) Genome-wide identification of SOC1 and SVP targets during the floral transition in *Arabidopsis*. Plant J **70**: 549–561

Tian Y, Zheng H, Zhang F, Wang S, Ji X, Xu C, He Y, Ding Y (2019) PRC2 recruitment and H3K27me3 deposition at *FLC* require FCA binding of *COOLAIR*. Sci Adv **5**: eaau7246

Tong M, Lee K, Ezer D, Cortijo S, Jung J, Charoensawan V, Box MS, Jaeger KE, Takahashi N, Mas P, et al (2020) The evening complex establishes repressive chromatin domains via H2A.Z deposition. Plant Physiol **182**: 612–625

Torres ES, Deal RB (2019) The histone variant H2A.Z and chromatin remodeler BRAHMA act coordinately and antagonistically to regulate transcription and nucleosome dynamics in *Arabidopsis*. Plant J **99**: 144–162

Wang C, Tian Q, Hou Z, Mucha M, Aukerman M, Olsen OA (2007) The *Arabidopsis thaliana AtPRP39-1* gene, encoding a tetratricopeptide repeat protein with similarity to the yeast pre-mRNA processing protein PRP39, affects flowering time. Plant Cell Rep **26**: 1357–1366

Wang ZW, Wu Z, Raitskin O, Sun Q, Dean C (2014) Antisense-mediated *FLC* transcriptional repression requires the P-TEFb transcription elongation factor. Proc Natl Acad Sci USA **111**: 7468–7473

Wang Z, Kang J, Armando Casas-Mollano J, Dou Y, Jia S, Yang Q, Zhang C, Cerutti H (2021) MLK4-mediated phosphorylation of histone H3T3 promotes flowering by transcriptional silencing of FLC/MAF in *Arabidopsis thaliana*. Plant J **105**: 1400–1412

Weber CM, Ramachandran S, Henikoff S (2014) Nucleosomes are context-specific, H2A.Z-modulated barriers to RNA polymerase. Mol Cell **53**: 819–830

Woude LC van der, Perrella G, Snoek BL, Hoogdalem M van, Novák O, Verk MC van, Kooten HN van, Zorn LE, Tonckens R, Dongus JA, et al (2019) HISTONE DEACETYLASE 9 stimulates auxin-dependent thermomorphogenesis in *Arabidopsis thaliana* by mediating H2A.Z depletion. Proc Natl Acad Sci USA **116**: 25343–25354

Wu, Keqiang, Lin Zhang, Changhe Zhou, Chun-Wei Yu VC (2008) HDA6 is required for jasmonate response, senescence and flowering in *Arabidopsis*. J Exp Bot **59**: 225–234

Xing D, Zhao H, Xu R, Li QQ (2008a) *Arabidopsis* PCFS4, a homologue of yeast polyadenylation factor Pcf11p, regulates *FCA* alternative processing and promotes flowering time. Plant J **54**: 899–910

Xing H, Vanderford NL, Sarge KD (2008b) The TBP–PP2A mitotic complex bookmarks genes by preventing condensin action. Nat Cell Biol 10: 1318–1323

Xu L, Zhao Z, Dong A, Soubigou-Taconnat L, Renou J-P, Steinmetz A, Shen W-H (2008) Di- and tri- but not monomethylation on histone H3 lysine 36 marks active transcription of genes involved in flowering time regulation and other processes in *Arabidopsis thaliana*. Mol Cell Biol **28**: 1348–1360

Xu Y, Guo C, Zhou B, Li C, Wang H, Zheng B, Ding H, Zhu Z, Peragine A, Cui Y, et al (2016) Regulation of vegetative phase change by SWI2/SNF2 chromatin remodeling ATPase BRAHMA. Plant Physiol **172**: 2416–2428

Xu C, Wu Z, Duan HC, Fang X, Jia G, Dean C (2021a) R-loop resolution promotes co-transcriptional chromatin silencing. Nat Commun **12**: 1–9

Xu Y, Li Q, Yuan L, Huang Y, Hung FY, Wu K, Yang S (2021b) MSI1 and HDA6 function interdependently to control flowering time via chromatin modifications. Plant J **10**: 1–13

Xue M, Zhang H, Zhao F, Zhao T, Li H, Jiang D (2021) The INO80 chromatin remodeling complex promotes thermomorphogenesis by connecting H2A.Z eviction and active transcription in *Arabidopsis*. Mol Plant **14**: 1799–1813

Yan Y, Shen L, Chen Y, Bao S, Thong Z, Yu H (2014) A MYB-domain protein EFM mediates flowering responses to environmental cues in *Arabidopsis*. Dev Cell **30**: 437–448

Yan Z, Jia J, Yan X, Shi H, Han Y (2017) *Arabidopsis* KHZ1 and KHZ2, two novel non-tandem CCCH zinc-finger and K-homolog domain proteins, have redundant roles in the regulation of flowering and senescence. Plant Mol Biol **95**: 549–565

Yan Z, Shi H, Liu Y, Jing M, Han Y (2019) KHZ1 and KHZ2, novel members of the autonomous pathway, repress the splicing efficiency of *FLC* pre-mRNA in *Arabidopsis*. J Exp Bot **71**: 1375–1386

Yin X, Romero-Campero FJ, de Los Reyes P, Yan P, Yang J, Tian G, Yang XZ, Mo X, Zhao S, Calonje M, et al (2021) H2AK121ub in Arabidopsis associates with a less accessible chromatin state at transcriptional regulation hotspots. Nat Commun **12**: 1–12

Yoo SK, Chung KS, Kim J, Lee JH, Hong SM, Yoo SJ, Yoo SY, Lee JS, Ahn JH (2005) CONSTANS activates *SUPPRESSOR OF OVEREXPRESSION OF CONSTANS 1* through FLOWERING LOCUS T to promote flowering in *Arabidopsis*. Plant Physiol **139**: 770–778

Yu CW, Liu X, Luo M, Chen C, Lin X, Tian G, Lu Q, Cui Y, Wu K (2011) HISTONE DEACETYLASE6 interacts with FLOWERING LOCUS D and regulates flowering in *Arabidopsis*. Plant Physiol **156**: 173–184

Yu CW, Chang KY, Wu K (2016) Genome-wide analysis of gene regulatory networks of the FVE-HDA6-FLD complex in *Arabidopsis*. Front Plant Sci **7**: 555

Yu Z, Lin J, Li QQ (2019) Transcriptome analyses of *FY* mutants reveal its role in mRNA alternative polyadenylation. Plant Cell **31**: 2332–2352

Yu X, Martin PGP, Zhang Y, Trinidad JC, Xu F, Huang J, Thum KE, Li K, Zhao SZ, Gu Y, et al (2021) The BORDER family of negative transcription elongation factors regulates flowering time in *Arabidopsis*. Curr Biol **31**: 5377-5384.e5

Yuan C, Hu Y, Liu Q, Xu J, Zhou W, Yu H, Shen L, Qin C (2023) MED8 regulates floral transition in *Arabidopsis* by interacting with FPA. Plant J **116**: 1234–1247

Yun J, Kim YS, Jung JH, Seo PJ, Park CM (2012) The AT-hook motif-containing protein AHL22 regulates flowering initiation by modifying *FLOWERING LOCUS T* chromatin in *Arabidopsis*. J Biol Chem **287**: 15307–15316

Zeng X, Gao Z, Jiang C, Yang Y, Liu R, He Y (2020) HISTONE DEACETYLASE 9 functions with Polycomb silencing to repress *FLOWERING LOCUS C* expression. Plant Physiol **182**: 555–565

Zhang Y, Gu L, Hou Y, Wang L, Deng X, Hang R, Chen D, Zhang X, Zhang Y, Liu C, et al (2015) Integrative genome-wide analysis reveals HLP1, a novel RNA-binding protein, regulates plant flowering by targeting alternative polyadenylation. Cell Res **25**: 864–876

Zhang D, Li Y, Zhang X, Zha P, Lin R (2016) The SWI2/SNF2 chromatin-remodeling ATPase BRAHMA regulates chlorophyll biosynthesis in *Arabidopsis*. Mol Plant **10**: 155–167

Zhang XN, Shi Y, Powers JJ, Gowda NB, Zhang C, Ibrahim HMM, Ball HB, Chen SL, Lu H, Mount SM (2017) Transcriptome analyses reveal SR45 to be a neutral splicing regulator and a suppressor of innate immunity in *Arabidopsis thaliana*. BMC Genomics **18**: 1–17

Zhang Y, Li Z, Chen N, Huang Y, Huang S (2020) Phase separation of *Arabidopsis* EMB1579 controls transcription, mRNA splicing, and development. PLoS Biol **18**: e3000782

Zhang Y, Fan S, Hua C, Teo ZWN, Kiang JX, Shen L, Yu H (2022) Phase separation of HRLP regulates flowering time in *Arabidopsis*. Sci Adv **8**: 5488

Zheng S, Hu H, Ren H, Yang Z, Qiu Q, Qi W, Liu X, Chen X, Cui X, Li S, et al (2019) The *Arabidopsis* H3K27me3 demethylase JUMONJI 13 is a temperature and photoperiod dependent flowering repressor. Nature **10**: 1–11

Zhou JX, Liu ZW, Li YQ, Li L, Wang B, Chen S, He XJ (2018) *Arabidopsis* PWWP domain proteins mediate H3K27 trimethylation on *FLC* and regulate flowering time. J Integr Plant Biol **60**: 362–368

Figure 1.1 Thermosensory and Autonomous repression of *FLC*. In heat-induced transcriptional repression of *FLC*, TAF15b complexes with CPL1 and DCP1 via LLPS to dephosphorylate RNA Pol II Ser5p. During *COOLAIR* transcript elongation, BDR and FPA cause Pol II pausing and an R-loop forms, stabilized by NDX and bound by VAL1. VALI recruits the PRC1 to ubiquitinate H2A and VAL1/VAL2 recruit HDACs. The ASAP complex (SAP18, ACINUS and SR45) also recruit the HDAC. Replisome stalling enables recruitment of the AuPC (FLD, FY, SDG26, LD, EFL2, EFL4 and APRF1) to halt H3K36me and H3K4me and recruit the HDAC. FCA, FY, FLL2, MTA, FPA, CstF64, CstF77, FIP1 and PRP8 clear the R-loop, adding a poly(A) tail to *COOLAIR*. The HDAC complex, consisting of FLD, FVE, MSI5, HDA5, HDA6, and HDA9, remove H2/H3ac and FVE, MSI5, LHP1, PDP1/2/3 recruit the PRC2. BRM prevents H2A.Z occupancy, enabling deposition of H3K27me3 by the PRC2. Proteins in green are recognized as autonomous pathway components. Majenta arrows indicate recruitment and magenta ovals indicate protein complexes.

Thermosensory and Autonomous repression of *FLC*

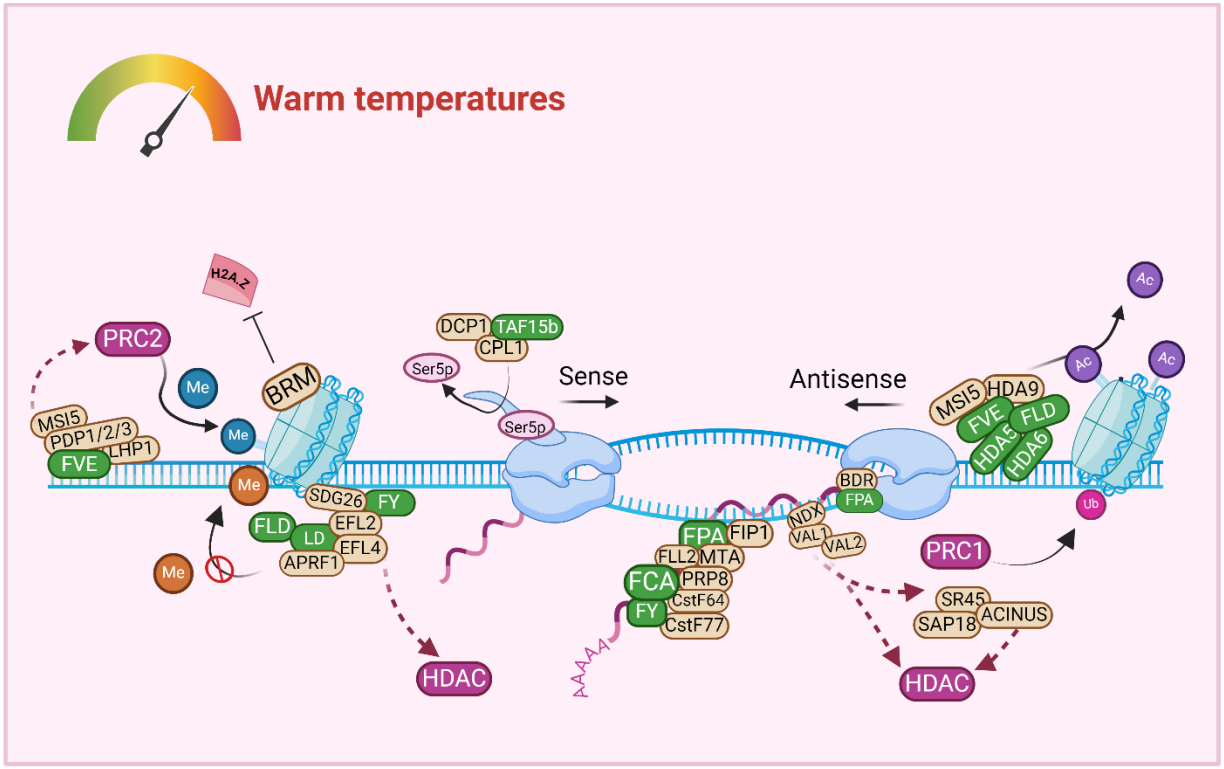

Figure 1.2 Thermosensory repression and activation of *FT*. Under cool temperatures, AHL22 recruits HDACs HDA19, HDA6 and HDA9 to deacetylate and SWC4 recruits PIE1 for H2A.Z deposition. PIE1, PKL and CLF act in H3K27me3 and FLM-β complexes with SVP. While *miR156* degrades *SPL3*, *miR169* degrades NF-YA2 and FT is sequestered in companion cell lipid membranes. Upon warming, H2A.Z is evicted, enabling binding and activation by PIF4. *FT* expression is also activated by the NF-Y complex and SPL3, and PKL and ATX1 facilitate activating H3K4me3. FCA acts in *miR172* maturation and *miR172* targets *AP2*, *TOE1/2/3*, *SNZ* and *SMZ*. While the nonfunctional FLM-δ isoform dominates, FVE and FCA act to repress *SVP* expression and *SVP* is degraded. FT is also released from companion cell lipid membranes. Autonomous pathway proteins are marked in green. Recruitment is marked by the magenta arrow, and protein complexes are marked by the magenta ovals

Thermosensory repression and activation of *FT*

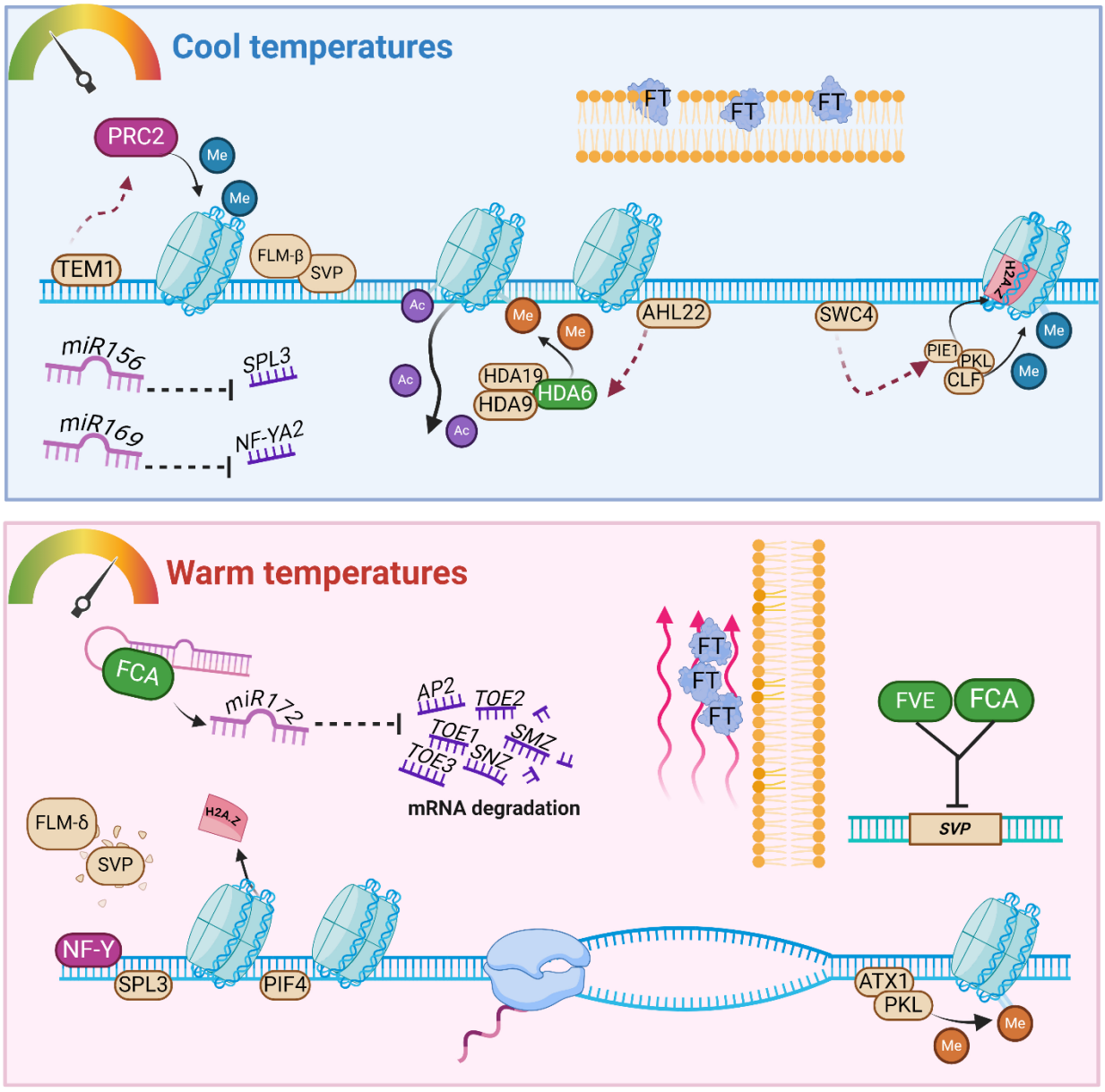

CHAPTER 2

AN IMPROVED METHOD FOR AGROBACTERIUM-MEDIATED GENETIC TRANSFORMATION OF ROMAINE, LEAF, AND BUTTERHEAD TYPES OF LETTUCE (LACTUCA SATIVA L.)

Abstract

In spite of the achievements in lettuce transformation and regeneration, there remains a genotype dependence upon the ability to efficiently transform and regenerate lettuce plants. In the present study, we have successfully developed an optimized *Agrobacterium*-mediated transformation protocol for elite lettuce cultivars, which belong to the romaine, leaf, and butterhead cultivar types. We found that a plant growth regulator combination of 1-naphthaleneacetic acid (NAA; 0.10 mg/L) and 6-benzyladenine (BA; 0.25 mg/L), the use of cotyledons and the first true leaf as explants, and the use of hygromycin (15 mg/L) for transgenic plant selection worked well for seven out of the eleven tested cultivars, achieving a 24.3% – 100% transformation efficiency. These seven cultivars include two romaine-types, three leaf-types, and two butterhead-types, and marks the first successful genetic transformation of the romaine cvs. 'Kahu' and 'Rosalita', the leaf lettuces 'Red Sails' and 'Royal Oak Leaf', and the butterhead 'Lollo Biondo'. While our optimized protocol did not successfully regenerate plants in the remaining four cultivars, successive use of kanamycin selection (40 mg/L) with the same plant growth regulators resulted in 64.3% transformation efficiency in the butterhead-type 'Mariska'. Thus, our newly optimized protocols are applicable in elite lettuce cultivars for *Agrobacterium*-mediated genetic transformation and regeneration when using hygromycin or kanamycin for selection.

Introduction

Lettuce (*Lactuca sativa* L.) is a diploid (2*n* = 2x = 18) species within the Asteraceae family (Davey et al., 2007) and a popular vegetable for production and consumption in the United States and Europe. Lettuce cultivation does not come without challenges, however, as increasing global temperatures and the ever-present threat of biological stresses push demand for cultivars with improved stress adaptations. Even with the advent of indoor cultivation, the desire for new cultivars, ideally suited to diverse environments, remains an objective for lettuce breeders. The floral morphology of lettuce promotes cleistogamy, hindering breeding by sexual means, and wild lettuce relatives have a limited gene pool of desirable traits, necessitating trait improvement via biotechnological means (Davey et al., 2007; Curtis, 2006). Utilization of biotechnological methods such as CRISPR/Cas9-mediated gene editing, however, are dependent upon the ability to efficiently regenerate plants after genetic transformation, thus necessitating the continuous development of ideal transformation and regeneration protocols (Bull and Michelmore, 2022).

Much research has been published in lettuce for the expression of foreign genes and downregulation of endogenous genes (Dan et al., 2014; Dong et al., 2014; Davey et al., 2002). Successful practices have been developed for *Agrobacterium rhizogenes*-mediated hairy root transformation (Vojin et al., 2014; Matvieieva et al., 2012), transient vacuum-infiltration (Negrouk et al., 2005; Joh et al., 2005; Wroblewski et al., 2005), electroporation (Chupeau et al., 1989), polyethylene glycol (PEG)- (Lelivelt et al., 2005) and biolistic bombardment- (Kanamoto et al., 2006; Ichikawa et al, 2010) mediated plastid transformation, and stable *A. tumefaciens*-mediated nuclear transformation (Michelmore et al., 1987; Davey et al., 2007; Curtis, 2006). The amenability to tissue culture and transformation, together with a short life cycle and fully

sequenced genome, makes lettuce a model leafy species in research (Darqui et al., 2021; Reyes-Chin-Wo et al., 2017).

Although generic protocols have been developed for a broad range of lettuce cultivars, there remains genotype-dependence for lettuce transformation and regeneration and a broad range of transformation efficiency (13% – 97%) has been observed when using said protocols (Curtis, 2006; Curtis et al., 1994). Thus, a method ideal to one lettuce genotype may not be optimal for another, and further protocol development is beneficial to the regeneration and transformation of additional lettuce cultivars (Curtis et al., 1994; Curtis, 2006; Armas et al., 2017).

When developing any improved transformation or regeneration protocol, it is necessary to test a variety of cultivars (Davey et al., 2007). In the present work, a new transformation and regeneration protocol was developed through the study of eleven lettuce cultivars, 'Kahu', 'Rosalita', 'Red Sails', 'Green Wave', 'Royal Oak Leaf', 'Cocarde', 'Girelle', 'Cobham Green', 'Lollo Biondo', 'Bronze Mignonette', and 'Mariska'. These eleven cultivars belong to three of the seven main types of lettuce; romaine, leaf, butterhead, crisphead, latin, stem, and oilseed (Davey et al., 2007). The 'Kahu' and 'Rosalita' cultivars belong to the romaine-type, characterized by long, upright, oval dark green leaves (van de Wiel et al., 1998; Ampomah-Dwamena et al., 1997). The 'Red Sails', 'Green Wave', 'Royal Oak Leaf', and 'Cocarde' cultivars belong to the leaf-type with a loose rosette (Martínez-González et al., 2011; Davey et al., 2007; Dinant et al., 1997; Zhang and Conner, 1992). The 'Girelle', 'Cobham Green', 'Lollo Biondo', 'Bronze Mignonette', and 'Mariska' cultivars are butterhead-type with a loosely-formed rosette and soft leaves (Ampomah-Dwamena et al., 1997; Mazier et al., 2007; Dinant et al., 1997). The eleven lettuce cultivars utilized in this study were chosen based upon previous

demonstration of transformation or regeneration success. The ‘Green Wave’ cultivar has been successfully transformed with the *Arabidopsis thaliana HSP17.8* gene (Kim et al., 2013), the toxin B subunit from *Escherichia coli* towards the development of edible vaccines (Martínez-González et al., 2011), and a chloroplast-expressed fructose gene from cyanobacteria to enhance photosynthetic capacity (Ichikawa et al., 2010). Both ‘Cocarde’ and ‘Girelle’ cultivars have been used to express lettuce mosaic virus coat protein (Dinant et al., 1997), and the ‘Cobham green’ cultivar was utilized in the inaugural transformation of lettuce (Michelmore et al., 1987). The ‘Mariska’ cultivar has been used to express the *Tnt1* retrotransposon from tobacco (Mazier et al., 2007), to express *Green Fluorescent Protein* (*GFP*) and *β-glucuronidase* (*GUS*) reporter genes in transient agroinfiltration assays (Wroblewski et al., 2005), and to silence the downy mildew resistance gene *Resistance Gene Candidate2* (*RGC2*) by RNAi (Wroblewski et al., 2007).

In addition, studies have been undertaken to develop tissue culture regeneration methods on non-transformed tissue in the cultivars used in this work. For example, ‘Red Sails’ and ‘Bronze Mignonette’ were utilized to develop regeneration protocols from mature leaf and cotyledon explants (Seabrook and Douglass, 2003; Zhang and Conner, 1992). The cotyledons of the ‘Cobham Green’ cultivar were also subject to a regeneration study ahead of initial transformation attempts (Brown et al., 1986). Regeneration has also been carried out on cotyledons of ‘Rosalita’, ‘Royal Oak Leaf’, ‘Cobham Green’, ‘Lollo Biondo’, and ‘Bronze Mignonette’ (Ampomah-Dwamena et al., 1997), and on cotyledons of ‘Rosalita’, ‘Cobham Green’, and ‘Bronze Mignonette’ in a separate study (Hunter and Burritt, 2002).

In the present study, different plant growth regulators (PGRs) and selection antibiotics were studied in the aforementioned eleven cultivars towards the goal of optimizing transformation and regeneration methods. This work demonstrates that an optimized protocol

was developed for *Agrobacterium*-mediated transformation and regeneration of these lettuce cultivars.

Results

Test of the effects of PGRs on callus induction and shoot regeneration

We first sought to identify a media composition, specifically that of the plant growth regulators, that would favor shoot regeneration of the eleven lettuce cultivars in tissue culture. A review of shoot regeneration studies across lettuce cultivars indicated that a base callus induction media containing Murashige & Scoog (MS), 3% sucrose, and 2 g/L Gelzan^{TM} with a pH of 5.8 has been most effective (Davey et al., 2007). However, ideal plant growth regulator combinations and the success in regeneration were highly genotype-dependent (Gómez -Montes et al., 2015; Dong et al., 2014; Zhang and Conner, 1992). Using the same base callus induction media in the present work, a PGR trial was performed on the explants (non-transformed cotyledons and the first leaf) of 7-day-old seedlings of cv. 'Kahu' to identify the ideal PGR combination for callus induction and shoot regeneration. The PGR combinations and concentrations considered were derived from successful regeneration studies across the literature (**Table 1; S1; S2**). Nine different combinations with different auxins (indole-3-acetic acid (IAA) and 1-naphthaleneacetic acid (NAA)) and cytokinins (kinetin and 6-benzyladenine (BA)) were studied. The effects of PGRs were assessed on their ability to develop callus and the rate at which shooting occurred (**Figures 1; 2**).

As expected, tissue yellowing and senescence was observed in the control media without PGRs with non-transformed 'Kahu' explants (**Figure 1A**). The callus induction media #2 and #3 containing IAA (2.00 and 1.00 mg/L, respectively) and kinetin (1.00 and 0.5 mg/L, respectively)

exhibited bright green callus growth but limited shooting (**Figure 1B; 1C**). The callus induction media #4 ~ #6 contained the same concentration of NAA (0.05 mg/L) and increasing concentrations of BA (0.25 – 1.00 mg/L). While the media #4 calli appeared mostly green with some yellowing, the media #5 and #6 calli tended towards white and brown, indicating a reduction in health with increased concentration of BA (**Figure 1D – 1F**). Callus induction media #7 – #9 contained the same concentration of NAA (0.10 mg/L), also with increasing concentrations of BA (0.25 – 1.00 mg/L). Media #7 yielded mostly green and bright yellow calli with a visible shift in preference for shoot induction, while media #8 and #9 yielded white and brown callus, once again, with reduced shooting (**Figure 1G – 1I**).

We also measured callus yield, shoot number per plate, and the percentage of shoot-producing explants of non-transformed 'Kahu' on each media at 28 days after callus induction. We found that callus induction media #4 – #9, containing NAA and BA, yielded a significantly greater mass of calli per callus cluster than media #2 and #3 containing IAA and kinetin. However, no statistical difference was observed when concentrations of auxin or cytokinin differed between the NAA/BA media (#4 – #9) and the IAA/kinetin media (#2 and #3) (**Figure 2A**). When the number of shoots generated per media were scored, media #7 was the best, averaging 61.67 ± 13.58 shoots per plate (**Figure 2B**). It was also observed that the use of NAA and BA in the media (#5 – #9) was more successful at generating shoots than that of the IAA and kinetin media (#2 and #3). In addition, the average number of shoot-producing explants was assessed (**Figure 2C**). While several of the media resulted in shoot induction, media #7 yielded the greatest percentage of shoot-producing explants (70.37% ± 6.42%). As a result, callus induction media #7 was most successful in producing healthy callus and shoots in the 'Kahu' cultivar, and was thus used in the successive transformation work.

Antibiotic selection in shoot induction Media

At the same time, we also tested the effects of the antibiotics kanamycin and hygromycin on the selection of transformed and non-transformed lettuce tissues. The 'Kahu', 'Red Sails', and 'Girelle' cultivars were selected to represent the romaine, leaf, and butterhead types, respectively, for the antibiotic kill curve analysis. Kanamycin is most commonly used as a selective agent for the transformation of lettuce and has been tested thoroughly in an array of cultivars (Dong et al., 2014; Curtis, 2006), with the effective concentrations of the antibiotics varying from cultivar to cultivar in different studies. The most effective concentrations of kanamycin were 50 mg/L in cv. 'Cobham Green' (Michelmore et al., 1987), 50 and 100 mg/L in cv. 'South Bay' (Torres et al., 1993), and 100 – 250 mg/L in cv. 'Kayser' (Enomoto et al., 1990), although it was reported that 100 mg/L kanamycin was more efficient than 50 mg/L for genotype-independent transformation of lettuce (Curtis et al., 1994; Curtis, 2006). Hygromycin is a less commonly used antibiotic in selection of transformed lettuce tissues, but has also proven successful in selecting for positive transformants. For example, the most effective concentrations of hygromycin were 10 mg/L in cvs. 'Veronica' and 'Solan Kriti' (Dias et al., 2006; Sharma et al., 2022), 20 mg/L in cv. 'Chongchima' (Vanjildorj et al., 2005), and 15 mg/L in cv. 'Ahvaz' (Mohebodini et al., 2014). Together, these works indicate that differing kanamycin and hygromycin concentrations may be ideal dependent upon genotype.

As hygromycin has been used for the transformation of cv. 'Ahvaz' (Mohebodini et al., 2014), a romaine-type (Mousavi et al., 2013), hygromycin was chosen for the kill curve analysis in cv. 'Kahu' in the present study. We tested the effect of hygromycin with differing concentrations (0, 10, 15, 20, 25 mg/L) in two differing callus induction media (e.g., media #3

and #7) on non-transformed cotyledons and the first leaf of cv. ‘Kahu’ (**Table 2**). On media #3, no callus growth occurred at 20 and 25 mg/L hygromycin, while calli were proliferative at concentrations of 0 and 10 mg/L, and moderate callus growth was observed at 15 mg/L hygromycin. Similarly, bleaching and necrosis and no callus growth were observed at higher hygromycin concentrations (20 and 25 mg/L), while moderate proliferation was observed at reduced hygromycin concentrations (10 mg/L), and minimal proliferation was observed at 15 mg/L hygromycin on media #7. As a result, 15 mg/L hygromycin was used in the successive studies in order to avoid potential transgene escape at a lower hygromycin concentration.

As kanamycin has been used for the transformation in the leaf lettuce cv. ‘Cocarde’ (Dinant et al., 1997) and the butterhead cv. ‘Cobham Green’ (Ampomah-Dwamena et al., 1997; Michelmore et al., 1987), kanamycin was chosen for the kill curve analysis on both transformed and untransformed tissue of ‘Red Sails’ (a leaf-type) and ‘Girelle’ (a butterhead-type) on callus induction media #3 in the present study. Concentrations of 0, 40, 80, 120, and 200 mg/L kanamycin were tested, and a visual assessment was performed (**Table 2**). When no antibiotics were used, a strong proliferation of callus and shooting was observed in both cultivars. Kanamycin concentrations of 120 mg/L and greater led to total necrosis of untransformed tissues with transformed tissues retaining some greenness but showing no callus growth (data not shown). While minimal callus growth was observed in transformed tissues of both cultivars at 80 mg/L kanamycin, no growth was observed in non-transformed tissues. When non-transformed ‘Red Sails’ was under 40 mg/L kanamycin selection, no growth was observed, while minimal-to-moderate callus growth was observed in transformed tissues. The ‘Girelle’ cultivar fared similarly, showing minimal-to-no growth in non-transformed tissue and moderate proliferation under 40 mg/L kanamycin selection (data not shown). As a result, 40 mg/L kanamycin was the

lowest concentration to kill off untransformed tissues and was used in the successive transformation studies.

Agrobacterium-mediated stable transformation of the tested lettuce cultivars

To conduct *Agrobacterium*-mediated stable transformation of the selected cultivars, *Agrobacterium* strain, co-cultivation time, explant type, seedling age, and rooting media from published literature were used as reference (**Table S1**). As LBA4404 has been the most favored *Agrobacterium* strain for lettuce transformation (Enomoto et al., 1990; Curtis, 2006) and the GV3101 strain has also been popular in lettuce transformation (Fallah-Ziarani et al., 2013; Liu et al., 2006; Paez-Valencia et al., 2013), both strains were chosen for the present study, with the assumption that they would have a similar effect on transformation efficiency here. The GV3101 strain was used with the pGFP-GUSPlus plasmid (hygromycin selection) containing the *35S:eGFP* and *35S:GUSPlus* reporter genes and the LBA4404 strain was used with the pGUSPlus plasmid (kanamycin selection) containing *35S:GUSPlus*. The *GUSPlus* reporter gene contains an intron, allowing GUS expression only in eukaryotic cells (Ohta et al., 1990; Vancanneyt et al., 1990; Liu et al., 2011; Huang et al., 2023). The working concentrations of both strains were a 1:10 dilution of *Agrobacterium* cells from a concentration of OD_{600} 1.1 – 1.6, as reported in Curtis et al. (1994). Also, due to the enhanced efficiency observed under short co-cultivation periods in the literature (Enomoto et al., 1990; Torres et al., 1993), a 2-day co-cultivation period was utilized in the present study.

As most studies indicated that cotyledons from 3–7-day-old seedlings were the ideal explants for transformation (Dong et al., 2014; Song et al., 2014), the cotyledons and the first leaf from seedlings 6 or 7 days after seeding were utilized as explants for transformation in the

present study. PGR-free rooting media was used to facilitate root development after transformation, as it was reported that the media producing the greatest root regeneration (up to 85%) was an MS base with sucrose and selective antibiotics alone, while the addition of auxin reduced the efficiency to 0% – 10% (Fallah-Ziarani et al., 2013).

We first tested the use of 15 mg/L hygromycin for *Agrobacterium*-mediated stable transformation on the explants from 25 seedling of each of the eleven lettuce cultivars with the GV3101 strain containing pGFP-GUSPlus plasmid. Utilizing our optimized lettuce transformation method as stated above, a wide array of success was observed (**Table 3**). We found that hygromycin selection worked successfully for the two romaine-type cultivars 'Kahu' and 'Rosalita'. In cv. 'Kahu', a 40.0% regeneration efficiency was realized with 10 plants regenerated. Half (50.0%) of the regenerated plants were positive for the *GUS* expression as detected by histological GUS staining and PCR amplification. Thirty-seven plants were regenerated in cv. 'Rosalita' with a 152.0% regeneration efficiency, while a mere 24.3% of them were GUS-positive, indicating a requirement for higher antibiotic concentration in future transformations.

We also observed that hygromycin selection worked well for three of the four leaf-type cultivars (**Table 3**). The 'Red Sails' cultivar produced 54 regenerants with a 212.0% regeneration efficiency, 69.8% of which were GUS-positive. The 'Green Wave' and 'Royal Oak Leaf' cultivars also delivered a 60.0% and 80.0% regeneration efficiency, respectively, with 100.0% and 50.0% of them positive for GUS, respectively. However, no plants were regenerated from the 'Cocarde' cultivar.

Unfortunately, hygromycin selection showed reduced success in the butterhead-type cultivars (**Table 3**). Limited regeneration and transformation efficiencies were realized for the

‘Cobham Green’ and ‘Lollo Biondo’ cultivars. In ‘Cobham Green’, 2 plants were regenerated with a regeneration efficiency of 8.0%, half of which were GUS-positive. In ‘Lollo Biondo’, 7 plants were regenerated (28.0% efficiency) with 71.4% of them positive for GUS. However, plants were not regenerated in the other three cultivars ‘Girelle’, ‘Bronze Mignonette’, and ‘Mariska’. Thus, the hygromycin selection or regeneration media was not ideal for the butterhead cultivars studied in the present work.

Next, we tested the effects of 40 mg/L kanamycin selection in one butterhead cultivar ‘Mariska’ by transforming it with the pGUSPlus plasmid, with cv. ‘Kahu’ for comparison (**Table 3**). In ‘Kahu’, 10 plants were regenerated, with a 32% regeneration efficiency and 42.9% transformation efficiency, similar to its performance under hygromycin selection. Unlike its performance under hygromycin selection, success was observed in the ability to regenerate plants from cv. ‘Mariska’ under kanamycin selection, with 15 regenerated plants and a 60% regeneration efficiency, 64.29% of them being GUS-positive. This study indicates that kanamycin selection may be preferential for transgenic plant selection in the butterhead-type cultivars.

Discussion

The transformation of lettuce remains genotype dependent. Here, we developed an improved method for *Agrobacterium*-mediated genetic transformation for eight of eleven elite lettuce cultivars of the romaine, leaf, and butterhead cultivar types. Various factors affect lettuce transformation and regeneration success, including *Agrobacterium* strain and concentration, co-cultivation time, explant tissue, antibiotic selection, and plant growth regulators.

The effects of *Agrobacterium* strain and concentration and co-cultivation period on lettuce transformation

While lettuce is not a natural host to *A. tumefaciens*, transformation attempts have been met with success (Michelmore et al., 1987). The most favored strain has been LBA4404, with its successful use in greater than 43 cultivars to date (Enomoto et al., 1990; Curtis, 2006). The GV3101 strain has also been commonly used in lettuce transformation (Fallah-Ziarani et al., 2013; Liu et al., 2006; Paez-Valencia et al., 2013), as well as EHA105 (Dias et al., 2006; Franklin et al., 2011; Pniewski et al., 2011; Vanjildorj et al., 2005; Ibrahim et al., 2017; Cui et al., 2011; Ren et al., 2011). Other strains including C58, EHA101, A208, GV3111, and GV2260 have been less commonly used in lettuce transformation (Chen et al., 2018; Park et al., 2005; Torres et al., 1993; Dinant et al., 1997; Michelmore et al., 1987; Mazier et al., 2007; Dubois et al., 2005). As the most favored *Agrobacterium* strains for lettuce transformation have been LBA4404 (Enomoto et al., 1990; Curtis, 2006) and GV3101 (Fallah-Ziarani et al., 2013; Liu et al., 2006; Paez-Valencia et al., 2013), both strains were utilized in the present study.

The concentration of *A. tumefaciens* cells is a critical component in the successful transformation of lettuce (Curtis et al., 1994). A study using an array of cultivars observed that a 1:10 dilution of *Agrobacterium* cells from a concentration of OD_{600} 1.1 – 1.6 yielded more transformed plants (Curtis et al., 1994). Thus, *Agrobacterium* concentration and dilution recommendations in Curtis et al. (1994) were followed for all transformations in the present study. In addition, the use of acetosyringone in lettuce transformation has been observed to add no benefit (Torres et al., 1993), so was not utilized in the present study.

The period of co-cultivation is also critical in enabling transformation by *A. tumefaciens*. When 1 - 5 days of co-cultivation were tested in the cultivar ‘South Bay’, transformation was

most successful using 3 or fewer days, as longer co-cultivation periods were observed to inhibit later shoot formation (Torres et al., 1993). When 2, 4, and 6 days of co-cultivation were tested in the cultivar 'Kayser', 2 days of co-cultivation was found to be the ideal period, while up to 5 days were effective in the leaf explant tissue of 'Cocarde' and 'Girelle' (Enomoto et al., 1990; Dinant et al., 1997). When 2, 3, and 4 days of co-cultivation were tested in the cultivar 'Solan Kriti', 3 days was found to be most efficient at generating transformants (Sharma et al., 2022). Due to the enhanced efficiency observed under shorter co-cultivation periods, a 2-day co-cultivation period was utilized in the current study.

Confounding effects of PGRs, antibiotic selection, and explant tissues

Regeneration alone has been attempted with different PGRs on the cultivars 'Rosalita', 'Royal Oak Leaf', Cobham Green', 'Lollo Biondo', and 'Bronze Mignonette' (Ampomah-Dwamena et al., 1997). In the regeneration study, the ideal media was defined to contain 0.1 mg/L IAA, 0.5 mg/L kinetin, and 0.05 mg/L zeatin, and the greatest regeneration ability was observed for 'Rosalita', 'Royal Oak Leaf', and 'Cobham Green' with 61%, 56%, and 60% of explants producing extensive calli, respectively (Ampomah-Dwamena et al., 1997). Limited success was observed with 'Lollo Biondo' and 'Bronze Mignonette', however, with 18 and 11% of explants producing extensive calli, respectively. The shoot development differed, with 'Rosalita' having the greatest success (55%), followed by 'Lollo Biondo' (50%), and 'Bronze Mignonette' (18%), and while 'Cobham Green' produced shoots (20%), it did not produce roots. In the present study, regeneration rates differed, with 'Rosalita' successfully regenerating plantlets at a rate of 152%, while 'Lollo Biondo' (28%) and 'Bronze Mignonette' (0%) exhibited reduced success, and shoots and roots were successfully regenerated in 'Cobham Green' (8%). In Ampomah-

Dwamena and coworkers (1997), ‘Royal Oak Leaf’ produced roots but did not yield shoots, indicating its recalcitrance to regeneration via the method utilized. In the present study, however, an 80% regeneration efficiency was achieved in ‘Royal Oak Leaf’.

Similar work towards the development of the ideal PGR combination in shoot regeneration of untransformed tissue arrived at ~0.1 mg/L NAA and ~0.1 mg/L BA as the ideal combination when 15 cultivars were tested (Hunter and Burritt, 2002). Among the cultivars tested, ‘Rosalita’, ‘Cobham Green’, and ‘Bronze Mignonette’ generated the most shoots under this PGR combination, with 73%, 78%, and 62% of explants generating shoots, respectively (Hunter and Burritt, 2002). Overall, these works demonstrate the wide degree of success achievable in different cultivars under differing regeneration methods, and the results in the current study, utilizing a differing protocol, attests to that.

A study to identify the ideal PGR combination to utilize in cultivars recalcitrant to transformation (‘Red Romaine’ and ‘Bibb’) identified 0.1 mg/L IAA combined with 1 mg/L 2ip (N-6(2-isopentenyl)-adenine) in an initial media, followed by regeneration in media supplemented with 0.4 mg/L BA and 0.05 mg/L NAA (Lim et al., 2011). Work to regenerate the recalcitrant cultivar ‘Rutgers Scarlet Lettuce’ achieved success when activated charcoal was added to the media together with 10 mg/L BA and 0.5 mg/L NAA (Armas et al., 2017).

In the present work, PGR combinations for regeneration were tested on non-transformed ‘Kahu’. When combinations of differing concentrations of auxins (IAA and NAA) and cytokinins (kinetin and BA) were tested, the ideal combination of PGRs for shoot regeneration was determined to be 0.1 mg/L NAA and 0.4 mg/L BA. This PGR combination and concentration have been successfully utilized in work transforming the *Tα1* (*Thymosin α1*) into the lettuce cv. ‘Zhouye’ (Cui et al., 2011) and to express *Oryza sativa chitinase* in the lettuce cv.

‘Solan Kriti’ (Sharma et al., 2022). However, the ability to develop quality callus and subsequent shooting differs greatly when tissue is untransformed and under no selection, versus having been transformed and under selection, as was the case in the present study. This observation was made in initial transformation attempts with the ‘Cobham Green’ cultivar as well (Michemore et al., 1987). While the ideal PGR combinations were developed under no selection pressure, minimal regeneration was observed when kanamycin (50 mg/l) was present, thus the authors concluded that that antibiotic may be slowing development of transformed tissues and that cultivars showing favorable regeneration ability when not transformed may yet still be recalcitrant to transformation or may decline in regeneration when under selection (Michelmore et al., 1987). Therefore, further elucidation of the ideal PGR and antibiotic combinations across cultivars would be beneficial to achieve the greatest success across lettuce genotypes.

When differing concentrations of NAA (0.05 and 0.1 mg/L) and BA (0.1, 0.2, and 0.4 mg/L) were tested, the ideal combination for regeneration when paired with 20 mg/L kanamycin was 0.05 mg/L NAA and 0.4 mg/L BA, yielding up to 48% shooting (Fallah-Ziarani et al., 2013). Even still, the highest transformation efficiency achieved was 19%, when transforming an Iranian landrace with *GCHI* (*GTP cyclohydrolase I*) (Fallah-Ziarani et al., 2013). Similarly, when regeneration of transformed leaf tissues was examined with cultivars ‘Cocarde’, ‘Girelle’ and ‘Mariska’, the ideal PGR combination was found to be 0.3 mg/L BA and 0.3 mg/L IAA, yielding 50 to 75% regeneration when under kanamycin selection (200 mg/L), while transformation efficiency ranged between 12 and 33% (Dinant et al., 1997). While a similar regeneration percentage was observed in cv. ‘Mariska’ under kanamycin selection (60%) in the current study, no plants were regenerated from ‘Cocarde’, ‘Girelle’ or ‘Mariska’ under hygromycin selection. This serves to further indicate the role that selection antibiotics play in

confounding tissue regeneration efficiency, and suggests that successive transformation attempts with ‘Cocarde’ and ‘Girelle’ may find success under kanamycin selection, as was observed in cv. ‘Mariska’, with a 64.3% transformation efficiency (**Table 3**).

When PGRs were tested in transformed ‘Chongchima’ cotyledons under selection with 20-25 mg/L hygromycin, 0.05 mg/L kinetin, and 0.05 mg/L NAA, a success rate of 10.8% was achieved (Vanjildorj et al., 2005). Vanjildorj et al. (2005) noted the importance of the ratio of cytokinin to auxin (with a ratio of 5:1 – 10:1 being ideal) rather than the concentration alone. In the present study, the most successful PGR combination for cv. ‘Kahu’ was media #7, which provided a ratio of cytokinin to auxin of 2.5:1 (0.1 mg/L NAA and 0.25 mg/L BA; **Table 1**). It may be possible that the ideal ratio differs in the other tested cultivars and may approach the suggested 5:1 – 10:1 ratio as reported in Vanjildorj et al. (2005), and enhanced regeneration ability can be realized by further protocol development.

Commonly, rooting takes place in PGR-free media (Kim et al., 2006; Gómez -Montes et al., 2015; Curtis, 2006). Interestingly, when differing rooting media compositions were tested, the media producing the greatest root regeneration (up to 85%) was an MS base with just sucrose and selective antibiotics (Fallah-Ziarani et al., 2013). The addition of auxin to the media reduced the efficiency to between 0 and 10%. Thus, in the present study, to facilitate root development no PGRs were added to rooting media.

We found that one cultivar (‘Red Sails’) proved considerably amenable to the transformation and regeneration methods put forth in the present study, with a 212.0% regeneration rate and a nearly 70% transformation rate (**Table 3**). A previous regeneration study utilized IAA (0.1 mg/L), kinetin (0.5 mg/L), and zeatin (0.05 mg/L) in a Schenk and Hildebrandt media base, and observed 46% of cotyledon explants developing shoots (Zhang and Conner,

1992). When mature leaf explants were used, only 14% of explants produced somatic embryos in cv. ‘Red Sails’, although the explant tissue and regeneration PGRs (IAA and kinetin) differed (Seabrook and Douglass, 2003). Thus, the combination of NAA and BA, hygromycin selection, and the cotyledon and first leaf explants worked very efficiently for cv. ‘Red Sails’ in the present study.

While seedlings differing in age have been utilized as explant sources, cotyledons have been the most effective explants for plant regeneration (Davey et al., 2002; Davey et al., 2007; Bull and Michelmore, 2022). A review of lettuce transformation developments cited 2 - 4 days post-germination as the most productive tissue age for successful callus generation and shooting, and most studies indicated that cotyledons from 3 - 7-day-old seedlings were the ideal explant for transformation (Dong et al., 2014; Song et al., 2014). However, there remains a cultivar effect for this preference. A transformation experiment using ‘Cocarde’ and ‘Girelle’ cultivars observed that regeneration was slow and minimal when cotyledons were used as an explant, and leaf explants were used instead (Dinant et al., 1997). As no shoots were regenerated from either cultivar in the present work, this previous study may be one clue as to this failure; the explant tissue, and future endeavors towards transformation and regeneration in the ‘Cocarde’ and ‘Girelle’ cultivars should take this into consideration. While the cotyledons and first leaf from seedlings 6-7 days after planting were utilized as explants for transformation in the present study, favoring leaf explants in these cultivars may be preferable.

Using our optimized protocol, we have successfully achieved 24.3% – 100% transformation efficiency for seven of the eleven lettuce cultivars (**Table 3**). However, our optimized protocol with hygromycin selection was unsuccessful in the four remaining cultivars, ‘Cocarde’, ‘Girelle’, ‘Bronze Mignonette’, and ‘Mariska’, which had 0% regeneration and

transformation efficiency. The overall poor regeneration ability of 'Bronze Mignonette' was highlighted previously, however (Ampomah-Dwamena et al., 1997). Transformation of these four cultivars may benefit from additional protocol development in the form of an increased cytokinin to auxin ratio (Vanjildorj et al., 2005), the use of a different selection antibiotic (Dinant et al., 1997; Chupeau et al., 1989; Mazier et al., 2007), or different explant tissue (Dinant et al., 1997).

The effects of the *35S* promoter and *Agrobacterium* strains on transgene expression in lettuce

The relative ease of transformation and regeneration in lettuce is overshadowed by misexpression of foreign genes and lack of transmission into subsequent generations, as transgene expression has been reported to be inconsistent, depending upon cultivar (Darqui et al., 2021; Davey et al., 2002). The *35S* promoter has been shown to be effective in lettuce (Dong et al., 2014) and *GUS* is the most commonly used reporter gene for lettuce transformation (Curtis, 2006). However, when *35S:GUS* was used as a reporter in cv. 'Mariska', blue staining was observed only at the edges of leaf punches from transformed leaves (Mazier et al., 2007). A study looking at transformation efficiency with *35S:GUS* in 13 different cultivars also observed an array of intensity in GUS staining, indicating that there could be a cultivar-effect on the *35S* promoter (Curtis et al., 1994). The two plasmids used in the current study enabled confirmation of transgene expression in transformed tissues via histological GUS staining, and similar results were observed here as well, as anything from blue spotting to deep blue staining across the leaf disc was observed (**Figures 3B; 4B**), indicating a potential cultivar-effect in transgene expression driven by the *35S* promoter.

Agrobacterium strain dependence on *35S:GUS* expression has also been observed in transient infiltration assays when the cultivar ‘Mariska’ was used (Wroblewski et al., 2005). While the strain 15955 yielded small blue spots across leaf tissues, the strain C58C1 yielded strong blue staining throughout the tissue, and the GV3101 strain exhibited small-to-moderate blue spotting of the transformed leaf tissues. In the present study, however, the one cultivar (‘Kahu’) with plants regenerated from transformation with different *Agrobacterium* strains (GV3101 and LBA4404) and different plasmids (pGFP-GUSPlus and pGUSPlus) showed no apparent difference in *35S:GUS* expression (**Figure 4B**), although confounding variables precludes a true side-by-side comparison.

Conclusion

We have developed an optimized transformation protocol utilizing hygromycin selection for seven of the eleven tested lettuce cultivars, and this work marks the first successful genetic transformation of the romaine cultivars ‘Kahu’ and ‘Rosalita’, the leaf lettuces ‘Red Sails’ and ‘Royal Oak’ Leaf’, and the butterhead ‘Lollo Biondo’. While this newly developed protocol had limited success in the remaining four cultivars, utilization of kanamycin selection led to successful transformation and regeneration in one additional cultivar, ‘Mariska’. Further protocol optimization is needed to effectively transform the remaining cultivars.

Materials and Methods

Plant Materials and Growth Conditions

The seeds of the lettuce cultivars ‘Kahu’ (PI 251501), ‘Rosalita’ (PI 601592), ‘Green Wave’ (PI 566589), ‘Royal Oak Leaf’ (PI 595576), ‘Cocarde’ (PI 657644), ‘Girelle’ (PI 665186), ‘Cobham

Green' (PI 612637), 'Lollo Biondo' (PI 617944), 'Bronze Mignonette' (PI 615072), and 'Mariska' (PI 665196) were obtained from USDA-ARS-GRIN, while the seeds of the lettuce cultivar 'Red Sails' were obtained from Johnny's Selected Seeds. Seeds were surface-sterilized by immersion in 10% bleach for 30 min, followed by three rinses with sterile ddH_20 (Curtis et al., 1994). Seeds were germinated in high-top, 9 cm, petri plates (13 seeds/plate) containing ½ MS media base (Murashige and Skoog, 1962), supplemented with 10% sucrose and solidified with 2 g/L Gelzan^{TM} (PhytoTech Labs), pH 5.8. Seeds were incubated at 23 ℃, under a 16 h photoperiod (18 $\mu mol \cdot m^{-2} \cdot s^{-1}$) for 6-7 days until regeneration and/or transformation procedures took place (Dong et al, 2014).

Plant Growth Regulators

Based on the published studies in the transformation and regeneration of lettuce, nine different media compositions were tested for their ability to regenerate healthy callus and shoots from untransformed cotyledon and first leaf tissues. On the seventh day after planting, the cotyledons and first leaf of cv. 'Kahu' were excised, wounded on the abaxial side across the midrib, and plated (3 replicates, 7-8 explants per plate) onto media #1 ~ #9, all having an MS base, 3% sucrose, and 2 g/L Gelzan^{TM} with a pH 5.8: media #1, no plant growth regulators (control); media #2, 2 mg/L IAA and 1 mg/L kinetin; media #3, 1 mg/L IAA and 0.5 mg/L kinetin; media #4, 0.05 mg/L NAA and 0.25 mg/L BA; media #5, 0.05 mg/L NAA and 0.5 mg/L BA; media #6, 0.05 mg/L NAA and 1.0 mg/L BA; media #7, 0.1 mg/L NAA and 0.25 mg/L BA; media #8, 0.1 mg/L NAA and 0.5 mg/L BA; and media #9, 0.1 mg/L NAA and 1 mg/L BA. Plates were maintained under the same conditions as germination plates and were assessed for callus and shoot growth 28 days after induction.

Plant Antibiotic Selection

A kill curve was performed with hygromycin on 6- or 7-day-old untransformed cotyledons and the first true leaf of cv. 'Kahu' with differing concentrations of hygromycin (0, 10, 15, 20, 25 mg/L) on the callus-induction media #3 (1 mg/L IAA and 0.5 mg/L kinetin) and #7 (0.1 mg/L NAA and 0.25 mg/L BA). Each test consisted of 3 replicated plates with 7-8 cotyledons per plate.

A kanamycin kill curve was performed using varied concentrations (0, 40, 80, 120, 160, and 200 mg/L) of kanamycin on 6- or 7-day-old transformed (with pGUSPlus) and untransformed cotyledons and first leaves of cvs. 'Red Sails' and 'Girelle' in callus-induction media #3 (1 mg/L IAA and 0.5 mg/L kinetin). Each test consisted of 3 replicated plates with 7-8 cotyledons per plate.

Vector Construction

The pGUSPlus plasmid (kanamycin selection) was generated as follows. The *35S:GusPlus-NosT* fragment was extracted from the pZP35SGusPlus plasmid with the help of *Eco*RI and *Hind*III, and inserted into *Eco*RI- and *Hind*III-digested pCAMBIA2200 plasmid (**Figure 5**). Digestion products were purified from an agarose gel using the QIAquick® Gel Extraction Kit (QIAGEN). Ligation products were transformed into *E. coli* DH5α competent cells using the freeze-thaw method (Inoue et al., 1990). Colony PCR was performed with primers M13F and M13R (**Table 4**). Positive colonies were increased for plasmid extraction with the QIAprep® Spin Miniprep Kit (QIAGEN) for subsequent Sanger sequencing with the M13F primer. The pGUSPlus T-DNA

contains *GusPlus*™ under the control of the *35S* promoter with a *Nos* terminator and *Kan*^{R} kanamycin resistance under the control of *35S* and a CaMV poly(A) signal (**Figure 5**).

The pGFP-GUSPlus plasmid was obtained from Addgene (plasmid #64401; hygromycin selection), and contains *GUSPlus* under the control of the *35S* promoter with a *Nos* terminator, *eGFP* under the control of *35S* with a *Nos* terminator, and *HygR* under the control of *35S* with a CaMV pol(A) signal (**Figure 5**).

Agrobacterium-mediated lettuce transformation

The pGFP-GUSPlus and pGUSPlus plasmids were transformed into the GV3101 and LBA4404 strains of *A. tumefaciens*, respectively, using the freeze-thaw method (Weigel and Glazebrook, 2006). Transformed *A. tumefaciens* cells were then plated onto solid YEP supplemented with 100 mg/L rifampicin and 20 mg/L chloramphenicol or 50 mg/L kanamycin. Colony PCR with M13F and M13R primers was performed on the resulting colonies to check for the presence of the plasmids. A single PCR-positive *Agrobacterium* colony was selected for each plasmid, and increased in 3 mL liquid YEP supplemented with 100 mg/L rifampicin and selection antibiotics at 28 ℃ overnight. Then, a 200 µL aliquot was transferred to 20 mL YEP with the same antibiotics in an Erlenmeyer flask and grown on a shaker at 150 rpm in the dark at 28 ℃ for 16-24 h until the optical density at 600 nm (OD_{600}) reached 1.1 – 1.6. The cells were centrifuged (20 min, 5000g), and in a sterile hood the pellet was resuspended in 200 mL liquid MS media supplemented with 30 g/L sucrose to a final ratio of 1:10 (Curtis et al., 1994) for lettuce transformation.

Plant transformation procedures were adapted from Curtis et al. (1994). Cotyledons and the first leaf were excised from 6- or 7-day-old seedlings and wounded on the abaxial side with

shallow cuts across the midrib. Wounded tissues were stirred gently in the *Agrobacterium* suspension for 10 min, then blotted dry on sterile Whatman blotting paper and placed abaxial side-down on co-cultivation media, containing MS, 0.25 mg/L BA, 0.1 mg/L NAA, 30 g/L sucrose, 2 g/L Gelzan™ with a pH of 5.8 (~8 explants per dish, ~25 ml media per plate). Co-cultivation took place in the dark at 25 ℃ for two days. After co-cultivation, explants were moved to selective callus induction media containing MS, 30 g/L sucrose, 0.25 mg/L BA, 0.1 mg/L NAA, 400 mg/L timentin, 2 g/L Gelzan™, 40 mg/L kanamycin or 15 mg/L hygromycin (**Tables 1 – 2**) with a pH of 5.8 (~33 ml media/plate) and placed in a growth chamber (23 ℃, 16 h photoperiod, 18 $\mu mol \cdot m^{-2} \cdot s^{-1}$). Living tissues were sub-cultured every 14 days onto fresh media and observed for shoot formation. Regenerated shoots were excised and cultured onto rooting media (MS, 30 g/L sucrose, 2 g/L Gelzan™, 400 mg/L timentin, and 7.5 mg/L hygromycin or 20 mg/L kanamycin) in Magenta® GA-7 boxes (~50 ml/box), and maintained until roots developed. After rooting, plantlets were carefully removed from culture, gel media rinsed free, and potted into potting soil (Sungro Horticulture Sunshine® Mix #1). Plantlets were maintained in a humid environment under plastic domes for one week, for hardening off and subsequent testing.

PCR confirmation of the presence of the transgene

Regenerated T_0 plants were confirmed for the presence of the transgenes via PCR. DNA was extracted from leaf discs using the DNeasy Plant Kit (QIAGEN). PCR amplification for genotyping was performed with EmeraldAmp® MAX (Takara) DNA polymerase and utilized primers GusPlus-F and GusPlus-R spanning a 1 kb region of the *GUSPlus* cassette (**Table 4; Figures 3C; 4C**).

Histological GUS staining

Histological GUS staining was used to confirm the expression of the transgene in the regenerated T_0 plants using the procedure of Jefferson et al. (1987). Leaf punches (~1 cm) were incubated in X-Gluc stain (1 mM X-gluc, 50 mM NaH_2PO_4, pH 7.0) overnight (~16 h) at 37 ℃ in the dark. Samples were then washed in 70% ethanol, with wash being replaced every few hours to clear greenness and de-stain (Jefferson et al., 1987). Stained discs were then visually assessed for the presence of blue staining and representative photographs were taken (**Figure 3B, 4B**).

References

Ampomah-Dwamena C, Conner AJ, Fautrier AG, Ampomah-Dwamena C, Conner AJ, Fautrier AG (1997) Genotypic response of lettuce cotyledons to regeneration in vitro. Sci Hortic (Amsterdam) **71**: 137–145

Armas I, Pogrebnyak N, Raskin I (2017) A rapid and efficient in vitro regeneration system for lettuce (*Lactuca sativa* L.). Plant Methods **13**: 1–9

Bříza J, Růžičková N, Niedermeierová H, Dusbábková J, Vlasák J (2010) Phosphomannose isomerase gene for selection in lettuce (*Lactuca sativa* L.) transformation. Acta Biochim Pol **57**: 63–68

Brown C, Lucas JA, Crute IR, Walkey DGA, Power JB (1986) An assessment of genetic variability in somacloned lettuce plants (*Lactuca sativa*) and their offspring. Ann Appl Biol **109**: 391–407

Bull T, Michelmore R (2022) Molecular determinants of in vitro plant regeneration: Prospects for enhanced manipulation of lettuce (*Lactuca sativa* L.). Front Plant Sci **13**: 888425

Chen Z, Zhao W, Ge D, Han Y, Ning K, Luo C, Wang S, Liu R, Zhang X, Wang Q (2018a) LCM-seq reveals the crucial role of *LsSOC1* in heat-promoted bolting of lettuce (*Lactuca sativa* L.). Plant J **95**: 516–528

Chupeau MC, Bellini C, Guerche P, Maisonneuve B, Vastra G, Chupeau Y (1989) Transgenic plants of lettuce (*Lactuca sativa*) obtained through electroporation of protoplasts. Nat Biotechnol **7**: 503–508

Cui L, Chen Y, Shen G, Zhao L, Tang K (2011) Expression of bioactive thymosin alpha 1 (Tα1) in marker-free transgenic lettuce (*Lactuca sativa*). Plant Mol Biol Report **29**: 466–472

Curtis IS, Power JB, Blackhall NW, de Laat AMM, Davey MR (1994) Genotype-independent transformation of lettuce using *Agrobacterium tumefaciens*. J Exp Bot **45**: 1441–1449

Curtis IS, He C, Power JB, Mariotti D, de Laat A, Davey MR (1996) The effects of *Agrobacterium rhizogenes rolAB* genes in lettuce. Plant Sci 115: 123–135

Curtis IS (2006) Lettuce (*Lactuca sativa* L.). In: Wang K (ed) Methods Mol. Biol., 2nd ed. Humana Press, Totowa, NJ, pp 449–458

Darqui FS, Radonic LM, Beracochea VC, Hopp HE, López Bilbao M (2021) Peculiarities of the transformation of Asteraceae family species: The cases of sunflower and lettuce. Front Plant Sci **12**: 767459

Davey MR, McCabe MS, Mohapatra U, Power BJ (2002) Genetic manipulation of lettuce. In: George YHH, Khachatourians C, Hui YH, Scorza R, Nip W-K (eds) Transgenic Plants Crop. CRC Press, pp 612–634

Davey MR, Anthony P, van Hooff P, Power JB, Lowe KC (2007) Lettuce. Biotechnol Agric For. **59**: 221–249

Dias BBA, Cunha WG, Morais LS, Vianna GR, Rech EL, Capdeville G, Aragao FJL (2006) Expression of an oxalate decarboxylase gene from *Flammulina sp.* in transgenic lettuce (*Lactuca sativa*) plants and resistance to *Sclerotinia sclerotiorum*. Plant Pathol **55**: 187–193

Dinant S, Maisonneuve B, Albouy J, Chupeau Y, Chupeau M-CC, Bellec Y, Gaudefroy F, Kusiak C, Souche S, Robaglia C, et al (1997) Coat protein gene-mediated protection in *Lactuca sativa* against lettuce mosaic potyvirus strains. Mol Breed **3**: 75–86

Dong H, Zhao Y, Wang Y, Li H (2014) Recombinant proteins expressed in lettuce. Indian J Biotechnol **13**: 427–436

Dubois V, Botton E, Meyer C, Rieu A, Bedu M, Maisonneuve B, Mazier M (2005) Systematic silencing of a tobacco nitrate reductase transgene in lettuce (*Lactuca sativa* L.). J Exp Bot **56**: 2379–2388

Enomoto S, Itoh H, Ohshima M, Ohashi Y (1990) Induced expression of a chimeric gene construct in transgenic lettuce plants using tobacco pathogenesis-related protein gene promoter region. Plant Cell Rep **9**: 6–9

Fallah-Ziarani M, Haddad R, Garoosi G, Jalali M (2013) *Agrobacterium*-mediated transformation of cotyledonary leaf of lettuce (*Lactuca sativa* L.) by the *GCHI* gene. Iran J Genet Plant Breed **2**: 47–55

Frankin G, Oliveria AL, Dias ACP (2011) In vitro flowering and viable seed setting of transgenic lettuce cultures. Plant Biotechnol **28**: 63–68

Gómez-Montes EO, Oliver-Salvador C, Durán-Figueroa N, Badillo-Corona JA, Salas CE (2015) Optimization of direct shoot regeneration using cotyledonary explants and true leaves from lettuce cv. Romaine (*Lactuca sativa* L.) by surface response methodology. Plant Growth Regul **77**: 327–334

Huang D, Gao L, McAdams J, Zhao F, Lu H, Wu Y, Martin J, Sherif SM, Subramanian J, Duan H, Liu W (2023). Engineered cleistogamy in *Camelina sativa* for bioconfinement. Hortic Res **10:** uhac280.

Hunter DC, Burritt DJ (2002) Improved adventitious shoot production from cotyledon explants of lettuce (*Lactuca sativa* L.). Sci Hortic (Amsterdam) **95**: 269–276

Ibrahim AB, Monteiro TR, Cabral GB, Aragão FJL (2017) RNAi-mediated resistance to whitefly (*Bemisia tabaci*) in genetically engineered lettuce (*Lactuca sativa*). Transgenic Res **26**: 613–624

Ichikawa Y, Tamoi M, Sakuyama H, Maruta T, Ashida H, Yokota A, Shigeoka S (2010) Generation of transplastomic lettuce with enhanced growth and high yield. GM Crops **1**: 322–326

Inoue H, Nojima H, Okayama H (1990) High efficiency transformation of Escherichia coli with plasmids. Gene **96**: 23–28

Jefferson RA, Kavanagh TA, Bevan MW (1987) GUS fusions: beta-glucuronidase as a sensitive and versatile gene fusion marker in higher plants. EMBO J **6**: 3901–3907

Joh LD, Wroblewski T, Ewing NN, VanderGheynst JS (2005) High-level transient expression of recombinant protein in lettuce. Biotechnol Bioeng **91**: 861–871

Kanamoto H, Yamashita A, Asao H, Okumura S, Takase H, Hattori M, Yokota A, Tomizawa KI (2006) Efficient and stable transformation of *Lactuca sativa* L. cv. Cisco (lettuce) plastids. Transgenic Res **15**: 205–217

Kim JH, Botella JR (2004) Etr1-1 gene expression alters regeneration patterns in transgenic lettuce stimulating root formation. Plant Cell Tissue Organ Cult **78**: 69–73

Kim YS, Kim BG, Kim TG, Kang TJ, Yang MS (2006) Expression of a cholera toxin B subunit in transgenic lettuce (*Lactuca sativa* L.) using *Agrobacterium*-mediated transformation system. Plant Cell Tissue Organ Cult **87**: 203–210

Kim DH, Xu Z-YY, Hwang I (2013) *AtHSP17.8* overexpression in transgenic lettuce gives rise to dehydration and salt stress resistance phenotypes through modulation of ABA-mediated signaling. Plant Cell Rep **32**: 1953–1963

Lelivelt CLC, McCabe MS, Newell CA, De Snoo CB, Van Dun KMP, Birch-Machin I, Gray JC, Mills KHG, Nugent JM (2005) Stable plastid transformation in lettuce (*Lactuca sativa* L.). Plant Mol Biol **58**: 763–774

Lim W, Park J, Park S (2011) Re-evaluation of the effects of growth regulators on callus induction and shoot regeneration in *Agrobacterium*-mediated transformation of lettuce. Acta Physiol Plant **33**: 1631–1637

Liu S, Hu Y, Wang X, Zhong J, Lin Z (2006) High content of resveratrol in lettuce transformed with a stilbene synthase gene of *Parthenocissus henryana*. J Agric Food Chem **54**: 8082–8085

Liu CW, Chen JJ, Kang CC, Wu CH, and Yiu JC (2012) Transgenic lettuce (*Lactuca sativa* L.) expressing H1N1 influenza surface antigen (neuraminidase). Sci Hortic (Amsterdam) **139**: 8–13

Liu W, Mazarei M, Rudis MR, Fethe MH, Stewart CN (2011) Rapid in vivo analysis of synthetic promoters for plant pathogen phytosensing. BMC Biotechnol **11**: 1-9.

Martínez-González L, Rosales-Mendoza S, Soria-Guerra RE, Moreno-Fierros L, López-Revilla R, Korban SS, Guevara-Arauza JC, Alpuche-Solís ÁG (2011) Oral immunization with a lettuce-derived *Escherichia coli* heat-labile toxin B subunit induces neutralizing antibodies in mice. Plant Cell Tissue Organ Cult **107**: 441–449

Matvieieva NA, Shakhovskij AM, Kuchuk MV (2012) Features of lettuce transgenic plants with the *ifn-α2b* gene regenerated after *Agrobacterium rhizogenes*-mediated transformation. Cytol Genet **46**: 150–154

Mazier M, Botton E, Flamain F, Bouchet J-P, Courtial B, Chupeau M-C, Chupeau Y, Maisonneuve B, Lucas H (2007) Successful gene tagging in lettuce using the Tnt1 retrotransposon from tobacco. Plant Physiol **144**: 18–31

Michelmore R, Marsh E, Seely S, Landry B (1987) Transformation of lettuce (*Lactuca sativa*) mediated by *Agrobacterium tumefaciens*. Plant Cell Rep **6**: 439–442

Mohebodini M, Jalali-Javaran M, Mahboudi F, Alizadeh H (2011) Effects of genotype, explant age and growth regulators on callus induction and direct shoot regeneration of Lettuce (*Lactuca sativa* L.). Aust J Crop Sci 5: 92–95

Mohebodini M, Jalali-Javaran M, Alizadeh H, Mahboudi F, Yarbakht M (2014) *Agrobacterium*-mediated transformation of lettuce (*Lactuca sativa* L.) to express IgG-binding protein A and human pro-insulin as a fusion protein. J Hortic Sci Biotechnol **89**: 719–725

Mousavi SH, Hassandokht MR, Choukan R, Ghanbari A, Papini A (2013) Genetic diversity of Iranian lettuce (*Lactuca sativa* L) accessions revealed by cytological traits. Caryologia **66**: 41–48

Murashige T, Skoog F (1962) A revised medium for rapid growth and bioassay with tobacco tissue cultures. Physiol Plant **15**: 473–479

Negrouk V, Eisner G, Lee H Il, Han K, Taylor D, Wong HC (2005) Highly efficient transient expression of functional recombinant antibodies in lettuce. Plant Sci **169**: 433–438

Ohta S, Mita S, Hattori T, Nakamura K (1990) Construction and expression in tobacco of a β-glucuronidase (*GUS*) reporter gene containing an intron within the coding sequence. Plant Cell Physiol **31**: 805-13.

Paez-Valencia J, Sanchez-Lares J, Marsh E, Dorneles LT, Santos MP, Sanchez D, Winter A, Murphy S, Cox J, Trzaska M, et al (2013) Enhanced proton translocating pyrophosphatase activity improves nitrogen use efficiency in Romaine lettuce. Plant Physiol **161**: 1557–1569

Park BJ, Liu Z, Kanno A, Kameya T (2005) Increased tolerance to salt- and water-deficit stress in transgenic lettuce (*Lactuca sativa* L.) by constitutive expression of *LEA*. Plant Growth Regul **45**: 165–171

Pileggi M, Pereira AAM, Suva JDS, Pileggi SAV, Verma DPS (2001) An improved method for transformation of lettuce by *Agrobacterium tumefaciens* with a gene that confers freezing resistance. Brazilian Arch Biol Technol **44**: 191–196

Pniewski T, Kapusta J, Bociąg P, Wojciechowicz J, Kostrzak A, Gdula M, Fedorowicz-Strońska O, Wójcik P, Otta H, Samardakiewicz S, et al (2011) Low-dose oral immunization with lyophilized tissue of herbicide-resistant lettuce expressing hepatitis B surface antigen for prototype plant-derived vaccine tablet formulation. J Appl Genet **52**: 125–136

Ren W, Zhao L, Wang Y, Cui L, Tang Y, Sun X, Tang K (2011) Overexpression of homogentisate phytyltransferase in lettuce results in increased content of vitamin E. African J Biotechnol **10**: 14046–14051

Reyes-Chin-Wo S, Wang Z, Yang X, Kozik A, Arikit S, Song C, Xia L, Froenicke L, Lavelle DO, Truco M-J, et al (2017) Genome assembly with in vitro proximity ligation data and whole-genome triplication in lettuce. Nat Commun **8**: 14953

Seabrook JEA, Douglass LK (2003) Somatic embryogenesis of lettuce from mature tissues. Acta Hortic **625**: 217–223

Sharma S, Gautam N, Thakur AK, Srivastava DK (2022) Transgenic lettuce (*Lactuca sativa* L.) harboring chitinase gene expressed resistance against a devastating fungus, *Sclerotinia sclerotiorum*. Vegetos **36**: 1265–1274

Song D, Han Q, Dong Z, He Z (2014) Genetic transformation of lettuce (*Lactuca sativa*): A review. African J Biotechnol **13**: 1686–1693

Tennigkeit J, Matzura H (1991) Nucleotide sequence analysis of a chloramphenicol-resistance determinant from *Agrobacterium tumefaciens* and identification of its gene product. Gene **98**: 113–116

Torres AC, Cantliffe DJ, Laughner B, Bienick M, Nagata R, Ashraf M, Ferl RJ (1993) Stable transformation of lettuce cultivar South Bay from cotyledon explants. Plant Cell Tissue Organ Cult **34**:

Vafaee Y, Alizadeh H (2018) Heterologous production of recombinant anti-HIV microbicide griffithsin in transgenic lettuce and tobacco lines. Plant Cell Tissue Organ Cult **135**: 85–97

Van de Wiel C, Arens P, Vosman B (1998) Microsatellite fingerprinting in lettuce (*Lactuca sativa* L.) and wild relatives. Plant Cell Rep **17**: 837–842

Vancanneyt G, Schmidt R, O'Connor-Sanchez A, Willmitzer L, Rocha-Sosa M (1990) Construction of an intron-containing marker gene: splicing of the intron in transgenic plants and its use in monitoring early events in *Agrobacterium*-mediated plant transformation. Mol General Genet **220**: 245-50.

Vanjildorj E, Bae TW, Riu KZ, Kim SY, Lee HY (2005) Overexpression of Arabidopsis *ABF3* gene enhances tolerance to drought and cold in transgenic lettuce (*Lactuca sativa*). Plant Cell Tissue Organ Cult **83**: 41–50

Vojin T, Snežana M, Aleksandar C, Marija P, Milana T, Dragana A, Jovan T, Angelina S (2014) Production of hairy root cultures of lettuce (*Lactuca sativa* L.). Cent Eur J Biol **9**: 1196–1205

Weigel D, Glazebrook J (2006) Transformation of Agrobacterium Using the Freeze-Thaw Method. Cold Spring Harb Protoc 2006: pdb.prot4666

Webster DE, Smith SD, Pickering RJ, Strugnell RA, Dry IB, Wesselingh SL (2006) Measles virus hemagglutinin protein expressed in transgenic lettuce induces neutralising antibodies in mice following mucosal vaccination. Vaccine **24**: 3538–3544

Wroblewski T, Tomczak A, Michelmore R (2005) Optimization of *Agrobacterium*-mediated transient assays of gene expression in lettuce, tomato and Arabidopsis. Plant Biotechnol J **3**: 259–273

Wroblewski T, Piskurewicz U, Tomczak A, Ochoa O, Michelmore RW (2007) Silencing of the major family of NBS-LRR-encoding genes in lettuce results in the loss of multiple resistance specificities. Plant J **51**: 803–818

Zhang X, Conner AJ (1992) Genotypic effects on tissue culture response of lettuce cotyledons. J Genet Breed **46**: 287–290

Table 2.1 Plant growth regulator trial for callus induction and shoot regeneration from cotyledon and first leaf of the lettuce cv. 'Kahu'.

	Present Study		Published Studies		
Media	**Auxin (mg/L)**	**Cytokinin (mg/L)**	**Auxin (mg/L)**	**Cytokinin (mg/L)**	**References**
#1	0.00	0.00	N/A	N/A	
	IAA	**Kinetin**	**IAA**	**Kinetin**	
#2	2.00	1.00	5.60	0.68	[1]
#3	1.00	0.50	-	-	[2]
	NAA	**BA**	**NAA**	**BA**	
#4	0.05	0.25	0.05	0.20	[3 – 7]
#5	0.05	0.50	-	-	[8]
#6	0.05	1.00	-	-	[9]
#7	0.10	0.25	-	-	[10, 11]
#8	0.10	0.50	-	-	[12 – 15]
#9	0.10	1.00	0.10	2.00	[16]

[1] Kim and Botella (2004); [2] Michelmore et al. (1987); [3] Pniewski et al. (2011); [4] Torres et al. (1993); [5] Pileggi et al. (2001); [6] Ibrahim et al. (2017); [7] Vafaee and Alizadeh (2018); [8] Brown et al. (1986); [9] Armas et al. (2017); [10] Cui et al. (2011); [11] Sharma et al. (2022); [12] Kim et al. (2006); [13] Liu et al. (2006); [14] Ren et al. (2011); [15] Liu et al. (2012); [16] Armas et al. (2017). Dash, not tested.

Table 2.2 Visual scoring of callus induction of three lettuce cultivars on hygromycin and kanamycin media. +, minimal callus growth; ++, moderate callus growth; +++, strong callus growth; -, no callus growth; and --, no callus growth and necrosis.

Media	**Hygromycin (mg/L)**					**Cultivar**	**Lettuce Type**
#	**0**	**10**	**15**	**20**	**25**		
#3	+++	++	+	-	--	Kahu (N.T.)	Romaine
#7	++	++	+	--	--	Kahu (N.T.)	
Media	**Kanamycin (mg/L)**					**Cultivar**	**Lettuce Type**
#	**0**	**40**	**80**	**120**	**200**		
#3	+++	-	-	--	--	Red Sails (N.T.)	Leaf
#3	+++	+	+	-	-	Red Sails (T.)	
#3	++	-	-	--	--	Girelle (N.T.)	Butterhead
#3	++	++	+	-	-	Girelle (T.)	

N.T., non-transformed. T., transformed.

Table 2.3 Plant regeneration efficiency and transformation efficiency of the eleven lettuce cultivars. Regeneration efficiency (%) was calculated by dividing the number of regenerated lines by the number of initial seedlings used for transformation. Transformation efficiency (%) was calculated by dividing the number of GUS and PCR positive lines by the number of regenerated lines. Each treatment utilized 50 cotyledon/first leaf explants from 25, 6- or 7-day-old seedlings. For transgenic plant selection, pGFP-GUSPlus transformation utilized 15 mg/L hygromycin, and pGUSPlus transformation utilized 40 mg/L kanamycin.

Cultivar	Plasmid	Regenerated plants/ initial seedlings	Regeneration %	Transformation %
Kahu	pGFP-GUSPlus	10/25	40.0	50.0
Rosalita		38/25	152.0	24.3
Red Sails		53/25	212.0	69.8
Green Wave		15/25	60.0	100.0
Royal Oak Leaf		20/25	80.0	50.0
Cocarde		0/25	0.0	N/A
Girelle		0/25	0.0	N/A
Cobham Green		2/25	8.0	50.0
Lollo Biondo		7/25	28.0	71.4
Bronze Mignonette		0/25	0.0	N/A
Mariska		0/25	0.0	N/A
Kahu	pGUSPlus	8/25	32.0	42.9
Mariska		15/25	60.0	64.3

Table 2.4 Primers used in this study

Primer Name	Primer Sequence (5' > 3')
M13F	TGTAAAACGACGGCCAGT
M13R	CAGGAAACAGCTATGAC
GusPlus-F	GACTGACCATCGATGTCTATG
GusPlus-R	GCCGAAATCTGGAATGTTGGT

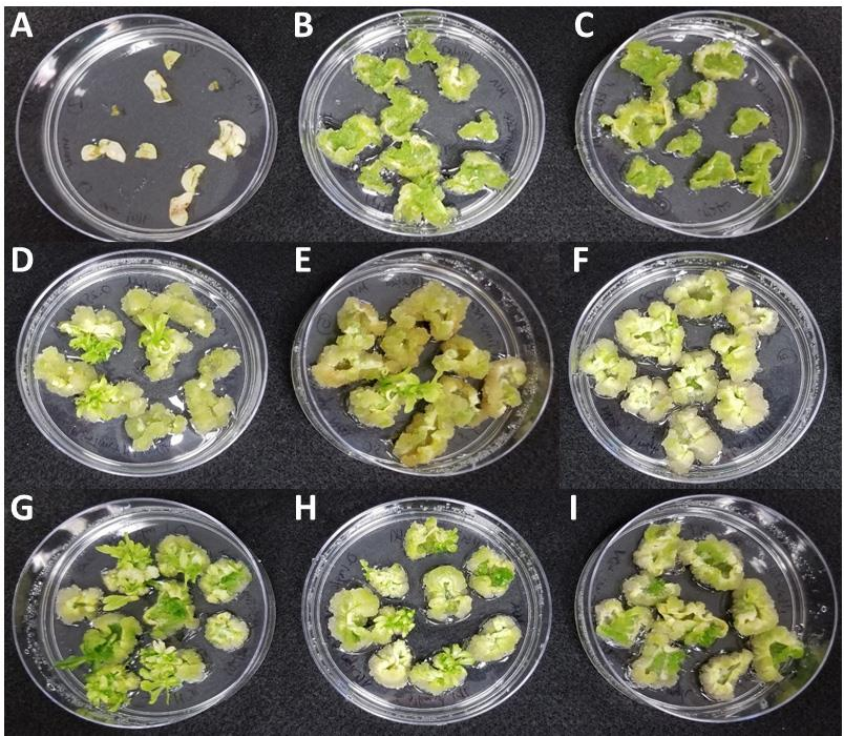

Figure 2.1 Representative images of the effects of plant growth regulators on callus induction and shoot regeneration from the cotyledon and first leaf explants of 6- or 7-day-old seedlings of lettuce cv. 'Kahu' at 28 days after callus induction. Media #1 (A), media #2 (B), media #3 (C), media #4 (D), media #5 (E), media #6 (F), media #7 (G), media #8 (H), media #9 (I) with PGR components as listed in (**Table 1**). Each plate is a representative of three replicates for each media.

Figure 2.2 The effects of plant growth regulators on callus induction (A), shoot regeneration (B), and the percentage of shoot-producing explants (C) from the cotyledon and first leaf explants of 6- or 7-day old seedlings of lettuce cv. 'Kahu' at 28 days after callus induction. Each value in (**A**) is based upon the average of 9 callus clusters for each treatment. Each value in (**B**) was based upon the average number of regenerated shoots per plate (n = 3) for each treatment. Each value in (**C**) is based upon the average percentage of shoot-developing explants per plate (9 explants/plate for 3 replicate plates) for each treatment. Error bars with compact letter display groupings (in A – B) represent significant differences based on one-way ANOVA ($p \leq 0.05$).

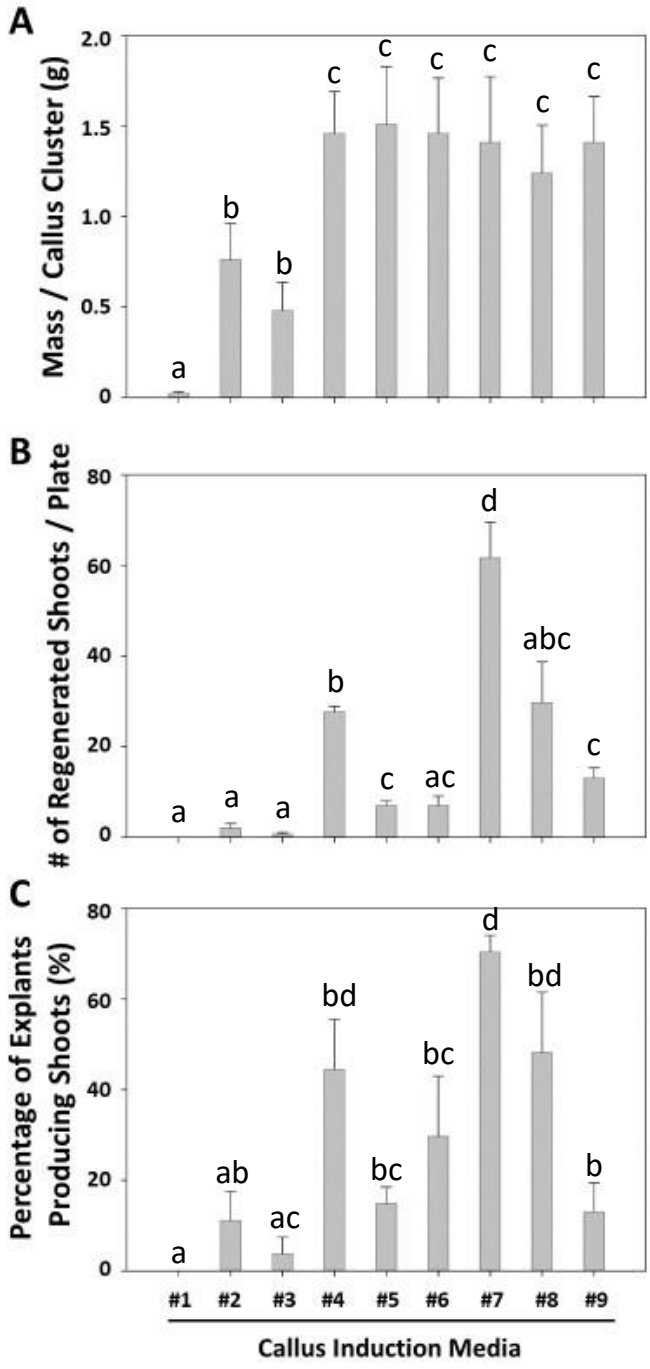
A
Mass / Callus Cluster (g)
2.0
1.5
1.0
0.5
0
a
b
b
c
c
c
c
c
c
B
# of Regenerated Shoots / Plate
80
60
40
20
0
a
a
a
b
c
ac
d
abc
c
C
Percentage of Explants Producing Shoots (%)
80
60
40
20
0
a
ab
ac
bd
bc
bc
d
bd
b
#1
#2
#3
#4
#5
#6
#7
#8
#9
Callus Induction Media

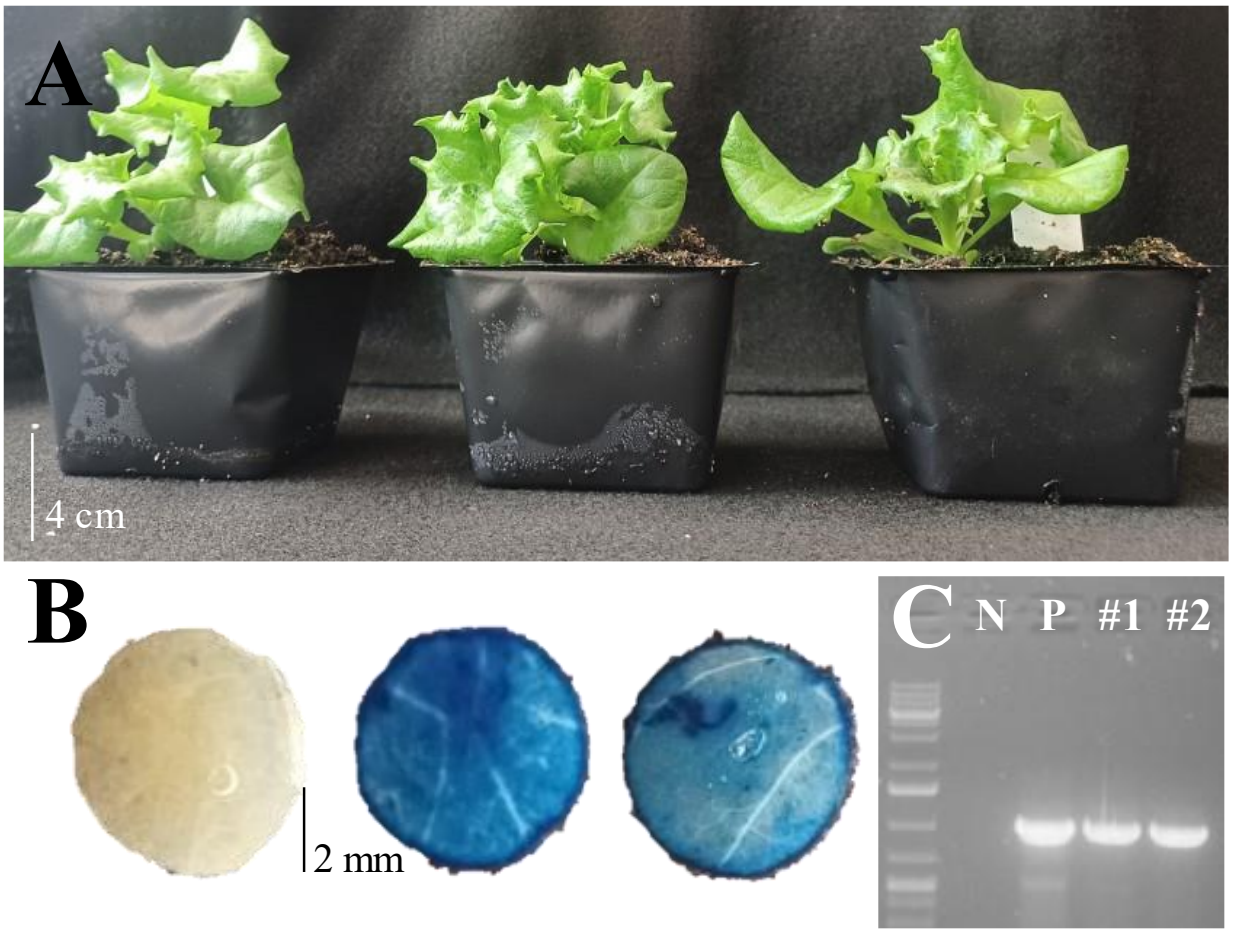

Figure 2.3 Representative images of T_1 cv. 'Red Sails' pGFP-GUSPlus (A), T_0 GUS staining (B) and T_0 PCR confirmation (C). Representative plants of cv. 'Red Sails' WT (left), cv. 'Red Sails' pGFP-GUSPlus line #1 (center), and 'Red Sails' pGFP-GUSPlus line #2 (right) positive for the transgene (A). Confirmation of transgene expression using histological GUS staining of leaf discs (B), with WT (left), cv. 'Red Sails' pGFP-GUSPlus line #1 (center) and cv 'Red Sails' pGFP-GUSPlus line #2 (right). PCR amplification of the *GUSPlus* gene with primers GusPlus-F and GusPlus-R (**Table 4**) spanning a 1 kb region of the *GUSPlus* cassette (C), with negative control (water, lane 2), positive control (pGFP-GUSPlus plasmid DNA, lane 3), cv. 'Red Sails' pGFP-GUSPlus line #1 (lane 4), and cv. 'Red Sails' pGFP-GUSPlus line #2 (lane 5).

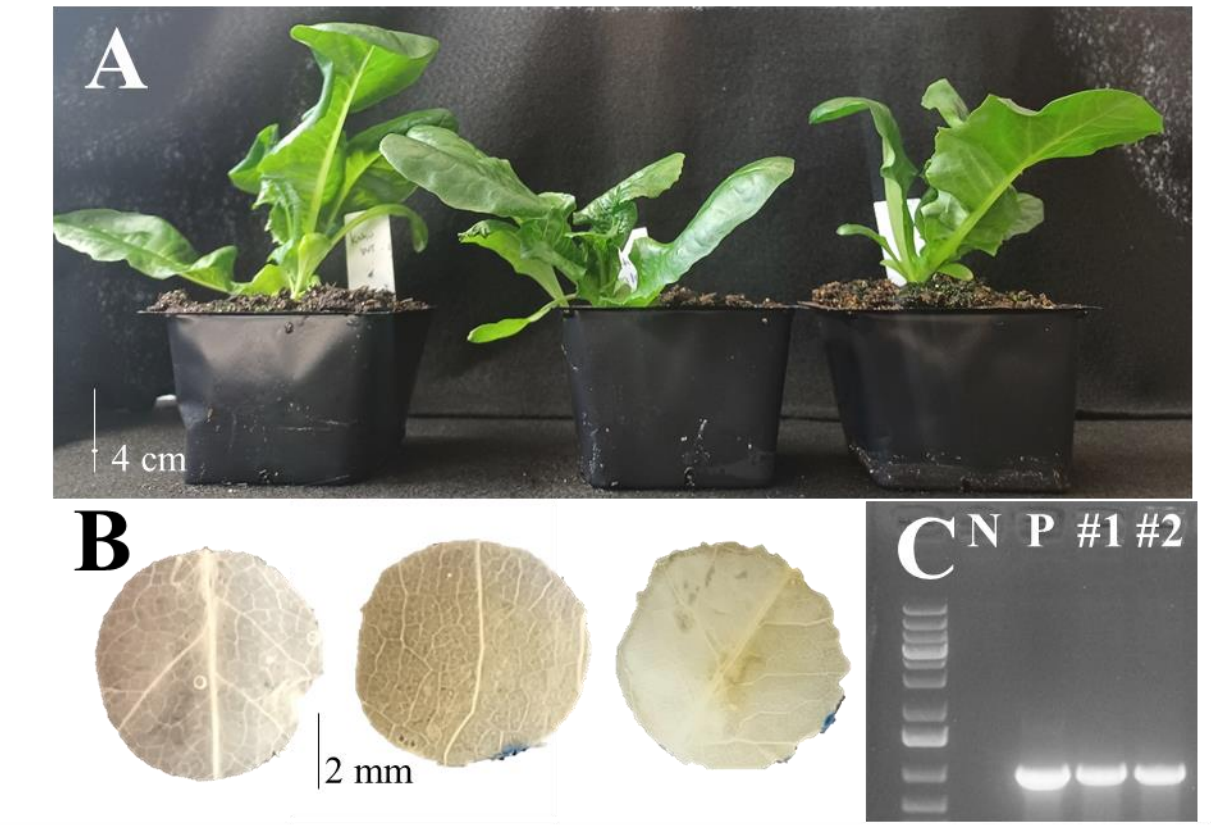

Figure 2.4 Representative images of T_1 cv. 'Kahu' pGUSPlus and pGFP-GUSPlus (A), T_0 GUS staining (B) and T_0 PCR confirmation (C). Representative plants of cv. 'Kahu' WT (left), cv. 'Kahu' pGUSPlus line #1 (center), and cv. 'Kahu' pGFP-GUSPlus line #1 (right) positive for the transgene (A). Confirmation of transgene expression using histological GUS staining of leaf discs (B), with WT (left), cv. 'Kahu' pGUSPlus line #1 (center) and cv 'Kahu' pGFP-GUSPlus line #2 (right). PCR amplification of the *GUSPlus* gene with primers GusPlus-F and GusPlus-R (**Table 4**) spanning a 1 kb region of the *GUSPlus* cassette (C), with negative control (water, lane 2), positive control (pGFP-GUSPlus plasmid DNA, lane 3), cv. 'Kahu' pGUSPlus line #1 (lane 4), and cv. 'Kahu' pGFP-GUSPlus line #2 (lane 5).

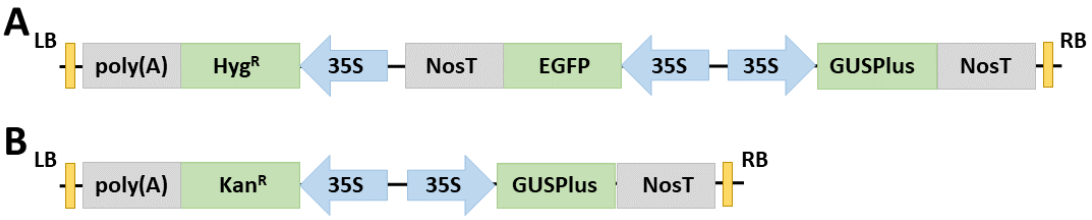

Figure 2.5 Scheme of the plasmids used in the present study. (**A**) The pGFP-GUSPlus plasmid containing *35S:HygR*, *35S:EGFP*, and *35S:GUSPlus*. (**B**) The pGUSPlus containing *35S:HygR* and *35S:GUSPlus*. LB, left border; RB, right border.

CHAPTER 3

GENE EDITING-ASSISTED GENERATION OF DELAYED BOLTING LETTUCE (LACTUCA SATIVA L.) FOR HIGH TEMPERATURE CONDITIONS

Abstract

Lettuce (*Lactuca sativa* L.) is a popular crop for cultivation and consumption, with the farming of lettuce increasing in popularity in recent years. With increased interest in this crop, growers are expanding into new cultivation systems, including indoor controlled-environment cultivation methods, such as greenhouses and vertical farms. Lettuce cultivation does not come without challenges, however, as increasing global temperatures push demand for cultivars with improved stress adaptations, and yield demands in indoor cultivation favor enhanced cultivation temperatures, in spite of the threat of premature bolting. Bolting reduces quality and makes the lettuce head unsalable, causing economic loss to growers. Thus, while climate change necessitates the development of crops adapted to warmer temperatures for field cultivation, so too can the breeding of crops for cultivation under new settings, such as controlled environments. Towards this goal, the primary objective of this work was to knockout floral promotion genes in lettuce to delay the onset of heat-induced bolting. CRISPR/Cas9 was utilized to target the endogenous lettuce genes, *LsFT*, *LsFLD* and *LsFCA* for editing, with the goal of delaying bolting in said warm environments. While bona fide editing of the target genes could not be confirmed, this effort produced lines with marked delays in lettuce bolting when cultivated under increased ambient temperatures, demonstrating its potential in future grower applications.

INTRODUCTION

Lettuce (*Lactuca sativa* L.) is a diploid (2n = 2x = 18) species within the Asteraceae family (Davey et al., 2007). Lettuce is a popular vegetable for production and consumption in the United States and Europe, and production area of lettuce and chicory in the U.S. has averaged over 100k ha since 1992, with yield per hectare steadily increasing (Davey et al., 2007; FAO, 2024). Lettuce is cultivated in an optimal temperature range of 15 – 20 ℃ and early bolting is induced at warmer temperatures (Ito et al., 1963; Hao et al., 2018). Bolting is the transition from vegetative to reproductive growth and is characterized by elongation of the stem, prior to floral bud differentiation (Hao et al., 2018). When bolting occurs, the lettuce head develops an undesirable appearance, a bitter flavor, a reduction in nutrients, and an overall decline in quality (Hao et al., 2018; Abbott, 2010). In lettuce production, being able to boost yield and predict harvest cycles is key. Because bolted plants are unsaleable and cause economic losses to growers, cultivar development to limit early bolting and lengthen the vegetative phase is a primary breeding objective (Leijten et al., 2018; Hao et al., 2018; Davey et al, 2007). Currently, controlled environment agricultural production utilizes cultivars developed for growth in the varied environments of fields and gardens (Folta, 2019). The advent of genetic modification technologies, like gene-editing offers a unique opportunity to tailor lettuce cultivars into those ideally suited for the challenges of indoor cultivation, which often differ vastly from those of outdoor cultivation (Folta, 2019). Thus, trait improvement via biotechnological means is a compelling strategy to combat high temperature-induced bolting in lettuce (Fukuda et al., 2016).

The transition to flowering is a complex process brought on by an array of environmental and endogenous signals. While several primary floral induction pathways have been defined in *Arabidopsis*, the intersection of the genes of the autonomous and thermosensory pathways were

of particular interest, considering the thermal induction of flowering observed in lettuce (Ito et al., 1963; Hao et al., 2018). Studies have been performed to identify genes in lettuce and across the Asteraceae, in the effort to investigate floral pathway preservation. Together, studies in sunflower (*Helianthus annuus L.*), New Zealand daisy (*Celmisia lyallii)*, chicory *(Cichorium intybus)*, chrysanthemum (*Chrysanthemum* sp.), *Cynara cardunculus* (cardoon), and lettuce reveal high conservation of autonomous and thermosensory floral pathways, indicating that studies in *Arabidopsis* can serve to inform gene function in species of the Asteraceae (Blackman et al., 2011; Samarth et al, 2021; Locascio et al., 2009; Nakano et al., 2015; Won et al., 2021; Puglia et al., 2015; Lavelle, 2009; Abbott, 2010).

FLOWERING LOCUS T (FT) is an active component of thermosensory flowering in *Arabidopsis*. Under warm ambient temperatures the mobile FT protein is transported from leaves to the shoot apex, to act in the promotion of flowering, while *ft* mutants are insensitive to temperature (Samach et al., 2000; Susila et al., 2021; Liu et al., 2020a; Balasubramanian et al., 2006). In lettuce, *LsFT* expression increases as plants cultivated under warm (35 ℃) temperatures transition to bolting (Fukuda et al., 2011), and *LsFT* expression is strongly induced in early bolting lines (Rosental et al., 2021; Fukuda et al., 2016). Overexpression of *LsFT* in *Arabidopsis ft* mutants complements the flowering phenotype, indicating its function is preserved across species (Abbott, 2010; Chen et al., 2018b).

Homologs to *AtFT* have been identified across species of the Asteraceae as well. In chicory, a parallel increase in *CiFT* expression was observed during heat-induced (38 ℃) floral initiation (Mathieu et al., 2020b), and in *C. lyallii*, significant upregulation of *ClFT* occurred after plants were exposed to high temperatures (Samarth et al., 2021). In *Chrysanthemum seticuspe*, the *AtFT* homolog *CsFTL3* was downregulated in response to enhanced temperatures

(30 ℃), as warm temperatures repress floral induction in this species (Nakano et al., 2015). In sunflower as well, the *Arabidopsis FT* homolog *HaFT,* was identified (Blackman et al., 2011).

Genes of the autonomous pathway promote flowering via repression of the potent floral repressor, *FLC*. FLC represses downstream floral activators *FT* and *SUPPRESSOR OF OVEREXPRESSION OF CONSTANS 1 (SOC1*) (He et al., 2003). Several main genes have been identified acting in the autonomous pathway in *Arabidopsis*, including *FLOWERING LOCUS D* (*FLD*), *FLOWERING CONTROL LOCUS A* (*FCA*), *FLOWERING LOCUS PA* (*FPA*), *FLOWERING LOCUS Y* (*FY*), *FLOWERING LOCUS VE* (*FVE*), *FLOWERING LOCUS K* (*FLK*), and *LUMINIDEPENDENS* (*LD*) (He et al., 2003), and autonomous pathway mutants are late flowering regardless of the photoperiod (Lee et al., 1994). *AtFLC* homologs have been identified in lettuce (Lavelle, 2009), cardoon (Puglia et al., 2015) sunflower (Blackman et al., 2011; Badouin et al., 2017) *Chrysanthemum nankingense* (Won et al., 2021), and *C. lyalli*, and increased expression of *ClFLC-like* was observed in vegetative plants (Samarth et al., 2021).

The RNA-binding protein, FLK, suppresses the splicing of functional *FLC* isoforms, and reduces the stability of *FLC* transcripts (Lim et al., 2004; Amara et al., 2023). In *C. lyallii*, *FLK* was strongly induced in plants prior to flowering (Samarth et al., 2021), and *LsFLK* is able to rescue the late-flowering of *Atflk* mutants, indicating functional preservation (Abbott, 2010). *AtFLK* homologs have also been identified in *Chrysanthemum morifolium* (Huang et al., 2021) and sunflower (Blackman et al., 2011; Badouin et al., 2017).

FCA, FPA and FY promote the proximal polyadenylation of *COOLAIR*, the antisense transcript of *FLC*, which enables subsequent deposition of repressive histone marks (Xu et al., 2021; Marquardt et al., 2014; Wang et al., 2014; Fang et al., 2020; Henderson et al., 2005; Yu et al., 2019; Simpson et al., 2003; Hornyik et al, 2010; Yuan et al., 2023). Homologs to *AtFCA*,

AtFPA, and *AtFY* have been identified in lettuce (Lavelle, 2009; Abbott, 2010), sunflower (Blackman et al., 2011; Badouin et al., 2017), and *C. lyallii* (Samarth et al., 2021), and an *FCA* homolog has additionally been identified in chrysanthemum (Su et al., 2024).

Arabidopsis LD scaffolds other proteins in a an *FLC* repressor complex, enabling the halting of active chromatin marks on *FLC,* and the subsequent deposition of repressive H3K27me3 (Qi et al., 2022; Liu et al., 2010; Fang et al., 2020; Xu et al., 2008). Expression of *LsLD* increases over the course of floral initiation, with greater increases observed in early-bolting lines (Fukuda et al., 2016). *C. lyallii LD* was also strongly induced prior to flowering (Samarth et al., 2021) and *LD* homologs have been identified in sunflower (Blackman et al., 2011; Badouin et al., 2017), and *C. morifolium* (Su et al., 2024).

In *Arabidopsis*, the histone deacetylase FVE complexes with HISTONE DEACETYLASE 6 (HDA6) and the histone demethylase FLD in suppressive *FLC* deacetylation (Ausín et al., 2004; Gu et al., 2011; Yu et al., 2016; He et al., 2003; Qi et al., 2022; Yu et al., 2011). Expression of both *LsFVE* and *LsFLD* increases over the course of floral initiation, with greater increases observed in early-bolting lines (Fukuda et al., 2016; Abbott, 2010). *FVE*, *FLD* and *HDA6* have also been identified in sunflower (Blackman et al., 2011; Badouin et al., 2017), and FVE in chrysanthemum (Samarth et al., 2019), with *ClFLD* and *ClHDA6* upregulation *observed* after daisy plants were exposed to high temperatures, indicating their contribution to the thermosensory induction of flowering (Samarth et al., 2021).

In addition to its autonomous suppression of the floral transition, FLC acts, and is acted upon, in the thermosensory pathway, both directly and via autonomous pathway components. Under warm temperatures, both FCA and FVE act in suppression of the thermosensory floral repressor *SVP* (Li et al., 2008). Under cool temperatures, SVP complexes with FLC in the

repression of flowering, via binding with TEMPRANILLO 1 (TEM1) (Mateos et al., 2015), with TEM1 directly repressing *FT* (Marín-Gonzalez et al., 2015). In *Chrysanthemum*, CmSVP binds and represses *CmFT* in a temperature-dependent manner (Cheng et al., 2018), and *CmSVP* delays flowering upon overexpression in *Arabidopsis* (Gao et al., 2017; Zhang et al., 2023). Heat treatment (35 ℃) induces flowering in chicory (Mathieu et al., 2014), and reduces *FLC-LIKE1* (*CiFL1*) expression (Mathieu et al., 2020a). *CiFL1* also complements *flc* mutants when expressed in *Arabidopsis* (Locascio et al., 2009; Périlleux et al., 2013). *LsFLC* expression is also downregulated in lettuce plants subjected to high temperature (33 ℃) treatment, leading to bolting (Hao et al., 2022). *SVP* homologs have also been identified in sunflower (Blackman et al., 2011; Badouin et al., 2017), and *C. nankingense* (Won et al., 2021), and these works further indicate conservation of the thermosensory flowering pathway in Asteraceae.

The body of knowledge of Asteraceae floral pathways is ever-expanding, but evidence indicates that flowering pathways are maintained between Asteraceae and *Arabidopsis* (Gao et al., 2017; Samarth et al., 2021, Huang et al., 2021; Abbott, 2010; Hao et al., 2022; Fukuda et al., 2016). This work was conducted to explore whether CRISPR/Cas9-mediated knockout of *LsFT*, *LsFCA*, and *LsFLD* could prevent heat-induced lettuce bolting.

Prior work has been performed in the pursuit of late-bolting lettuce lines. In a grand effort, EMS mutagenized cultivars ‘Larissa’ and ‘Saladin’, *Tnt1*-transformed ‘Jessy’, and wild lettuce accessions from *L. serriola*, *L. saligna*, and *L. virosa* were screened for late-bolting. Late-bolting lines were identified in the mutagenized ‘Larissa’, ‘Saladin’, and ‘Jessy’ cultivars, but none of the genes at play could be confirmed (Abbott, 2010). The auxin response factor *LsARF3* observed to directly activate *LsCO*, was targeted for gene knockout and, and homozygous knockout plants were observed to bolt as much as 20 days later than WT in the early bolting

cultivar ‘GB-30’ (Li et al., 2022). *SQUAMOSA PROTEIN BINDING PROTEIN LIKE 13* (*LsSPL13),* as well, has been a target of CRISPR/Cas9-mediated knockout. This effort led to delayed flowering in the ‘Grand Rapids’ cultivar by up to ~15 days (Beracochea et al., 2023). In *Arabidopsis*, SPL13 is a *FT* activator (Han et al., 2010; Kim et al., 2012). When *LsSOC1* was subjected to knockdown by RNAi in the heat-sensitive cultivar ‘S39’, bolting was delayed by an average of 14 days, and heat insensitivity at high temperatures (35 ℃) was observed in transformed lines (Chen et al., 2018a). In subsequent work, *LsSOC1* was targeted for CRISPR/Cas9-mediated gene editing and a single base insertion led to a delay in flowering of 5 days when T_1 mutants were screened under prevailing outdoor conditions (Choi et al., 2022).

Results

CRISPR guide selection and vector construction

Two sgRNAs per gene were designed to target exons in *LsFT, LsFCA,* and *LsFLD* (**Figure 1**). The *LsFT* sgRNAs LsFT1 and LsFT2 target sequences in the first and fourth exons of *LsFT,* respectively. The *LsFCA* sgRNAs, LsFCA1 and LsFCA2 target sequences in the first exon and the *LsFLD* sgRNAs, LsFLD1 and LsFLD2 also target sequences in the first exon. The sgRNAs for each gene were cloned individually under the control of the *Arabidopsis AtU6* promoter into the pMDC plasmid containing *35S:GFP, 35S:Cas9,* and *35S:Hyg*^{R} cassettes in the T-DNA. The resulting pMDC destination plasmids were named pLsFT1, pLsFT2, pLsFCA1, pLsFCA2, pLsFLD1, and pLsFLD2 and each contained a single sgRNA. The sgRNAs for each gene were cloned under the control of the rice (*Oryza sativa*) *OsU3* promoter and multiplexed in the pRGEB31m plasmid containing *35S:Cas9* and *35S:Hyg*^{R} in the T-DNA (**Figure 1**). The resultant

pRGEB31 destination plasmids were named pLsFTm, pLsFCAm, and pLsFLDm, each containing two sgRNAs targeting a single gene.

Generation of transgenic lettuce lines

The destination plasmids pLsFT1 and pLsFT2, each containing a single sgRNA, were transformed individually into the lettuce cultivars 'Red Sails', 'Kahu', and 'Royal Oak Leaf', using an optimized lettuce transformation protocol (see Chapter 2). An array of success was observed in plant regeneration after transformation, based upon cultivar, construct, and transformation attempt (**Table 1)**. As an example, the three transformation attempts in the 'Red Sails' cultivar with the pLsFT1 plasmid yielded 425, 85, and 318 T_0 lines, respectively, while transformation attempts with the pLsFT2 plasmid yielded 47, 252, and 0 T_0 lines, respectively. A total of 828 and 299 T_0 lines were obtained in 'Red Sails' for pLsFT1 and pLsFT2, respectively (**Table 1**). Considerably less success was observed in the regeneration of T_0 plants from the 'Kahu' and 'Royal Oak Leaf' cultivars. The three transformation attempts of 'Kahu' with pLsFT1 yielded 94 T_0 lines, while those with pLsFT2 generated 80 T_0 lines in total (**Table 1**). 'Royal Oak Leaf', however, yielded a mere 14 total transformants (6 for pLsFT1 and 8 for pLsFT2) (**Table 1**).

Due to the success observed with the 'Red Sails' cultivar in the transformation efforts with pLsFT1 and pLsFT2, 'Red Sails' alone was utilized in successive transformations (three replicates/plasmid). More consistent results were obtained in transformation with the destination plasmids pLsFCA1, pLsFCA2, pLsFLD1, and pLsFLD2 into 'Red Sails'. As shown in **Table 1**, 152 T_0 lines were regenerated from the pLsFCA1 transformation, and 97 T_0 lines were obtained

from the pLsFCA2 transformations. As well, the pLsFLD1 transformations resulted in 70 T_0 lines, while the pLsFLD2 transformations resulted in 130 T_0 lines total.

In 'Red Sails', utilizing the multiplex destination plasmids pLsFTm, pLsFCAm, and pLsFLDm, each containing two sgRNAs targeting one gene, transformations with pLsFLDm were most successful, yielding 303 T_0 lines, while transformations with pLsFTm and pLsFCAm yielded 127 and 119 T_0 lines, respectively (**Table 1**). Results of this nature indicate the importance of replicated transformations to ensure successful generation of transgenic plants and the importance of using an optimized transformation protocol for the cultivar of interest.

Mutant phenotypic screening under high temperature conditions

After harvesting T_1 seed from T_0 plants, a random selection of T_1 lines were grown under high temperature (30.38 ± 1.92 ℃) controlled-environment conditions to identify the lines exhibiting delayed bolting. Here, bolting was defined as stem length reaching 8 cm or greater (Hao et al., 2018; Ito et al., 1963), while delayed bolting was defined as a time period of greater than 7 days elapsing in the observance of bolting in a line when compared to the wild type (WT) of the same cultivar. As shown in **Table 1**, 27, 18 and 1 T_1 lines were screened from the pLsFT1-transformed 'Red Sails', 'Kahu' and 'Royal Oak Leaf' cultivars, respectively, while 17, 16, and 1 T_1 lines were screened for pLsFT2 in the same cultivars. While as low as 11.1% (pLsFT1) and 25.0% (pLsFT2) of T_1 in 'Kahu' lines yielded plants with a delayed-bolting phenotype, moderate success was achieved in 'Red Sails,' with 40.7% (pLsFT1) and 35.3% (pLsFT2) of T_1 lines producing at least one plant with a delayed-bolting phenotype. All lines tested in 'Royal Oak Leaf' produced plants with a delayed-bolting phenotype as compared to WT, although only one line was phenotyped per construct (**Table 1**). A difference in the percentage of T_1 lines

exhibiting a delayed-bolting phenotype was observed between pLsFCA1 and pFCA2 (26.7% vs. 50.0%), as well as pLsFLD1 and pLsFLD2 lines (57.1% vs. 37.5%) as well (**Table 1**).

Phenotyping of T_1 lines arising from the multiplex plasmids pLsFTm and pLsFCAm in 'Red Sails' resulted in the emergence of the delayed-bolting phenotype in 62.5% and 57.1% of T_1 lines, respectively (**Table 1**). Both numbers were slightly higher than that of their respective single sgRNA plasmids. In screening of pLsFLDm T_1 lines, 41.2% produced at least one plant with a delayed-bolting phenotype, which was comparable to the single sgRNA plasmid T_1's (**Table 1**).

T_1 plants with a delayed bolting phenotype were maintained to collect T_2 seeds for further screening. Depending on timing of T_1 seed maturation, T_2 lines were screened in either a modified shipping container (vertical farm) under the same aforementioned conditions, or were planted into potting soil in a greenhouse with similar ambient temperature (28.41 ± 3.54 ℃). Photoperiod was the primary difference in the growing conditions between the vertical farm and greenhouse controlled-environments. As the greenhouse utilized natural lighting, plants were subject to the prevailing photoperiod during the trial (~10 to ~14.5 hours), in addition to the increased ratio of far-red (FR) light that comes with exposure to a sunlight spectrum. Natural sunlight has approximately 19% FR (Zhen and Bugbee, 2020), depending on location, whereas the highest percentage of FR utilized in the affixed LED in the vertical farm was 5%.

All told, delays in bolting were observed across all cultivars and constructs, several with quite lengthy delays in bolting, maintaining the phenotype into subsequent generations. In screening of pLsFTm plants, 120 of the 1,121 screened plants were delayed in bolting (>7 days later than WT), and had an average delay of 20.2 ± 11.6 days, with the greatest delay being 77 days. In the 'Red Sails' cultivar, the pLsFT1 lines produced 32 individual plants delayed in

bolting (of 1324 screened), with an average delay of 14.7 ± 6.3 days, with 33 days being the greatest delay observed. With the same cultivar, the pLsFT2 lines produced 100 individual plants delayed in bolting (of 1018 screened), with the largest observed delay of 43 days, and an average delay of 17.6 ± 6.6 days. The 'Kahu' cultivar produced 80 delayed-bolting plants (of 1155 screened) from the pLsFT1-transformed lines, with an average delay of 21.4 ± 6.8 days. In the same cultivar, the pLsFT2 lines yielded a mere 8 plants delayed in bolting (of 1035 screened), with an average delay of 14.8 ± 5.6 days. While in the screening of 'Royal Oak Leaf', only one line per construct was screened, each line yielded plants with a delayed-bolting phenotype and the greatest delay in bolting observed was 33 days in the pLsFT2 line, with a 25-day delay observed in the pLsFT1 line. While the delayed phenotype of the pLsFT1 lines did not carry into the T_2 generation, candidates were obtained in the pLsFT2 line, with plants delayed in bolting by 16 and 33 days, as compared to WT.

Delays were observed in the bolting of *LsFCA* knockout lines as well. In 'Red Sails', the pLsFCAm lines produced a total of 47 individual plants (of 659 screened) delayed in bolting, with an average delay of 16.5 ± 4.7 days observed, and a largest delay of 47 days. The pLsFCA2 lines yielded 85 plants with a delayed bolting phenotype (of 613 screened), with an average observed delay of 18.9 ± 13.7 days, and the lengthiest delay being 69 days. Somewhat reduced success was observed in the screening of pLsFCA1 lines, with the longest delay observed amid a total of 19 late-bolting plants (of 479 screened) having been 30 days, and the average delay having been 15.7 ± 5.6 days.

In lines where *LsFLD* was targeted for knockout, delayed bolting under heat treatment was also observed. The pLsFLDm lines produced a total of 78 delayed-bolting plants (of 655 screened), with a lengthiest delay of 38 days. The average delay observed was 15.9 ± 3.7 days.

Similarly, the greatest delay observed among the 65 delayed-bolting plants (of 633 screened) in the screened pLsFLD1 lines was 33 days, while the average delay was 13.9 ± 4.3 days. Shorter bolting delays were observed with the pLsFLD2 lines, with a lengthiest delay of just 22 days, and an average of delay of just 12.8 ± 3.9 days, among the 20 total delayed plants (of 511 screened). Overall, the average delay observed among all delayed plants was 17.6 ± 8.9 days.

Tracing of phenotype segregation revealed that while a few lines, like pLsFLDm #106 and pLsFLD1 #18, did exhibit the expected Mendelian segregation ratio of 1:2:1, most did not (**Table 2**). Instead, most ratios favored the WT phenotype, with a spectrum of shorter bolting delays and few plants exhibiting strong bolting delays, as with pLsFLD2 #15, pLsFT1 #286, and pLsFCA1 #5. When a majority of delayed bolting was observed in a line ('Red Sails' pLsFTm #6 and 'Kahu' pLsFT1 #51), as would be expected in a homozygous edit, dwarfism was also observed, likely confounding the maturity measurement. Several of the T_2 lines maintaining a delayed-bolting phenotype (**Table 1**), were subject to genotyping in order to confirm whether gene-editing had taken place. When time allowed, a third generation was also screened under high-temperature treatment, and T_3 candidates were included for genotyping.

Genotyping of delayed-bolting candidates

All told, phenotype screening resulted in 235 T_2 plants and 124 T_3 plants delayed in bolting. Approximately one-third of these individuals (123), encompassing the majority of lines exhibiting a phenotype, were subject to Sanger sequencing of target amplicons with DNA amplified from leaf punches. As no sequences revealed homozygous edits, sequencing chromatograms were decoded by the Tracking of Indels by Decomposition (TIDE) program to estimate the frequency of indels in the cell population (**Table 3**; Brinkman et al., 2014; Pan et al.,

2022; Zhang et al., 2020). A selection of plants representing all constructs, predicted by TIDE to have undergone editing in the target region ('Red Sails' pLsFT1 #268, pLsFT2 #82, pLsFCA1 #5, pLsFCA2 #72, pLsFLD1 #18, pLsFLD2 #15, pLsFTm #6, pFCAm #93, pFCAm #116, pFLDm #106, 'Kahu pLsFT1 #51, and 'Royal Oak Leaf' pLsFT2 #5; **Figures 3; 4**) were then subject pCR^{TM}8/GW/TOPO cloning of PCR amplicons, with successive sequencing of individual resultant colonies, as well as deep amplicon sequencing. While SNPs were revealed in the sequencing of target regions, the frequency was low for each tested line. For example, in pLsFCA1 #5, a T_2 late in bolting by 30 days, 20% of pCR^{TM}8/GW/TOPO of colonies sequenced revealed a 1 bp deletion in the 15th base from the PAM in the LsFCA1 sgRNA target. Deep amplicon sequencing of pLsFCA1 #5 revealed, however, that only 27.6% of aligned reads were modified, with the most common read (30.9% of edited reads) being a 3 bp deletion occurring 9 bases from the PAM. An array of other mutations in the target region were presenting as well, including deletions further from the PAM and base insertions nearer to it. Similarly, in pLsFCAm #93, a T_2 late in bolting by 20 days, 5% of pCR^{TM}8/GW/TOPO colonies revealed a 1 bp deletion in the 14th base from the PAM in the LsFCA1 sgRNA target, and while, 33.9% of aligned reads were modified, the most common edit (7.8% of edited reads) was also a 3 bp deletion occurring 9 bases from the PAM. An array of other edits were presenting here as well, including a single base deletion in the same position and deletions downstream of the sgRNA target. The presence of multiple, differing low-frequency reads among all samples are indicative of chimerism (Bertier et al., 2018; Nguyen et al., 2021). Unfortunately, no editing frequencies, as revealed by pCR^{TM}8/GW/TOPO or deep amplicon sequencing, approached the expected Mendelian ratios indicative of heterozygous or homozygous edits, disallowing certainty as to whether or not editing had indeed occurred in any of the tested lines. Thus, while many plants

were delayed in bolting and thus possessing the desired phenotype, this work is unable to conclude that this phenotype was arrived at via bona fide gene-editing, and not a result of T-DNA insertional mutations, off-target editing, PCR error, or environmental stress that may have led to presentation of the phenotype. It is possible, however, that further work in seeking out DNA edits in the remaining lines, or additional screening would reveal lines possessing both the desired phenotype and genotype.

Discussion

This study sought to delay the heat-induced bolting of lettuce via CRISPR/Cas9-mediated gene editing of the flowering pathway genes *LsFT*, *LsFCA* and *LsFLD*. While a delay in bolting was achieved for all gene targets, unfortunately, it could not be determined whether bona fide editing had occurred in tested lines. Thus, while this work serves to indicate that delaying heat-induced bolting of lettuce is indeed achievable, and appreciable delays in bolting and subsequent flowering can be achieved, non-Mendelian segregation of the delayed bolting phenotype along with lack of legitimate evidence of gene-editing, indicate that further work would need to take place in order to apply these efforts towards the goal of generating a lettuce line cultivatable under increased ambient temperatures while retaining quality.

The light and thermal component to flowering response in LsFT-, LsFLD- and LsFCA-targeted lines

Lettuce is a quantitative long day plant (Waycott, 1995). Contrary to previous assertions that high temperature alone is not sufficient to induce bolting and a long-day photoperiod is required (Waycott, 1995), plants under high temperature in this treatment were observed to bolt readily

even under a short-day photoperiod. In *Arabidopsis* as well, while flowering is more accelerated in long photoperiods than in short, cultivation of *Arabidopsis* under warm temperatures (27 ℃) bypasses the long-day requirement by direct promotion of *AtCO* and successive promotion of *AtFT*. Thus, under warm temperatures, full acceleration of flowering requires the action of functional FT (Fernández et al., 2016), and as AtCO cannot promote *AtSOC1* in the absence of *AtFT* expression, floral promotion is delayed (Yoo et al., 2005). In the current study, T_2 lines were assayed for late-bolting under the prevailing photoperiod (~10 – 14.5) hours, with the consistent presence of high temperatures. In *Arabidopsis*, flowering time in warm ambient conditions (27 ℃) under short days is approximately equivalent to that observed under cooler ambient conditions (21 - 23 ℃) under a long day photoperiod (Fernández et al., 2016; Balasubramanian et al., 2006), indicating how an increase in ambient temperature is equally as potent at triggering flowering, as prolonging the photoperiod. These works also serve to indicate how the thermosensory induction of flowering at least partially occurs through FT, and thus indicates how knockout of *FT* can be a tool to delay thermally-induced flowering. A strategic effort to identify the most important residues in *AtFT* determined that *FT* is quite robust to an array of mutations, even those occurring in conserved regions (Ho and Weigel, 2014). This may indicate why a limited number of late-bolting lines were recovered when *LsFT* was targeted for knockout, as even though edits may have occurred, there may not have been a concurrent reduction in *LsFT* expression leading to the late bolting phenotype.

Flowering is promoted by FT via the photoperiod pathway, and *Arabidopsis* mutants of *ft* are less sensitive to the light environment, but still retain a response and flower earlier under far-red-enriched light (Bagnall, 1993). In WT as well, variation in flowering time across *Arabidopsis* accessions has been attributed to variation in *AtFT* alleles, and ecotypes with a reduced response

to FR show reduced *AtFT* expression (Schwartz et al., 2017). The Bla-6 ecotype exhibits reduced sensitivity to FR light, due to the presence of a weak *AtFY* allele, leading to increased At*FLC* expression, and concurrently, reduced *AtFT* expression (Adams et al., 2009). This indicates that enhanced *FLC* expression, due to knock-down/knockout of autonomous pathway genes can successfully suppress *FT*, in spite of the FR-induced expression of *FT*. Indeed, the repression of *FLC* via *COOLAIR* has been demonstrated as a biological safeguard in case of the loss of *FT* function (Luo et al., 2019). In the current study, lines generated from plasmids targeting *LsFT* bolted significantly earlier (15.0 ± 10.4 days; one-way ANOVA, $\alpha = 0.05$) under sunlight than under any of the LED light spectra, indicating that these lines retained sensitivity to the enhanced FR (~19%) in the natural light environment (Zhen and Bugbee, 2020; Meng et al., 2019). The observation of bolting in all tested light qualities, however, including those that did not contain far-red, is indicative of the influence of the autonomous and temperature-mediated floral pathways in inducing bolting in lettuce.

The *FT* gene has been targeted for gene-knockout by CRISPR/Cas9 to modulate flowering time in an array of species, including *Arabidopsis*, soybean, sorghum and tomato (Kishchenko et al., 2020). Downregulation of lettuce *FT* by RNAi in the bolting-sensitive line 'S39' led to a delay in bolting of 7 to 37 days, with a correlative decrease in *LsFT* expression of 29 – 56% when cultivated at 25 ℃ (Chen et al., 2018b). A similar time to bolting was observed in knockdown lines treated with heat (37 ℃) (Chen et al., 2018b). The study by Chen and coworkers indicated that a similar delay in bolting may be observed in *LsFT* knockout lines, and motivated this exploration in the current study (Chen et al., 2018b). Indeed, under heat treatment, delays in bolting of up to 77 days were observed in screened lines derived from *LsFT* knockout

plasmids, with an average delay observed across *LsFT* constructs in 'Red Sails, 'Kahu' and 'Royal Oak leaf' cultivars of 18.4 ± 9.9, 20.8 ± 8.8, and 14.4 ± 6.5 days, respectively.

In addition to its role in shade avoidance, it is known that *Arabidopsis* flowers more rapidly under FR-enriched light (Halliday et al., 2003). While they remain delayed in flowering, autonomous pathway mutants do respond to high a FR light environment, as they remain photoperiod-responsive (Bagnall, 1993). While mutants of *Atfca* show profound delays in flowering under red light (Mockler et al., 1999), the introduction of FR to the light environment hastens flowering, though plants are still delayed as compared to WT (Sanda and Amasino, 1996a; Bagnall, 1993; Halliday et al., 1994). Similarly, *Atfld* mutants flower considerably sooner when the R:FR ratio shifts from 4.6 to 0.8, but remain delayed as compared to WT (Sanda and Amasino, 1996b). Green light also contributes to hastening flowering in *Arabidopsis*, and has been observed to promote the shade avoidance response in lettuce (Meng and Runkle, 2019; Meng et al., 2019). Thus, contrary to expectations, in lettuce lines transformed with plasmids targeting both *LsFCA* and *LsFLD*, plants under the 15B:38G:47R spectral combination bolted significantly later (21.7 ± 11.4 and 17.2 ± 9.4 days, respectively (one-way ANOVA, $\alpha = 0.05$)) than those under the 16B:15G:69R spectrum (16.2 ± 4.6 and 13.9 ± 4.8 days, respectively), while there was no significant difference in bolting time across the other spectral treatments. Wild type plants, however, showed the expected phenotype, exhibiting greater stem elongation under the 38% green light combination (13.9 ± 6.9 cm), and less elongation under 15% green light (11.5 ± 4.8 cm) (Hernández and Spalholz, 2019).

While studies have not examined the delay in flowering brought on by *FLD* lesions in lettuce to date, research on the phenotypes of mutant *fld* lines in *Arabidopsis* are plentiful. Mutants of *fld* show hyperacetylation at *FLC* histones H3/H4, and increased H3K4 dimethylation

and trimethylation (Yu et al., 2011; He et al., 2003; Liu et al., 2007), leading to increased expression of *FLC* and delayed flowering (He et al., 2003). *Atfld* mutants are insensitive to temperature as well, and acceleration of flowering is not observed at increased ambient temperatures (27 ℃ vs. 23 ℃) (He et al., 2003; Balasubramanian et al., 2006). In the current study, the average delay across all lines derived from *LsFLD* knockout constructs was 15.0 ± 6.2 days. Although this study only observed plants under high ambient temperatures, it would be interesting to study the potential flowering delay under cooler ambient temperatures as well.

Lesions in *fca* also lead to temperature insensitivity (Balasubramanian et al., 2006). Studies conducted across temperatures 15 – 27 ℃, indicate that flowering is not accelerated in *Atfca-1* mutants under heightened temperatures, while flowering is accelerated in Ler WT (Balasubramanian et al., 2006; Blázquez et al., 2003; Wendell et al., 2017). A photoperiod response is maintained, however in mutants of *fca,* with long days accelerating the transition to flowering (Macknight et al., 2002; Henderson et al., 2005; Fujiwara et al., 2010). In the current study, under long day conditions, the lines transformed with plasmids targeting *LsFCA* bolted an average of 17.0 ± 8.8 days later than WT (32.4 ± 6.7 days), while those cultivated under SD photoperiods bolted an average of 21.5 ± 10.5 days later than WT (35.5 ± 5.4 days), with both WT and *LsFCA* lines showing a significant difference between photoperiods (one-way ANOVA $\alpha = 0.05$), indicating that photoperiod, rather than ambient temperature, may have contributed predominantly to bolting response in *LsFCA*-targeted lines.

When lettuce plants of the butterhead ‘Wayahead’ lettuce cultivar were treated with high ambient temperatures (23 ℃ - 30 ℃), as compared to cool ambient temperatures (17 ℃), bolting occurred approximately 35 - 15 days, respectively, after the initiation of the treatment (Ito et al., 1963). At 23 ℃, the iceberg cultivar ‘New York’, bolted in 15 days, while the romaine cultivar

‘Paris Market’ took 50 days at the same temperature (Ito et al., 1963). In a study of iceberg cultivars ‘Capitata’ and ‘Saladin Supreme’, a clear correlation was also observed between stem length and cultivation temperature, and prolonged time at increased temperatures (25 ℃ vs. 13 ℃) led to bolting induction (Al-Said et al., 2018). In the current study, bolting of WT plants took 23.8 ± 2.3 days in the romaine ‘Kahu’, 30.8 ± 5.7 in the leaf cultivar ‘Red Sails’, and 33.8 ± 1.0 days in the leaf cultivar ‘Royal Oak Leaf’ when cultivated under high temperature conditions (Van de Wiel et al., 1998; Xinrun and Conner, 1992; Ampomah-Dwamena et al., 1997). Together, these works indicate that different genotypes of lettuce have differing sensitivities to cultivation temperature and differing rates at which flowering is induced.

Past efforts in delaying lettuce bolting and gene-editing studies across species inform the current work

CRISPR/Cas-9 works by making site-directed double-stranded cuts in genomic DNA (Burner et al., 2022). When the cuts are repaired by error-prone endogenous DNA-repair mechanisms like Non-Homologous End-Joining (NHEJ), insertions, deletions and substitutions are made in the DNA sequence. Typical mutations occurring via CRISPR/Cas9 occur at the position three nucleotides upstream of the PAM, although mutations occurring from bases 1 to 5 from the PAM have also been observed (Burner et al., 2022; Pan et al., 2016; Biswas et al., 2020; Yang et al., 2017). Mutations often present as single base insertions, deletions, or base transitions (Burner et al., 2022). CRISPR/Cas-9 mediated gene editing in lettuce has been gaining popularity in recent years, with several efforts published towards optimization of the technology (Woo et al., 2015; Bertier et al., 2018).

In the initial gene-editing effort in lettuce, protoplasts of 'Cheongchima' were transfected with purified *Cas9* and sgRNA to target *BRASSINOSTEROID INSENSITIVE 2* (*LsBIN2*). In this work, 5.7% of tested calli had monoallelic mutations, 40% had biallelic mutations, and the T_0 and T_1 plants regenerated from biallelic homozygous mutants were determined to be carrying the mutation (Woo et al., 2015). In a subsequent work, *9-cis-EPOXYCAROTENOID DIOXYGENASE 4 (LsNCED4*) was targeted for editing (Bertier et al., 2018). This effort sought to prevent thermoinhibition in germination by knockout of *LsNCED4*, and enabled study of the heritability of CRISPR/Cas9-induced mutations. While nearly half of recovered T_1's had editing events (46%) at the target, a quarter (22%) were mono-allelic, and only ~7% of recovered T_1's had bi-allelic editing events. The remaining events were determined to be chimeric 'late-events' with an array of alleles presenting (Bertier et al., 2018). Chimerism in gene-editing is defined as having two or more mutation-types, in addition to WT sequence, present at the target site (Feng et al., 2014; Pan et al., 2016). In a work by the same group, a leaf variegation gene, *LsVAR2*, was targeted for CRISPR/Cas9-mediated gene editing (Nguyen et al., 2021). In this effort, 40% of T_1's also contained an array of mutations in the target gene, and the array of variegation phenotypes presenting correlated with the array of mutations observed. While two of the 10 edited lines produced homozygous edits, and thus clean sequencing chromatograms, the remaining eight lines exhibited noise in the sequencing chromatograms, indicating heterogenous mutations were present. Similar to the work of Bertier and coworkers, de novo late events due to continued expression of *Cas9* were theorized to be contributing to the phenotypic and genotypic chimerism in T_1 plants, with a differing range of edits detected in sequenced regions even across the same leaf (Nguyen et al., 2021; Bertier et al., 2018). Chimeric edits have also been reported in CRISPR/Cas9-mediated gene editing efforts in rice (Jang et al., 2016; Ishizaki, 2016), tomato

(Pan et al., 2016; Zhang et al., 2020; Debbarma et al., 2023), *Arabidopsis* (Feng et al., 2014; Ma et al., 2015), soybean (Michno et al., 2020), citrus (Peng et al., 2017; Song et al., 2023), grapevine (Yu et al., 2024), poinsettia (Nitarska et al., 2021), *Brassica* (Yang et al., 2017; Xiong et al., 2019), cotton (Janga et al., 2017), and tobacco (Song et al., 2022a), indicating that observations in lettuce are not isolated. In the current study, as well, it became challenging to identify edits via Sanger sequencing by visually examining sequencing chromatograms (Yang et al., 2017). As such, the TIDE program was utilized to decode chromatograms and a selection of plants with a high likelihood of possessing edits (**Table 3**) were subject to pCR^{TM}8/GW/TOPO cloning (Brinkman et al., 2014; Pan et al., 2022; Zhang et al., 2020). In sequencing of individual amplicons, an array of alleles presented across target regions, indicating that the tested lines were also chimeric (Bertier et al., 2018; Nguyen et al., 2021). In grapevine and poinsettia as well, an array of edits were observed across the target region in sequencing of cloned amplicons, in addition to WT sequence (Yu et al., 2024; Nitarska et al., 2021).

Non-mendelian segregation of the delayed-bolting phenotype was predominantly observed in this study (**Table 2**). Non-mendelian segregation has commonly been observed in lines edited by CRISPR/Cas9 when somatic editing has taken place (Michno et al., 2020; Feng et al., 2014; Pan et al., 2016; Xu et al., 2015; Gao et al., 2016) and/or when the *Cas9* remains active in subsequent generations (Feng et al., 2014; Pan et al., 2016; Xu et al., 2015; Ishizaki, 2016; Song et al., 2022b; Yang et al., 2017), and chimerism often coincides with somatic editing (Pan et al., 2016; Feng et al., 2014). When somatic editing does not result in germline transmission, stable transmission of edits does not reliably occur, leading to the non-Mendelian segregation of editing genotypes (Gao et al., 2016; Song et al., 2022b). Coupled with continued expression of *Cas9*, generating new, potentially different, somatic edits across generations (Ishizaki, 2016;

Song et al., 2022b), it soon becomes difficult to track the presence of induced mutations. Thus, the chimerism of different low-frequency mutations, along with the observed non-Mendelian segregation across generations indicates that if editing has indeed occurred in the current work, the edits are thus likely somatic, and germline transmission has not occurred in the tested lines. Germline transmission of chimeric edits has been observed to occur from T_2 to T_3 generations in *Arabidopsis*, however, indicating that further study of these lines may yet produce homozygous edits (Feng et al., 2014).

Interestingly, phenotypic changes have been brought about in lines where chimeric edits were observed. In *Arabidopsis,* delayed bolting was observed across genotypes, including chimeras, when *AtFT* was subject to knockout (Hyun et al., 2015). In rice, chimeric edits of *SD1* led to the dwarf stature sought by researchers (Biswas et al., 2020). In orange, chimeric edits of *CsLOB1* achieved the goal of citrus canker resistance (Peng et al., 2017), and in grapevine, lines with chimeric edits to *VvEDR1* developed powdery mildew resistance superior to that of homozygous edited lines, whose severe hypersensitive response served to kill the plant (Yu et al., 2024). Chimerism in editing the flavonoid gene *F3'H* led to orange mottling amid red tissues in poinsettia bracts (Nitarska et al., 2021), and the aforementioned chimerism in *LsVAR2* edits led to an array of variegation patterns across lettuce leaves (Nguyen et al., 2021). In the current study, delayed bolting phenotypes were repeatedly documented for every tested construct, indicating the possibility that chimeric somatic edits of target genes were indeed contributing towards the phenotype.

Research has been conducted in recent years towards improving gene-editing efficiency in lettuce. In one study, where *AtU6-26* was used to drive the sgRNA targeting *LsARF3*, 25% homozygous edits were achieved in T_1 (Li et al., 2022) In a subsequent study, using an

endogenous *U6* promoter (*LsU6-10*) to drive the sgRNA targeting *LsPHOT2* was observed to be more effective (73% efficiency) in gene-editing than *AtU6-26* (48% efficiency) (Riu et al., 2023). When *Cas9* was driven by the parsley ubiquitin promoter (*PcUbi*), homozygous edits were derived in the T_2 generation (Bertier et al., 2018). To further boost editing efficiency in lettuce, Pan and coworkers (2022) used an intron-enhanced *35S* promoter ahead of a *Cas9*-sgRNA linked transcript, as well as co-expression of the developmental regulator *GROWTH REGULATING FACTOR 5* (*GRF5*). This effort increased editing efficiency from 14 - 28% to 54 - 81% and improved the rate of homozygous and biallelic edits in the T_0 generation (Pan et al., 2022). In the current work, two differing base plasmids were utilized, with the sgRNA under the control of either *AtU6* (pMDC) or *OsU3* (pRGEB31m) (**Figure 2**). While the rice polymerase III promoter (*OsU3*) driving the sgRNA in pRGE3-based plasmids is designed to be utilized in monocot transformation (Xie and Yang, 2013), gene-editing success has been observed when this plasmid was used for examining HDR efficiency in *Populus trichocarpa* (Movahedi et al., 2022), and knockout of *A622* genes and the alkaloid synthetic gene *QPT2* in *Nicotiana tabacum* (Burner et al., 2022; Smith et al., 2022). Thus, while researchers are eager to perform gene knockout in *L. sativa*, there remains room for progress in editing efficiency, as was discovered in the current study, and future efforts would do well to consider methods that have brought success in lettuce gene-editing.

Materials and Methods

Plant materials and growth conditions

Seeds of the ‘Red Sails’ cultivar were obtained from Johnny’s selected seeds and seeds of ‘Royal Oak Leaf’ (PI 595576), and ‘Kahu’ (PI 251501) were obtained from USDA-ARS-GRIN. Seeds

were incubated at 23 ± 2 ℃ under a 16 h photoperiod (18 $\mu mol \cdot m^{-2} \cdot s^{-1}$) for 6-7 days until transformation procedures took place (Dong et al., 2014).

gRNA design

Two sgRNA target sites in each of the *LsFT*, *LsFCA* and *LsFLD* genes were designed through the following steps (**Figure 1**). The amino acid sequence of each respective gene was retrieved from NCBI (ncbi.nlm.nih.gov; Reyes-Chin-Wo et al., 2017) and blasted to the current *L. sativa* annotation (v8) in Phytozome (phytozome-next.jgi.doe.gov/). Matching amino acid and cDNA sequences were retrieved and aligned to each target gene amino acid and cDNA sequence utilizing ClustalX software (clustal.org/). Alignments were manually adjusted to identify locations in each gene with minimal hits to other regions in the genome. Genomic sequences were then plugged into CRISPOR (crispor.tefor.net/) and compared against the *L. sativa* genome (NCBI GCA_002870075.2 (Lsat_Salinas_v7)) to identify sequences with proximal NGG PAMs and high specificity. The resulting potential guides were compared against the manual alignments to select guides with a minimal risk of off-target editing. Oligos with sticky ends to anneal to restriction sites for *Bsa*I in the pRGEB31 plasmid and *Bae*I in the pSK35S-AtU6-ccdB-gRNA plasmid (Liu et al., 2020b) were synthesized by Integrated DNA Technologies, Inc. (Coralville, IA, USA). Oligos were dimerized in a thermocycler by an initial linearization step (94 ℃, 10 min), followed by annealing (25 ℃, 60 min).

Plasmid cloning

Each sgRNA was individually cloned into the pMDC plasmid to generate six destination plasmids for the three target genes, according to the following steps. pSK35S-AtU6-CsCLG-

18gRNA and pSKPvU6-2.1p-gRNA-ccdB were first digested with *Spe*I and *Hind*III to extract ccdB-gRNA from pSKPvU6-2.1p-gRNA-ccdB and ligate it into pSK-35S-AtU6-CsCLG-18gRNA. The resulting plasmid was named pSK35S-AtU6-ccdB-gRNA and was transformed into *Escherichia coli* DB3.1. Colonies were increased in 3 ml liquid LB (37 ℃) on a shaker for ~16 h, and plasmid DNA was extracted with the QIAprep® Spin Miniprep Kit (QIAGEN). Cloned inserts were confirmed by colony PCR, followed by Sanger sequencing with the T7 primer. The resulting pSK35S-AtU6-ccdB-gRNA plasmid was then digested with *Bae*I to remove the ccdB cassette, and each of the six sgRNA dimers were cloned into the plasmid backbone in individual reactions. Ligation products were transformed into *E. coli* DH5α and colonies screened for the insert and confirmed by Sanger sequencing with the T7 primer. Each resultant plasmid was named p35S-AtU6-gRNA. Next, each p35S-AtU6-gRNA and pMDC35S-mGFPNosT-35SRev-Cas9-35S-AtU6-26p-ccdB-gRNA (Liu et al., 2020b) were digested with *Asc*I and *Hind*III in order to extract each AtU6-gRNA cassette from each p35S-AtU6-gRNA and remove the AtU6-26p-ccdB-gRNA sequence from pMDC35S-mGFPNosT-35SRev-Cas9-35S-AtU6-26p-ccdB-gRNA. Then, each AtU6-gRNA fragment was cloned into the pMDC35S-mGFPNosT-35SRev-Cas9-35S plasmid backbone, confirmed by sequencing. The resulting destination plasmids were named pLsFT1, pLsFT2, pLsFCA1, pLsFCA2, pLsFLD1 and pLsFLD2, each containing *SpCas9* driven by the CaMV *35S* promoter, the sgRNA driven by the *AtU6-26* promoter, and hygromycin resistance (Hyg^R) driven by the *35S* promoter (**Figure 2A**).

The multiplex pRGEB31m plasmids were generated as follows from the pRGEB31 backbone (addgene.org/51295) to make one destination plasmid containing two sgRNAs for each target gene. pSKPvU6-2.1p-gRNA-ccdB was PCR amplified with PrimeSTAR® Max high-fidelity DNA polymerase (Takara Bio) to amplify the *Bae*I restriction site and sgRNA scaffold,

adding a 5' *Spe*I restriction site and 3' *Sbf*I-*EcoR*I restriction sites with primers SpeI-BaeI-gRNAscaf-for and EcoRI-SbfI-gRNAscaf-rev **(Table 4**). After digestion with *Spe*I and *EcoR*I, the amplicon was cloned into the intermediate vector pSK4xPRI-35SPAP1 (Liu et al., 2011; 2013), which had also been digested with *Spe*I and *EcoR*I to open the backbone. The *OsU3* promoter was PCR amplified from pRGEB31 with PrimeSTAR® Max to add 5' *Not*I and *Sbf*I restriction sites and a 3' *Xba*I restriction site with primers NotI-SbfI-OsU3-for and XbaI-OsU3-rev (**Table 4**). After the amplicon and destination plasmid were digested with *Not*I and *Xba*I, the NotI-SbfI-OsU3-XbaI fragment was cloned into pSK4xPRI-35SPAP1 directly upstream of the BaeI-gRNA scaffold cassette. The intermediate plasmid and pRGEB31 plasmids were then digested with *Sbf*I and the SbfI-OsU3-BaeI-gRNA-SbfI cassette was cloned into pRGEB31. The resulting plasmid was named pRGEB31m. The sgRNA pair for each of the three target genes were cloned stepwise into the *Bsa*I and *Bae*I restriction sites downstream of each *OsU3* promoter. The resultant destination plasmids were named pLsFTm, pLsFLDm, and pLsFCAm, which have *35S* promoter-driven hygromycin resistance (Hyg^R), *OsU3* promoter-driven sgRNAs, and *35S*-driven *SpCas9* with a Nos terminator.

Transformation procedure

Lettuce transformation was conducted as described in the transformation chapter. Briefly, the destination plasmids were transformed into the GV3101 strain of *A. tumefaciens* using rifampicin (10 mg/mL) and kanamycin (50 mg/ml) for bacterial selection. When the optical *Agrobacterium* density at 600 nm (OD_{600}) reached 1.1 – 1.6, the *Agrobacterium* was centrifuged and resuspended to a final ratio of 1:10 for use in lettuce transformation. Cotyledons from 7-day old seedlings were used as the explants. The co-cultivation media contained an MS (Musashige and

Skoog, 1962) media base, 0.1 mg/L NAA, 0.25 mg/L BA, 20 g/L sucrose, 2g/L Gelzan™, pH 5.8 (~8 cotyledons/dish). Co-cultivation took place in the dark at 25 ℃ for two-to-four days. After co-cultivation, explants were moved to selective callus-induction media containing MS, 0.1 mg/L NAA, 0.25 mg/L BA, 15 mg/L hygromycin, 400 mg/L timentin, 30 g/L sucrose, 2 g/L Gelzan™, pH 5.8 (~30 ml/plate) and were placed in a growth chamber (23 ± 2 ℃, 16 h photoperiod, 18 $\mu mol \cdot m^{-2} \cdot s^{-1}$). Living tissues were sub-cultured every 14 days onto fresh media. Developed shoots were excised and cultured onto rooting media (MS, 30 g/L sucrose, 7.5 mg/L hygromycin, 400 mg/L timentin, 2 g/L Gelzan™, pH 5.8) and maintained until roots developed. After rooting, plantlets were carefully removed from culture, potted into potting soil (Sungro Horticulture Sunshine® Mix #1), and maintained until seed set, at which point seed was harvested for subsequent screening.

Mutant phenotyping under high temperature conditions

A portion of T_1 lines, derived from T_0 plants from all cultivars and plasmids, were selected at random to phenotype under high temperature conditions. One-hundred seeds of each T_1 line (or the total amount of seed in the T_1 line if it was less than 100) and WT seeds, comprising 16.67% of each planting, were planted into moistened Grodan® ROCKWOOL® cubes (AO 36×40 10 cm x 10 cm) for germination under room temperature conditions for ~ 9 days. Seedlings were distributed into Nutrient Film Technique (NFT) channels with 1 WT plant randomly assigned for every 5 T_1 plants (planting density of 58.1 plants/m^2), with its position being determined by Random Number Generator® (UXAPPSLTD). Plants were screened in a modified shipping container outfitted with GE Arize® LED light bars, under a 20-hour photoperiod. Four different spectral combinations were utilized, i.e., PKB, BRI, PPV, and PKF. PKB lights yield

16B:15G:69R spectrum (89.8 $\mu mol \cdot m^{-2} \cdot s^{-1}$), BRI is 15B:38G:47R (76.9 $\mu mol \cdot m^{-2} \cdot s^{-1}$), PPV yield 40B:60R (58.1 $\mu mol \cdot m^{-2} \cdot s^{-1}$) , and PKF yields 8B:15G:72R:5FR (57.4 $\mu mol \cdot m^{-2} \cdot s^{-1}$). Temperatures were maintained at a constant 30.38 ± 1.92 ℃, CO_2 was maintained at ~400 ppm, and relative humidity (RH) averaged 67.06 ± 12.78%. Plants were fertilized with Peter's Professional 20-20-20 (400 ppm) supplemented with $CaCl_2$ (316 ppm) and fertigation solution E.C. was maintained at ~1.64 mS/cm, pH 5.8.

An assessment of WT plant maturity was performed to determine the ideal time to collect data, i.e. when a majority of WT plants exhibited stem elongation ≥8 cm, as lettuce plants with elongated stems of 8 cm in length were considered 'bolting' (Hao et al., 2018; Ito et al., 1963). T_1 plants that had not bolted were retained for an observation period of an additional 7 days. T_1's that had still not bolted were retained in the treatment conditions to clock the time of bolting, and plants were maintained for seed set. Upon seed harvest, T_2 lines were either screened under the same conditions, or in a greenhouse from 12/3/23 (9 hours and 53 minutes photoperiod) – 6/15/24 (14 hours and 34 minutes photoperiod) with an average temperature of 28.41 ± 3.54 ℃ and RH of 49.21 ± 13.49%, with the same fertilizer regime and ambient CO_2. The planting density was 77.5 plants/m^2. Twenty seeds of each T_2 line were planted for vertical farm screening, while 14 seeds of each T_2 line were planted for greenhouse screening. Wild-type plants were included in vertical farm screenings (16.67% per planting) and greenhouse screenings (12.5% per planting), as described above.

Genotyping

DNA was extracted from leaf discs using the DNeasy® Plant Mini Kit (QIAGEN). PCR amplification for sequencing was performed with PrimeSTAR® Max high-fidelity DNA

polymerase using primers flanking gRNA targets (LsFT186_fw, LsFT186_rv, LsFT456_fw, LsFT456_rv, LsFLD_400_fw, LsFLD_786_rv, LsFCA_40_fw, LsFCA_210_rv; **Table 4**). PCR amplicons from candidate lines were purified with the QIAquick® PCR Purification kit. Amplicons were subject to Sanger sequencing and subsequent chromatogram decoding with the TIDE program to estimate the frequency of indels in the sample (Brinkman et al., 2014; Pan et al., 2022; Zhan et al., 2020). A selection of amplicons estimated to have an indel frequency ≥5% were then subject to cloning with the pCR^{TM}8/GW/TOPO (Invitrogen) entry vector. After cloning, ligation products were transformed into DH5α competent cells. After selection on LB plates containing 200 μg/mL spectinomycin, positive colonies were Sanger sequenced with the T7 primer and the DNA sequence analyzed for edits using Sequencher 5.4.6 software (genecodes.com). Ten colonies per procedure were sequenced to identify edits in the target region. Lines subject to analysis by cloning were further assessed for edits by deep amplicon sequencing (Oxford Nanopore long read) and analysis by CRISPResso2 (Clement et al., 2019), to identify edits that may not have been identified by clone sequencing.

References

Abbott A (2010) The isolation of flowering time genes from lettuce to enable the manipulation of bolting time (Doctoral dissertation). University of Warwick

Adams S, Allen T, Whitelam GC (2009) Interaction between the light quality and flowering time pathways in *Arabidopsis*. Plant J **60**: 257–267

Al-Said F, Hadley P, Pearson S, Khan MM, Iqbal Q (2018) Effect of high temperature and exposure duration on stem elongation of iceberg lettuce. Pakistan J Agric Sci **55**: 95–101

Amara U, Hu J, Cai J, Kang H (2023) FLK is an mRNA m6A reader that regulates floral transition by modulating the stability and splicing of *FLC* in *Arabidopsis*. Mol Plant **16**: 919–929

Ampomah-Dwamena C, Conner AJ, Fautrier AG, Ampomah-Dwamena C, Conner AJ, Fautrier AG (1997) Genotypic response of lettuce cotyledons to regeneration in vitro. Sci Hortic (Amsterdam) **71**: 137–145

Ausín I, Alonso-Blanco C, Jarillo JA, Ruiz-García L, Martínez-Zapater JM (2004) Regulation of flowering time by FVE, a retinoblastoma-associated protein. Nat Genet **36**: 162–166

Badouin H, Gouzy J, Grassa CJ, Murat F, Staton SE, Cottret L, Lelandais-Brière C, Owens GL, Carrère S, Mayjonade B, et al (2017) The sunflower genome provides insights into oil metabolism, flowering and Asterid evolution. Nature **546**: 148–152

Bagnall D (1993) Light quality and vernalization interact in controlling late flowering in *Arabidopsis* ecotypes and mutants. Ann Bot **71**: 75–83

Balasubramanian S, Sureshkumar S, Lempe J, Weigel D (2006) Potent induction of *Arabidopsis thaliana* flowering by elevated growth temperature. PLoS Genet **2**: e106

Biswas S, Tian J, Li R, Chen X, Luo Z, Chen M, Zhao X, Zhang D, Persson S, Yuan Z, et al (2020) Investigation of CRISPR/Cas9-induced *SD1* rice mutants highlights the importance of molecular characterization in plant molecular breeding. J Genet Genomics **47**: 273–280

Blackman BK, Rasmussen DA, Strasburg JL, Raduski AR, Burke JM, Knapp SJ, Michaels SD, Rieseberg LH (2011) Contributions of flowering time genes to sunflower domestication and improvement. Genetics **187**: 271–287

Blázquez MA, Ahn JH, Weigel D (2003) A thermosensory pathway controlling flowering time in *Arabidopsis thaliana*. Nat Genet **33**: 168–171

Beracochea V, Stritzler M, Radonic L, Bottero E, Jozefkowicz C, Darqui F, Ayub N, Bilbao ML, Soto G (2023) CRISPR/Cas9-mediated knockout of *SPL13* radically increases lettuce yield. Plant Cell Rep **42**: 645–647

Bertier LD, Ron M, Huo H, Bradford KJ, Britt AB, Michelmore RW (2018) High-resolution analysis of the efficiency, heritability, and editing outcomes of CRISPR/Cas9-induced modifications of *NCED4* in lettuce (*Lactuca sativa*). G3 **8**: 1513–1521

Brinkman EK, Chen T, Amendola M, Van Steensel B (2014) Easy quantitative assessment of genome editing by sequence trace decomposition. Nucleic Acids Res **42**: e168–e168

Burner N, Kernodle SP, Steede T, Lewis RS (2022) Editing of *A622* genes results in ultra-low nicotine whole tobacco plants at the expense of dramatically reduced growth and development. Mol Breed **42**: 1–10

Chen Z, Zhao W, Ge D, Han Y, Ning K, Luo C, Wang S, Liu R, Zhang X, Wang Q (2018a) LCM-seq reveals the crucial role of LsSOC1 in heat-promoted bolting of lettuce (*Lactuca sativa* L.). Plant J **95**: 516–528

Chen Z, Han Y, Ning K, Ding Y, Zhao W, Yan S, Luo C, Jiang X, Ge D, Liu R, et al (2018b) Inflorescence development and the role of LsFT in regulating bolting in lettuce (*Lactuca sativa* L.). Front Plant Sci **8**: 2248

Cheng P, Dong B, Wang H, Cao P, Liu T, Liu Y, Gao J, Liao Y, Fang W, Chen S, et al (2018) A transcriptomic analysis targeting genes involved in the floral transition of winter-flowering *Chrysanthemum*. J Plant Growth Regul **37**: 220–232

Choi SH, Ahn WS, Jie EY, Cho HS, Kim SW (2022) Development of late-bolting plants by CRISPR/Cas9-mediated genome editing from mesophyll protoplasts of lettuce. Plant Cell Rep **41**: 1627–1630

Clement K, Rees H, Canver MC, Gehrke JM, Farouni R, Hsu JY, Cole MA, Liu DR, Joung JK, Bauer DE, et al (2019) CRISPResso2 provides accurate and rapid genome editing sequence analysis. Nat Biotechnol **37**: 224–226

Davey MR, Anthony P, Van Hooff P, Power JB, Lowe KC (2007) Lettuce. In: Pua EC, Davey MR (eds) Transgenic Crops IV. Biotechnology in Agriculture and Forestry, vol 59. Springer, Berlin, Heidelberg, pp 221–249

Debbarma J, Saikia B, Singha DL, Das D, Keot AK, Maharana J, Velmurugan N, Arunkumar KP, Reddy PS, Chikkaputtaiah C (2023) CRISPR/Cas9-Mediated Mutation in *XSP10* and *SlSAMT* Genes Impart Genetic Tolerance to Fusarium Wilt Disease of Tomato (*Solanum lycopersicum* L.). Genes (Basel) **14**: 488

Dong, Hao; Yijun Zhao, Yingli Wang HL (2014) Recombinant proteins expressed in lettuce. Indian J Biotechnol **13**: 427–436

Fang X, Wu Z, Raitskin O, Webb K, Voigt P, Lu T, Howard M, Dean C (2020) The 3' processing of antisense RNAs physically links to chromatin-based transcriptional control. Proc Natl Acad Sci USA **117**: 15316–15321

Feng Z, Mao Y, Xu N, Zhang B, Wei P, Yang DL, Wang Z, Zhang Z, Zheng R, Yang L, et al (2014) Multigeneration analysis reveals the inheritance, specificity, and patterns of CRISPR/Cas-induced gene modifications in *Arabidopsis*. Proc Natl Acad Sci USA **111**: 4632–4637

Fernández V, Takahashi Y, Le Gourrierec J, Coupland G (2016) Photoperiodic and thermosensory pathways interact through CONSTANS to promote flowering at high temperature under short days. Plant J **86**: 426–440

Folta KM (2019) Breeding new varieties for controlled environments. Plant Biol **21**: 6–12

Fujiwara S, Nakagawa M, Oda A, Kato K, Mizoguchi T (2010) Photoperiod pathway regulates expression of *MAF5* and *FLC* that encode MADS-box transcription factors of the FLC family in *Arabidopsis*. Plant Biotechnol **27**: 447–454

Fukuda M, Matsuo S, Kikuchi K, Kawazu Y, Fujiyama R, Honda I (2011) Isolation and functional characterization of the *FLOWERING LOCUS T* homolog, the *LsFT* gene, in lettuce. J Plant Physiol **168**: 1602–1607

Fukuda M, Yanai Y, Nakano Y, Sasaki H, Uragami A, Okada K (2016) Isolation and gene expression analysis of flowering-related genes in lettuce (*Lactuca sativa* L.). Hortic J **36**: 1–9

Gao X, Chen J, Dai X, Zhang D, Zhao Y (2016) An Effective Strategy for Reliably Isolating Heritable and Cas9-Free *Arabidopsis* Mutants Generated by CRISPR/Cas9-Mediated Genome Editing. Plant Physiol **171**: 1794–1800

Gao Y, Gao Y, Fan M, Yuan L, Wu Z, Zhang Q (2017) Overexpression of *Chrysanthemum morifolium SVP* gene delays blossoming and regulates inflorescence architecture in transgenic *Arabidopsis*. Can J Plant Sci **97**: 1130–1139

Gu X, Jiang D, Yang W, Jacob Y, Michaels SD, He Y (2011) *Arabidopsis* homologs of retinoblastoma-asociated protein 46/48 associate with a histone deacetylase to act redundantly in chromatin silencing. PLoS Genet **7**: e1002366

Halliday KJ, Koornneef M, Whitelam GC (1994) Phytochrome B and at Least One Other Phytochrome Mediate the Accelerated Flowering Response of *Arabidopsis thaliana* L. to Low Red/Far-Red Ratio. Plant Physiol **104**: 1311–1315

Halliday KJ, Salter MG, Thingnaes E, Whitelam GC (2003) Phytochrome control of flowering is temperature sensitive and correlates with expression of the floral integrator *FT*. Plant J **33**: 875–885

Han Y, Zhu B, Luan F, Zhu H, Shao Y, Chen A, Lu C, Luo Y (2010) Conserved miRNAs and their targets identified in lettuce (*Lactuca*) by EST analysis. Gene **463**: 1–7

Hao JH, Zhang LL, Li PP, Sun YC, Li JK, Qin XX, Wang L, Qi ZY, Xiao S, Han YY, et al (2018) Quantitative proteomics analysis of lettuce (*Lactuca sativa* L.) reveals molecular basis-associated auxin and photosynthesis with bolting induced by high temperature. Int J Mol Sci **19**: 2967

Hao J, Yang J, Liu X, Pan G, Li Y, Zhang X, Han Y, Fan S, Zhou Z (2022) Molecular basis of high temperature-induced bolting in lettuce revealed by multi-omics analysis. BMC Genomics **23**: 1–9

He Y, Michaels SD, Amasino RM (2003) Regulation of flowering time by histone acetylation in *Arabidopsis*. Science **302**: 1751–1754

Henderson IR, Liu F, Drea S, Simpson GG, Dean C (2005) An allelic series reveals essential roles for FY in plant development in addition to flowering-time control. Development **132**: 3597–3607

Hernández R, Spalholz H (2019) Characterization of Solar Radiation Spectral Contribution in Lettuce Bolting and Flowering Using LEDs in an Indoor Setting (Conference Presentation). Am. Soc. Hortic. Sci. Annu. Conf.

Ho WWH, Weigel D (2014) Structural features determining flower-promoting activity of *Arabidopsis* FLOWERING LOCUS T. Plant Cell **26**: 552–564

Hornyik C, Terzi LC, Simpson GG (2010) The spen family protein FPA controls alternative cleavage and polyadenylation of RNA. Dev Cell **18**: 203–213

Huang Y, Xing X, Tang Y, Jin J, Ding L, Song A, Chen S, Chen F, Jiang J, Fang W (2021) CmERF110 interacts with CmFLK to accelerate flowering through the circadian clock in *Chrysanthemum morifolium*. In: *The 8th International Horticulture Research Conference*.

Hyun Y, Kim J, Cho SW, Choi Y, Kim JS, Coupland G (2015) Site-directed mutagenesis in *Arabidopsis thaliana* using dividing tissue-targeted RGEN of the CRISPR/Cas system to generate heritable null alleles. Planta **241**: 271–284

Ishizaki T (2016) CRISPR/Cas9 in rice can induce new mutations in later generations, leading to chimerism and unpredicted segregation of the targeted mutation. Mol Breed **36**: 1–15

Ito H, Kato T, Konno Y (1963) Factors associated with the flower induction in lettuce. Tohoku J Agric Res **12**: 51–65

Jang G, Lee S, Um TY, Chang SH, Lee HY, Chung PJ, Kim JK, Do Choi Y (2016) Genetic chimerism of CRISPR/Cas9-mediated rice mutants. Plant Biotechnol Rep **10**: 425–435

Janga MR, Campbell LAM, Rathore KS (2017) CRISPR/Cas9-mediated targeted mutagenesis in upland cotton (*Gossypium hirsutum* L.). Plant Mol Biol **94**: 349–360

Kim JJ, Lee JH, Kim W, Jung HS, Huijser P, Ahn JH (2012) The *microRNA156*-SQUAMOSA PROMOTER BINDING PROTEIN-LIKE3 module regulates ambient temperature-responsive flowering via *FLOWERING LOCUS T* in *Arabidopsis*. Plant Physiol **159**: 461–478

Kishchenko O, Zhou Y, Jatayev S, Shavrukov Y, Borisjuk N (2020) Gene editing applications to modulate crop flowering time and seed dormancy. aBIOTECH **1**: 233–245

Lavelle DO (2009) Genetics of candidate genes for developmental and domestication-related traits in lettuce (Doctoral dissertation). University of California, Davis

Lee I, Aukerman MJ, Gore SL, Lohman KN, Michaels SD, Weaver LM, John MC, Feldmann KA, Amasino RM (1994) Isolation of *LUMINIDEPENDENS*: A gene involved in the control of flowering time in *Arabidopsis*. Plant Cell **6**: 75–83

Leijten W, Koes R, Roobeek I, Frugis G (2018) Translating flowering time from *Arabidopsis thaliana* to Brassicaceae and Asteraceae crop species. Plants **7**: 111

Li D, Liu C, Shen L, Wu Y, Chen H, Robertson M, Helliwell, CA, Ito T, Meyerowitz E, Yu H (2008) A repressor complex governs the integration of flowering signals in *Arabidopsis*. Dev Cell **15**: 110–120

Li Y, Zhu J, Feng Y, Li Z, Ren Z, Liu N, Liu C, Hao J, Han Y (2022) LsARF3 mediates thermally induced bolting through promoting the expression of *LsCO* in lettuce (*Lactuca sativa* L.). Front Plant Sci **13**: 958833

Lim MH, Kim J, Kim YS, Chung KS, Seo YH, Lee I, Kim J, Hong CB, Kim HJ, Park CM (2004) A new *Arabidopsis* gene, *FLK*, encodes an RNA binding protein with K homology motifs and regulates flowering time via *FLOWERING LOCUS C*. Plant Cell **16**: 731–740

Liu F, Quesada V, Crevillé P, Bä Urle I, Swiezewski S, Dean C (2007) The *Arabidopsis* RNA-binding protein FCA requires a lysine-specific demethylase 1 homolog to downregulate *FLC*. Mol Cell **28**: 398–407

Liu F, Marquardt S, Lister C, Swiezewski S, Dean C (2010) Targeted 3′ processing of antisense transcripts triggers *Arabidopsis FLC* chromatin silencing. Science **327**: 94–97

Liu W, Mazarei M, Rudis MR, Fethe MH, Stewart CN (2011) Rapid in vivo analysis of synthetic promoters for plant pathogen phytosensing. BMC Biotechnol **11**: 1-9.

Liu W, Mazarei M, Rudis MR, Fethe MH, Peng Y, Millwood RJ, Schoene G, Burris JN, Stewart Jr CN (2013) Bacterial pathogen phytosensing in transgenic tobacco and *Arabidopsis* plants. Plant Biotechnol J **11**: 43-52.

Liu L, Zhang Y, Yu H (2020a) Florigen trafficking integrates photoperiod and temperature signals in *Arabidopsis.* J Integr Plant Biol **62**: 1385–1398

Liu W, Rudis MR, Cheplick MH, Millwood RJ, Yang JP, Ondzighi-Assoume CA, Montgomery GA, Burris KP, Mazarei M, Chesnut JD, et al (2020b) Lipofection-mediated genome editing using DNA-free delivery of the Cas9/gRNA ribonucleoprotein into plant cells. Plant Cell Rep **39**: 245–257

Locascio A, Lucchin M, Varotto S (2009) Characterization of a *MADS FLOWERING LOCUS C-LIKE* (*MFL*) sequence in *Cichorium intybus*: A comparative study of *CiMFL* and *AtFLC* reveals homologies and divergences in gene function. New Phytol **182**: 630–643

Luo X, Chen T, Zeng X, He D, He Y (2019) Feedback regulation of *FLC* by FLOWERING LOCUS T (FT) and FD through a 5' *FLC* promoter region in *Arabidopsis*. Mol Plant **12**: 285–288

Ma X, Zhang Q, Zhu Q, Liu W, Chen Y, Qiu R, Wang B, Yang Z, Li H, Lin Y, et al (2015) A Robust CRISPR/Cas9 System for Convenient, High-Efficiency Multiplex Genome Editing in Monocot and Dicot Plants. Mol Plant **8**: 1274–1284

Macknight R, Duroux M, Laurie R, Dijkwel P, Simpson G, Dean C (2002) Functional significance of the alternative transcript processing of the *Arabidopsis* floral promoter *FCA*. Plant Cell **14**: 877–888

Marín-González E, Matías-Hernández L, Aguilar-Jaramillo AE, Lee JH, Ahn JH, Suárez-López P, Pelaz S (2015) SHORT VEGETATIVE PHASE up-regulates *TEMPRANILLO2* floral repressor at low ambient temperatures. Plant Physiol **169**: 1214–1224

Marquardt S, Raitskin O, Wu Z, Liu F, Sun Q, Dean C (2014) Functional consequences of splicing of the antisense transcript *COOLAIR* on *FLC* transcription. Mol Cell **54**: 156

Mateos JL, Madrigal P, Tsuda K, Rawat V, Richter R, Romera-Branchat M, Fornara F, Schneeberger K, Krajewski P, Coupland G (2015) Combinatorial activities of SHORT VEGETATIVE PHASE and FLOWERING LOCUS C define distinct modes of flowering regulation in *Arabidopsis*. Genome Biol **16**: 1–23

Mathieu AS, Lutts S, Vandoorne B, Descamps C, Perilleux C, Dielen V, Van Herck J-C, Quinet M (2014) High temperatures limit plant growth but hasten flowering in root chicory (*Cichorium intybus*) independently of vernalisation. J Plant Physiol **171**: 109–118

Mathieu AS, Périlleux C, Jacquemin G, Renard ME, Lutts S, Quinet M (2020a) Impact of vernalization and heat on flowering induction, development and fertility in root chicory (*Cichorium intybus* L. var. *sativum*). J Plant Physiol **254**: 153272

Mathieu AS, Dobrev PI, Tarkowská D, Pospíšil J, Motyka V, Jacquemin G, Quinet M, Lutts S (2020b) Phytohormone profile and *CiFL1* expression in young seedlings of *Cichorium intybus* L. var. *sativum* exposed to high temperature in relation to vernalization and de-vernalization processes. Environ Exp Bot **178**: 104127

Meng Q, Runkle ES (2019) Regulation of flowering by green light depends on its photon flux density and involves cryptochromes. Physiol Plant **166**: 762–771

Meng Q, Kelly N, Runkle ES (2019) Substituting green or far-red radiation for blue radiation induces shade avoidance and promotes growth in lettuce and kale. Environ Exp Bot **162**: 383–391

Michno JM, Virdi K, Stec AO, Liu J, Wang X, Xiong Y, Stupar RM (2020) Integration, abundance, and transmission of mutations and transgenes in a series of CRISPR/Cas9 soybean lines. BMC Biotechnol **20**: 1–13

Movahedi A, Wei H, Zhou X, Fountain JC, Chen ZH, Mu Z, Sun W, Zhang J, Li D, Guo B, et al (2022) Precise exogenous insertion and sequence replacements in poplar by simultaneous *HDR* overexpression and NHEJ suppression using CRISPR-Cas9. Hortic Res **9**: uhac154

Murashige T, Skoog F (1962) A revised medium for rapid growth and bioassay with tobacco tissue cultures. Physiol Plant **15**: 473–479

Nakano Y, Higuchi Y, Sumitomo K, Oda A, Hisamatsu T, Naro (2015) Delay of flowering by high temperature in *Chrysanthemum*: heat-sensitive time-of-day and heat effects on *CsFTL3* and *CsAFT* gene expression. J Hortic Sci Biotechnol **90**: 143–149

Nguyen CD, Li J, Mou B, Gong H, Huo H, Nguyen CD, Li J, Mou B, Gong H, Huo H (2021) A case study of using an efficient CRISPR/Cas9 system to develop variegated lettuce. Veg Res **1**: 1–10

Nitarska D, Boehm R, Debener T, Lucaciu RC, Halbwirth H (2021) First genome edited poinsettias: targeted mutagenesis of flavonoid 3′-hydroxylase using CRISPR/Cas9 results in a colour shift. Plant Cell Tissue Organ Cult **147**: 49–60

Pan C, Ye L, Qin L, Liu X, He Y, Wang J, Chen L, Lu G (2016) CRISPR/Cas9-mediated efficient and heritable targeted mutagenesis in tomato plants in the first and later generations. Sci Rep **6**: 1–9

Pan W, Liu X, Li D, Zhang H (2022) Establishment of an efficient genome editing system in lettuce without sacrificing specificity. Front Plant Sci **13**: 930592

Peng A, Chen S, Lei T, Xu L, He Y, Wu L, Yao L, Zou X (2017) Engineering canker-resistant plants through CRISPR/Cas9-targeted editing of the susceptibility gene *CsLOB1* promoter in citrus. Plant Biotechnol J **15**: 1509–1519

Périlleux C, Pieltain A, Jacquemin G, Bouché F, Detry N, D'Aloia M, Thiry L, Aljochim P, Delansnay M, Mathieu A, et al (2013) A root chicory MADS box sequence and the *Arabidopsis* flowering repressor *FLC* share common features that suggest conserved function in vernalization and de-vernalization responses. Plant J **75**: 390–402

Puglia G, Raccuia SA, Pappalardo H, Genovese C, Argento S, Melilli MG (2015) Characterization of a *MADS FLOWERING LOCUS C - LIKE* (*MFL*) in *Cynara cardunculus*

var. *altilis* under different sowing and planting density. In: *IX International Symposium on Artichoke, Cardoon and Their Wild Relatives 1147*, pp. 301-308

Qi PL, Zhou HR, Zhao QQ, Feng C, Ning YQ, Su YN, Cai XW, Yuan DY, Zhang ZC, Su XM, et al (2022) Characterization of an autonomous pathway complex that promotes flowering in *Arabidopsis*. Nucleic Acids Res **50**: 7380–7395

Reyes-Chin-Wo S, Wang Z, Yang X, Kozik A, Arikit S, Song C, Xia L, Froenicke L, Lavelle DO, Truco M-J, et al (2017) Genome assembly with in vitro proximity ligation data and whole-genome triplication in lettuce. Nat Commun **8**: 14953

Riu YS, Kim GH, Chung KW, Kong SG (2023) Enhancement of the CRISPR/Cas9-based genome editing system in lettuce (*Lactuca sativa* L.) using the endogenous *U6* promoter. Plants **12**: 878

Rosental L, Still DW, You Y, Hayes RJ, Simko I (2021) Mapping and identification of genetic loci affecting earliness of bolting and flowering in lettuce. Theor Appl Genet **134**: 3319–3337

Samach A, Onouchi H, Gold SE, Ditta GS, Schwarz-Sommer Z, Yanofsky MF, Coupland G (2000) Distinct roles of constans target genes in reproductive development of *Arabidopsis*. Science **288**: 1613–1616

Samarth, Lee R, Song J, Macknight RC, Jameson PE (2019) Identification of flowering-time genes in mast flowering plants using *de novo* transcriptomic analysis. PLoS ONE **14**: e0216267

Samarth, Lee R, Kelly D, Turnbull MH, Macknight RC, Poole AM, Jameson PE (2021) Molecular control of the floral transition in the mast seeding plant *Celmisia lyallii* (Asteraceae). Mol Ecol **30**: 1846–1863

Sanda SL, Amasino RM (1996a) Interaction of FLC and late-flowering mutations in *Arabidopsis thaliana*. Mol Gen Genet **251**: 69–74

Sanda SL, Amasino RM (1996b) Ecotype-specific expression of a flowering mutant phenotype in *Arabidopsis thaliana*. Plant Physiol **111**: 641–644

Schwartz CJ, Lee J, Amasino R (2017) Variation in shade-induced flowering in *Arabidopsis thaliana* results from *FLOWERING LOCUS T* allelic variation. PLoS ONE **12**: e0187768

Simpson GG, Dijkwel PP, Quesada V, Henderson I, Dean C (2003) FY is an RNA 3′ end-processing factor that interacts with FCA to control the *Arabidopsis* floral transition. Cell **113**: 777–787

Smith WA, Matsuba Y, Dewey RE (2022) Knockout of a key gene of the nicotine biosynthetic pathway severely affects tobacco growth under field, but not greenhouse conditions. BMC Res Notes **15**: 1–6

Song GQ, Urban G, Ryner JT, Zhong GY (2022a) Gene Editing Profiles in 94 CRISPR-Cas9 Expressing T_0 Transgenic Tobacco Lines Reveal High Frequencies of Chimeric Editing of the Target Gene. Plants **11**: 3494

Song H, Ahn JY, Yan F, Ran Y, Koo O, Lee GJ (2022b) Genetic Dissection of CRISPR-Cas9 Mediated Inheritance of Independently Targeted Alleles in Tobacco *α-1,3-Fucosyltransferase 1* and *β-1,2-Xylosyltransferase 1* Loci. Int J Mol Sci **23**: 2450

Song X, Xie Y, Tian X, Wang N, Zhou Y, Xie Z, Ye J, Deng X (2023) CRISPR/Cas9 editing characteristics of multiple transgenic generations in *Fortunella hindsii*, an early flowering mini-citrus. Sci Hortic (Amsterdam) **321**: 112236

Su J, Lu Z, Zeng J, Zhang X, Yang X, Wang S, Zhang F, Jiang J, Chen F (2024) Multi-locus genome-wide association study and genomic prediction for flowering time in *Chrysanthemum*. Planta **259**: 1–18

Susila H, Jurić S, Liu L, Gawarecka K, Chung KS, Jin S, Kim S-J, Nasim Z, Youn G, Suh MC, et al (2021) Florigen sequestration in cellular membranes modulates temperature-responsive flowering. Science **373**: 1137–1142

Van de Wiel C, Arens P, Vosman B (1998) Microsatellite fingerprinting in lettuce *(Lactuca sativa* L.) and wild relatives. Plant Cell Rep **17**: 837–842

Wang ZW, Wu Z, Raitskin O, Sun Q, Dean C (2014) Antisense-mediated *FLC* transcriptional repression requires the P-TEFb transcription elongation factor. Proc Natl Acad Sci USA **111**: 7468–7473

Waycott W (1995) Photoperiodic response of genetically diverse lettuce accessions. J Am Soc Hortic Sci **120**: 460–467

Wendell M, Ripel L, Lee YK, Rognli OA, Torre S, Olsen JE (2017) Thermoperiodic control of floral induction involves modulation of the diurnal *FLOWERING LOCUS T* expression pattern. Plant Cell Physiol **58**: 466–477

Won SY, Jung JA, Kim JS (2021) Genome-wide analysis of the MADS-Box gene family in *Chrysanthemum*. Comput Biol Chem **90**: 107424

Woo JW, Kim J, Kwon S Il, Corvalán C, Cho SW, Kim H, Kim SG, Kim ST, Choe S, Kim JS (2015) DNA-free genome editing in plants with preassembled CRISPR-Cas9 ribonucleoproteins. Nat Biotechnol **33**: 1162–1164

Xie K, Yang Y (2013) RNA-guided genome editing in plants Using a CRISPR–Cas system. Mol Plant **6**: 1975–1983

Xinrun Z, Conner AJ (1992) Genotypic effects on tissue culture response of lettuce cotyledons. J Genet Breed **46**: 287–290

Xiong X, Liu W, Jiang J, Xu L, Huang L, Cao J (2019) Efficient genome editing of *Brassica campestris* based on the CRISPR/Cas9 system. Mol Genet Genomics **294**: 1251–1261

Xu L, Zhao Z, Dong A, Soubigou-Taconnat L, Renou JP, Steinmetz A, Shen WH (2008) Di- and tri- but not monomethylation on histone H3 lysine 36 marks active transcription of genes involved in flowering time regulation and other processes in *Arabidopsis thaliana*. Mol Cell Biol **28**: 1348–1360

Xu RF, Li H, Qin RY, Li J, Qiu CH, Yang YC, Ma H, Li L, Wei PC, Yang JB (2015) Generation of inheritable and "transgene clean" targeted genome-modified rice in later generations using the CRISPR/Cas9 system. Sci Rep **5**: 1–10

Xu C, Wu Z, Duan HC, Fang X, Jia G, Dean C (2021) R-loop resolution promotes co-transcriptional chromatin silencing. Nat Commun **12**: 1–9

Yang H, Wu JJ, Tang T, Liu K De, Dai C (2017) CRISPR/Cas9-mediated genome editing efficiently creates specific mutations at multiple loci using one sgRNA in *Brassica napus*. Sci Rep **7**: 1–13

Yoo SK, Chung KS, Kim J, Lee JH, Hong SM, Yoo SJ, Yoo SY, Lee JS, Ahn JH (2005) CONSTANS activates *SUPPRESSOR OF OVEREXPRESSION OF CONSTANS 1* through *FLOWERING LOCUS T* to promote flowering in *Arabidopsis*. Plant Physiol **139**: 770–778

Yu CW, Liu X, Luo M, Chen C, Lin X, Tian G, Lu Q, Cui Y, Wu K (2011) HISTONE DEACETYLASE6 interacts with FLOWERING LOCUS D and regulates flowering in *Arabidopsis*. Plant Physiol **156**: 173–184

Yu CW, Chang KY, Wu K (2016) Genome-wide analysis of gene regulatory networks of the FVE-HDA6-FLD complex in *Arabidopsis*. Front Plant Sci **7**: 555

Yu Z, Lin J, Li QQ (2019) Transcriptome analyses of *FY* mutants reveal its role in mRNA alternative polyadenylation. Plant Cell **31**: 2332–2352

Yu XN, Guo Y, Yang Q, Yu H, Lu MJ, Zhao L, Jin ZS, Xu X, Feng JY, Wen YQ (2024) Chimeric mutations in grapevine *ENHANCED DISEASE RESISTANCE1* improve resistance to powdery mildew without growth penalty. Plant Physiol **195:** 1995–2015

Yuan C, Hu Y, Liu Q, Xu J, Zhou W, Yu H, Shen L, Qin C (2023) MED8 regulates floral transition in *Arabidopsis* by interacting with FPA. Plant J **116**: 1234–1247

Zhang N, Roberts HM, Van Eck J, Martin GB (2020) Generation and Molecular Characterization of CRISPR/Cas9-Induced Mutations in 63 Immunity-Associated Genes in Tomato Reveals Specificity and a Range of Gene Modifications. Front Plant Sci **11:** 510955

Zhang Z, Hu Q, Gao Z, Zhu Y, Yin M, Shang E, Liu G, Liu W, Hu R, Cheng H, et al (2023) Flowering repressor CmSVP recruits the TOPLESS corepressor to control flowering in *Chrysanthemum*. Plant Physiol **193**: 2413–2429

Zhen S, Bugbee B (2020) Far-red photons have equivalent efficiency to traditional photosynthetic photons: Implications for redefining photosynthetically active radiation. Plant Cell Environ **43**: 1259–1272

Table 3.1 Counts of regenerated and screened lines, and candidates with a delayed-bolting phenotype. The # of # indicates how many lines had a delayed bolting phenotype of those screened. Dash, not screened yet.

Cultivar	Plasmid	T_0	T_1	T_1 Phenotyped	Delayed Bolting		
					T_1	T_2	T_3
	pLsFT1	828	546	27	11 (40.7%)	2 of 8	2 of 2
	pLsFT2	299	208	17	6 (35.3%)	2 of 4	1 of 2
	pLsFCA1	152	88	15	4 (26.7%)	2 of 3	-
	pLsFCA2	97	59	16	8 (50.0%)	4 of 5	-
'Red Sails'	pLsFLD1	70	44	14	6 (42.9%)	5 of 6	2 of 2
	pLsFLD2	130	66	16	6 (37.5%)	2 of 5	-
	pLsFTm	119	59	16	10 (62.5%)	7 of 7	2 of 2
	pLsFCAm	127	45	14	8 (57.1%)	5 of 6	-
	pLsFLDm	303	143	17	7 (41.2%)	3 of 3	1 of 1
'Kahu'	pLsFT1	94	73	18	2 (11.1%)	2 of 2	1 of 2
	pLsFT2	80	57	16	4 (25.0%)	1 of 3	0 of 1
'Royal Oak	pLsFT1	6	6	1	1 (100.0%)	0 of 1	-
Leaf'	pLsFT2	8	5	1	1 (100.0%)	1 of 1	-

Table 3.2 Observed segregation ratios in the delayed-bolting phenotype of screened lines. Observed counts of individual plants displaying each of three phenotypes is reported. The ratio #:#:# values indicate the number of plants that bolted with WT: the number of plants with a mild bolting delay (1 -7 days): the number of plants having a bolting delay of greater than 7 days. Values in bold were not significantly different from the expected 1:2:1 ratio, according to the Chi-square goodness-of-fit test at $\alpha = 0.05$.

		Observed Segregation Ratios		
Cultivar	**Line**	**T1**	**T2**	**T3**
'Red Sails'	pLsFT1 #268	15:15:2	10:0:2	-
	pLsFT2 #82	5:0:1	1:5:31	**2:9:2**
	pLsFCA1 #5	62:11:2	13:6:4	-
	pLsFCA2 #72	26:15:20	**5:2:4**	-
	pLsFLD1 #18	**8:6:9**	**3:0:2**	-
	pLsFLD2 #15	19:2:1	21:4:4	-
	pLsFTm #6	21:6:6	0:0:13	-
	pLsFCAm #93	35:16:4	**5:7:2**	-
	pLsFCAm #116	**0:0:1**	10:2:2	-
	pLsFLDm #106	**9:15:8**	**5:5:2**	-
'Kahu'	pLsFT1 #51	24:4:5	0:0:10	0:0:3
'Royal Oak Leaf'	pLsFT2 #5	29:31:4	6:2:2	-

Table 3.3 Indel frequency estimate in candidate lines by Sanger amplicon sequencing and TIDE analysis. PCR amplicons from candidate lines were subject to Sanger sequencing and subsequent chromatogram decoding with the TIDE program (shinyapps.datacurators.nl/tide/; Brinkman et al., 2014). The percentage listed estimates frequency of indels in the pool of cells for the target region.

Cultivar	**Plasmid**	**Line**	**Gen.**	**Days delayed**	**sgRNA**	**Estimated % of indels (by TIDE)**	**pCR8 cloning**
'Red Sails'	*pLsFT1*	#268-6	T2	17	LsFT1	16.3	X
	pLsFT2	#82-1	T3	18	LsFT2	17.7	
		#82-2	T3	11		92.6	X
		#82-3	T3	33		89.3	
		#82-35	T2	12		89.1	
	pLsFCA1	#5-25	T2	30	LsFCA1	12.1	X
	pLsFCA2	#72-1	T2	33	LsFCA2	87.3	X
		#72-5	T2	40		10.3	
		#72-7	T2	42		51.6	
		#72-8	T2	38		11.8	
	pLsFLD1	#18-9	T2	19	LsFLD1	95.4	X
		#68-8	T2	14		95.6	
	pLsFLD2	#15-7	T2	14	LsFLD2	97.3	X
	pLsFTm	#6-2	T2	24	LsFT1	12.0	X
					LsFT2	3.5	
		#34-26	T2	28	LsFT1	0.6	

Table 3.3 (Continued)

Cultivar	Plasmid	Line	Gen.	Days delayed	sgRNA	Estimated % of indels (by TIDE)	pCR8 cloning
					LsFT2	5.9	
	pLsFCAm	#93-14	T2	20	LsFCA1	94.5	X
					LsFCA2	93.0	
		#116-24	T2	26	LsFCA1	7.2	X
					LsFCA2	5.9	
	pLsFLDm	#106-8	T2	27	LsFLD1	97.4	X
					LsFLD2	98.0	
		#220-5	T2	39	LsFLD1	79.9	
					LsFLD2	94.1	
‘Kahu’	*pLsFT1*	#51-1	T3	27	LsFT1	5.8	
		#51-2	T3	33		97.3	X
		#51-4	T3	21		8.6	
		#51-6	T2	11		32.8	
		#51-7	T2	12		15.4	
		#51-8	T3	31		5.8	
		#51-9	T2	20		75.1	
		#51-10	T3	29		11.6	
		#51-12	T2	20		9.8	
‘Royal Oak Leaf”	*pLsFT2*	#5-7	T2	33	LsFT2	5.6	X

Table 3.4 Primers used in the present study.

Name	Sequence (5'>3')
T7	TAATACGACTCACTATAGGG
AtU6	TTAGGCATCGAACCTTCAAG
182rv_LsFTgRNA_pMDC_top	AGGCTGATTTACCACCTGAGGTTTT
M13f	ACTGGCCGTCGTTTTAC
182rv_LsFT_gRNA_pMDC_bot	CTCAGGTGGTAAATCAGCCTCGGTG
456fw_LsFT_gRNA_pMDC_top	CGACAAACTGTGTATGCCCCGTTTT
456fw_LsFT_gRNA_pMDC_bot	GGGGCATACACAGTTTGTCGCGGTG
40fw_LsFCA_gRNA_pMDC_top	GAGGAGGAGGAGACAGGTACGTTTT
40fw_LsFCA_gRNA_pMDC_bot	GTACCTGTCTCCTCCTCCTCCGGTG
210fw_LsFCA_gRNA_pMDC_top	CCTCGTTATTCTCTTAGCGGGTTTT
210fw_LsFCA_gRNA_pMDC_bot	CCGCTAAGAGAATAACGAGGCGGTG
400fw_LsFLD_gRNA_pMDC_top	TCTTCTGTAAGTACATCCGCGTTTT
400fw_LsFLD_gRNA_pMDC_bot	GCGGATGTACTTACAGAAGACGGTG
786rv_LsFLD_gRNA_pMDC_top	TTGGAAGGAAGAAAACGTCCGTTTT
786rv_LsFLD_gRNA_pMDC_bot	GGACGTTTTCTTCCTTCCAACGGTG
182rv_LsFT_gRNA_pRGE_top	GGCAGGCTGATTTACCACCTGAG
182rv_LsFT_gRNA_pRGE_bot	AAACCTCAGGTGGTAAATCAGCCT
456fw_LsFT_gRNA_pRGE_top	GCACGACAAACTGTGTATGCCCC
456fw_LsFT_gRNA_pRGE_bot	AAACGGGGCATACACAGTTTGTCG
40fw_LsFCA_gRNA_pRGE_top	GGCAGAGGAGGAGGAGACAGGTAC
40fw_LsFCA_gRNA_pGRE_bot	AAACGTACCTGTCTCCTCCTCCTC

Table 3.4 (Continued)

Name	Sequence (5'>3')
210fw_LsFCA_gRNA_pGRE_top	GGCACCTCGTTATTCTCTTAGCGG
210fw_LsFCA_gRNA_pGRE_bot	AAACCCGCTAAGAGAATAACGAGG
400fw_LsFLD_gRNA_pRGE_top	GGCATCTTCTGTAAGTACATCCGC
400fw_LsFLD_gRNA_pRGE_bot	AAACGCGGATGTACTTACAGAAGA
786rv_LsFLD_gRNA_pRGE_top	GGCATTGGAAGGAAGAAAACGTCC
786rv_LsFLD_gRNA_pGRE_bot	AAACGGACGTTTTCTTCCTTCCAA
LsFT186_fw	ACCGGCTTTAAAGAAACACAAC
LsFT186_rv	CATCAGGATCGACCATCACCT
LsFT456_fw	TCCCGGATCAAATGCCGAAA
LsFT456_rv	TCGTGATAATATGGTGTGCAAGC
SpeI-BaeI-gRNAscaf-for	TTTTACTAGTCCGGATCCACG
EcoRI-SbfI-gRNAscaf-rev	GAGAATTCCTGCAGGAAAAAAGCACCGACTCG
NotI-SbfI-OsU3-for	ATGCGGCCGCCTGCAGGAAGGAATCTTTAAACA TACG
XbaI-OsU3-rev	AGTCTAGATGCCACGGATCATCTGCACAAC
pRGEB31_Cas9_fw	CATCGAGCAGATCAGCGAGT
pRGEB31_Cas9_rv	CGATCCGTGTCTCGTACAGG
pRGEB31_HygR_fw	CAATGACCGCTGTTATGCGG
pRGEB31_HygR_rv	GCTCTCGATGAGCTGATGCT
pMDC_AtU6_rv1	CCAGGGGCCTTTGAAGATTA
pMDC_AtU6_rv2	TGCTTCTCTTCTTTCAGATTC

Table 3.4 (Continued)

Name	Sequence (5'>3')
LsFLD_400_fw	AGCAGCACAAGTAGGTGTATCC
LsFLD_786_rv	CCCAAGAGGGTTTCCATGTGTA
LsFCA_40_fw	GCAAAACTCATGTCAGGGGG
LsFCA_210_rv	AAGCAAGCTACCTGGAGAAGG

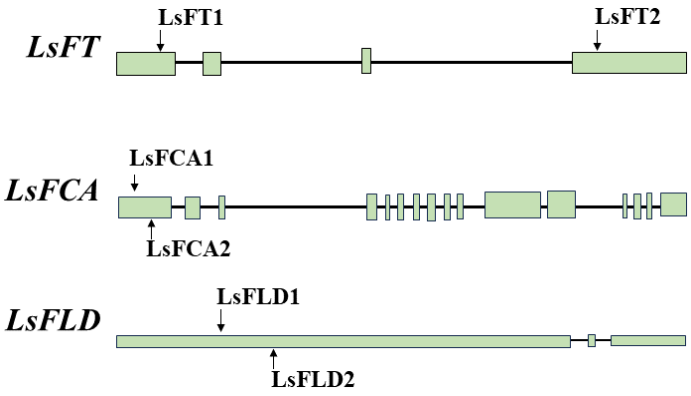

Figure 3.1 Relative position of guides on target genes. The relative position of guides on each of *LsFT* (LsFT1, LsFT2), *LsFCA* (LsFCA1, LsFCA2) and *LsFLD* (LsFLD1, LsFLD2) is shown. Exons are represented by green bars and introns are represented by black lines. Images not to scale.

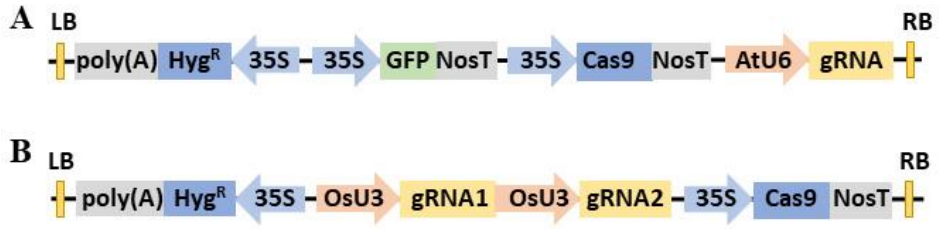

Figure 3.2 Plasmids used in this study. (A) Plasmid map of p-sgRNA. (B) Plasmid map of p-sgRNAm.

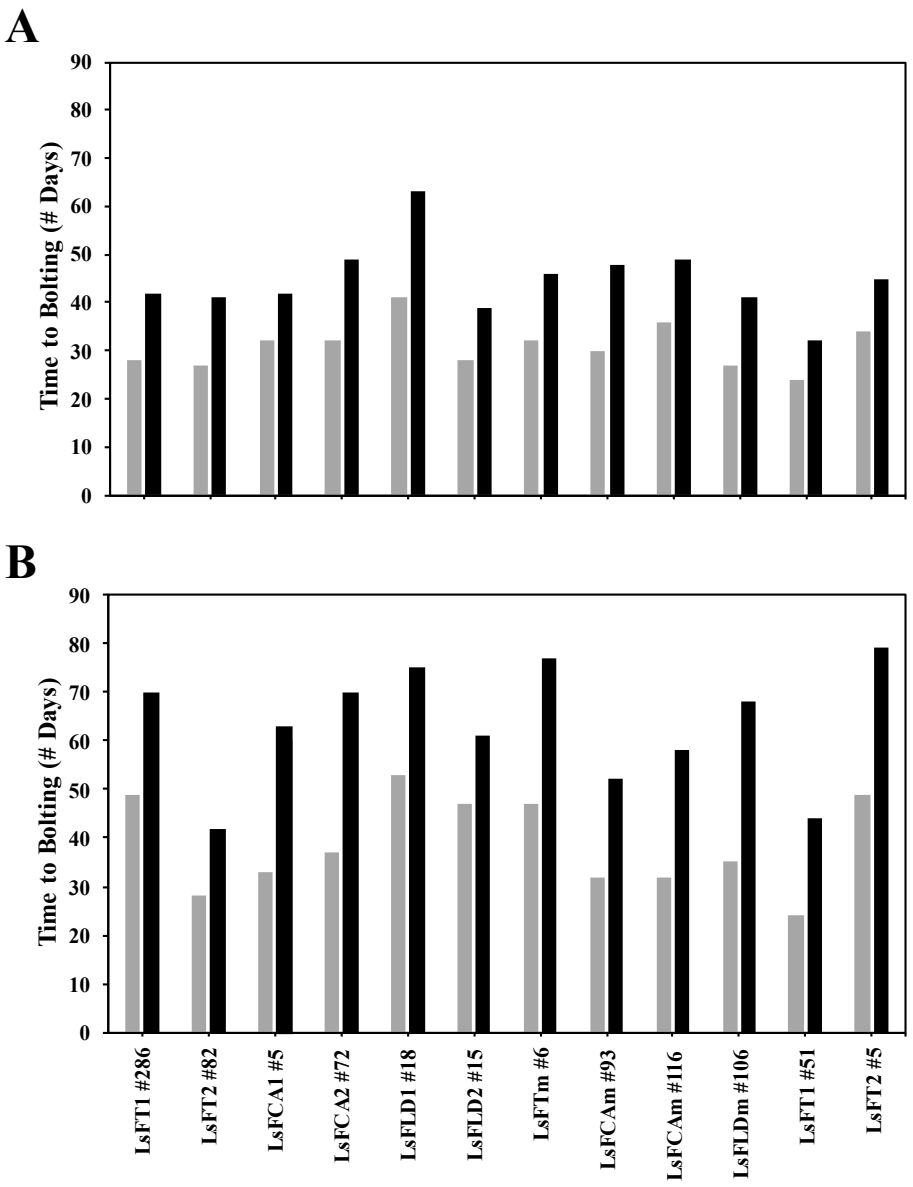

Figure 3.3 Measure of delayed-bolting days in candidate T_1 (A) and T_2 (B) lines. The number of days delayed indicates the time (day) difference for the plant stem to reach 8 cm in length between each indicated line and its respective cultivar WT.

Figure 3.4 Images of delayed-bolting plants. For each image, a representative WT plant, planed in the treatment at the same time, sits to the left. A. ‘Red Sails’ pLsFT1 #268, B. ‘Red Sails pLsFT2 #82, C. ‘Red Sails’ pLsFCA1 #5, D. ‘Red Sails’ pLsFCA2 #72, E. ‘Red Sails’ pLsFLD1 #18, F. ‘Red Sails’ pLsFLD2 #15, G. ‘Red Sails’ pLsFTm #6, H. ‘Red Sails’ pLsFCAm #93, I. ‘Red Sails’ pLsFCAm #116, J. ‘Red Sails’ pLsFLDm #106, K. ‘Kahu’ pLsFT1 #51, and L. ‘Royal Oak Leaf’ pLsFT2 #5.


A
8 cm
B
8 cm
C
8
D
8 cm
E
8 cm
F
8 cm
G
8 cm
H
8 cm
I
8 cm
J
8 cm
K
8 cm
L
8 cm

APPENDICES

Appendix A

Table A1. Literature review of *A. tumefaciens*-mediated lettuce transformation and regeneration methods.

Cultivar	Explant	Explant Age (days)	Antibiotic Conc. (mg/L)	*Agro* Strain	OD^{600}	Co-cultivation Time (days)	Auxin (mg/L)	Cytokinin (mg/L)	Ref
'Achát'	Cotyledon	10	100 Kan	LBA4404	0.9	1	0.93 NAA	0.56 BA	[1]
'Zhouye'	Cotyledon	N/A	50 Kan	EHA105	0.5 - 0.6	1.5	0.1 NAA	0.25 BA	[2]
'Lake Nyah', 'Mantillia', 'Bastion', 'Carvello', 'Cortina', 'Evola', 'Flora', 'Luxor', 'Omega', 'Reflex', 'Danilla', 'Impulse', 'Lobjoits'	Cotyledon	7	50-**100** Kan	LBA4404	1.1 - 1.6	2	0.04 NAA	0.5 BA	[3]
'Lake Nyah'	Cotyledon	7	100 Kan	LBA4404	N/A	2	0.04 NAA	0.5 BA	[4]
'Saladin'	Cotyledon	7	50, 100 Kan	LBA4404	1.1 - 1.6	2	0.04 NAA	0.5 BA	[5]
'Veronica'	Cotyledon	2	10 Hyg	EHA105	N/A	0.01	0.1 IBA	0.1 BA	[6]
'Cocarde', 'Girelle', 'Jessy'	Leaf	7	200 Kan	GV2260	N/A	1 - 5	0.3 IAA	0.3 BA	[7]
'Kayser'	Cotyledon	5	0, **50, 100, 250**, 500 Kan	LBA4404	N/A	**2**, 4, 6	0.05 IAA	0.01 BA	[8]
'Iranian landrace'	Cotyledon	3	0, 10, **20**, 30, 40, 50 Kan	GV3101	0.8 - 1.0	1, 2, **4**, 6	**0.05**, 0.1 NAA	0.1, 0.2, **0.4** BA	[9]

Table A1 (Continued)

Cultivar	Explant	Explant Age (days)	Antibiotic Conc. (mg/L)	*Agro* Strain	OD^{600}	Co-cultivation Time (days)	Auxin (mg/L)	Cytokinin (mg/L)	Ref
'Batavia Blonde'	Cotyledon	6	100 Kan	EHA105	0.5 - 0.8	5 - 7	0.1 NAA	0.1 BA	[10]
'Verônica'	Cotyledon	2	4 PPT	EHA105	0.5 - 1.0	2	0.05 NAA	0.2 BA	[11]
'LE126', 'Seagreen'	Cotyledon	6	50 Kan	LBA4404	1.1 - 1.6	2	5.6 IAA	0.68 Kin	[12]
N/R	Cotyledon	5 – 7	0.5 PPT	LBA4404	N/R	2	0.1 NAA	0.5 BA	[13]
'Green Wave'	Cotyledon	5	25 PPT	N/R	N/A	2	0.05 NAA; 2 2,4-D	0.25 Kin	[14]
'Simpson', 'Red Romaine', 'Bibb'	Leaf	42	100 Kan	LBA4404	1.0	3	**0.05**, 0.1 NAA; 0.1 IAA	1 2ip; 0.4 BA; 1 Zeatin	[15]
N/A	Cotyledon	7	1 PPT	GV3101	N/A	N/A	0.1 NAA	0.5 BA	[16]
'Grand Rapids'	Cotyledon	7	100 Kan	LBA4404	N/A	3	0.1 NAA	0.5 BA	[17]
'Potosina', 'Green Wave'	Cotyledon	7	100 Kan	LBA4404	2.0	2	0.02 NAA	0.5 BA	[18]
'Mariska', 'Jessy'	Leaf	10	200 Kan	GV2260	N/A	2	0.3 IAA	0.15 BA	[19]

Table A1 (Continued)

Cultivar	Explant	Explant Age (days)	Antibiotic Conc. (mg/L)	*Agro* Strain	OD^{600}	Co-cultivation Time (days)	Auxin (mg/L)	Cytokinin (mg/L)	Refs
'Cobham Green'	Cotyledon	4	0, 10, 25, **50**, 100, 250, 500 Kan	GV3111	0.5	2	1 IAA	0.5 Kin	[20]
'Ahvaz'	Cotyledon	7	0 - 20 (**15**) Kan	LBA4404	0.8 - 1.0	0.08	0.1 NAA	0.1 BA	[21]
'Grand Rapids'	Cotyledon	1 – 2	300 Kan	LBA4404	5.2	3	0.05 NAA	0.2 BA	[22]
'Syrena'	Cotyledon	2 – 3	2.5 PPT	EHA105	1.0	2	0.05 NAA	0.2 BA	[23]
'Longifolia'	Cotyledon	4-7	40 Kan	EHA105	0.8 - 1.0	1.5 - 2	0.1 NAA	0.5 BA	[24]
'Solan Kriti'	**Leaf,** petiole	15 – 20	10 Hyg, PPT	LBA4404	0.5	2, **3**, 4	**0.1** NAA	0.75 Kin; **0.25** BA	[25]
'South Bay'	Cotyledon	**1, 2, 3**, 4, 5	0, 25, **50, 100**, 200 Kan	A208	0.7	**1, 2, 3**, 4, 5	0.05 NAA	0.2 BA	[26]
'TN-96-39'	Cotyledon	4	10 Kan	LBA4404	0.6	1	0.05 NAA	0.2 BA	[27]
'Chongchima'	Cotyledon	7	5, 10, **20**, 30, 40, 50 Hyg	EHA105	0.6 - 0.8	3	0.0, **0.05**, 0.1, 0.2, 0.4, 1.6 NAA	0.0, 0.25, **0.5**, 1.0, 2.0 Kin	[28]
'Crystal'	Cotyledon	7	50 Kan	LBA4404	0.5	2	0.04 NAA	0.5 BA	[29]

Table A1 (Continued)

*Bold, the best explant age or concentration. [1] Bříza et al., 2010. [2] Cui et al., 2011. [3] Curtis et al., 1994. [4] Curtis et al., 1996. [5] Curtis et al., 1999. [6] Dias et al., 2006. [7] Dinant et al., 1997. [8] Enomoto et al., 1990. [9] Fallah-Ziarani et al., 2013. [10] Franklin et al., 2011. [11] Ibrahim et al., 2017. [12] Kim and Botella, 2004. [13] Kim et al., 2006. [14] Kim et al., 2013. [15] Lim et al., 2011. [16] Liu et al., 2006. [17] Liu et al., 2012. [18] Martínez-González et al., 2011. [19] Mazier et al., 2007. [20] Michelmore et al., 1987. [21] Mohebodini et al., 2014. [22] Pileggi et al., 2001. [23] Pniewsji et al., 2011. [24] Ren et al., 2011. [25] Sharma et al., 2022. [26] Torres et al., 1993. [27] Vafaee and Alizadeh, 2018. [28] Vanjildorj et al., 2005. [29] Webster et al., 2006. Hyg, hygromycin; Kan, kanamycin; Kin, Kinetin; PPT, phosphinothricin; 2,4-D, 2,4-Dichlorophenoxyacetic acid; IBA, indole-3-butyric acid; 2ip, 6-(γ,γ-Dimethylallylamino)purine.

Table A2 Literature review of lettuce regeneration methods

Cultivars tested	**Explant**	**Explant Age (days) ***	**Auxin (mg/L) ***	**Cytokinin (mg/L) ***	**Ref**
'Bronze Mignonette', 'Bambino', 'Iceberg', 'Cobham Green', 'Sweet Butter', 'Simpson Elite', 'Rosalita', 'Paris White', 'Lollo Biondo', 'Royal Oak Leaf', 'Red Salad Bowl', 'South Bay', 'Black Seeded Simpson', 'Lollo Rosso', 'Mainspring', 'Oak Leaf', 'Tango', 'Prize Head', 'Sangria', 'Mini-Green', 'Nevada', 'New York Head'	Cotyledon	2	0.1 IAA	0.5 Kin; 0.05 zeatin	[1]
'Rutgers Scarlet', 'Winter Destiny'	Cotyledon	3	0.05, 0.1, 0.125, 0.15, 0.2, 0.25, 0.3, 0.35, 0.4, 0.45, **0.5 NAA**	0.009, 1.0, 2.0, 3.0, 4.0, 5.0, 6.0, 7.0, 8.0, 9.0 BA; 2.0 Kin; 2.0 thidiazuron; 2.0 zeatin; 2.0, 2.5, 5.0, **10.0 BA**; **200 activated charcoal**	[2]
'Cobham Green', 'Hilde', 'Avondefiance', 'Continuity', 'Sabine', 'Capitan', 'Reskia', 'Dandie', 'Little Gem', 'Lobjoits Cos', 'Pennlake', 'Salad Bowl', 'Red Salad Bowl'	Cotyledon and first leaf	7, 14	0.05 NAA	0.5 BA	[3]
'Romaine'	Cotyledon, leaf	7, 40	0.03, 0.05, **0.1**, 0.15, 0.17 NAA	0.1, **0.4**, 0.7, 0.82 BA	[4]
'Red Oak Leaf', 'Red Coral', 'Grand Rapids', 'Black Seeded Simpson', 'Great Lakes', 'Greenway', 'Bambino', 'Webb Wonderful', 'Iceberg', 'Cos', 'Paris White', 'Rosalita', 'Buttercrunch', 'Bronze Mignonette', 'Cobham Green'	Cotyledon	3 – 14 (**3-5**)	0 - 1.0 NAA (**0.1** NAA); 0.1, 5.0 IAA	0 - 1.0 BA; 6.88 Kin; 0.05 Zeatin; 0.5 Kin; **0.1 BA**	[5]
'Yazd', 'Ahvaz'	Cotyledon	**3**, 7	0.02, 0.05, **0.1**, 0.5, 1.0 **NAA**	**0.1**. 0.4, 0.5, 1.0 **BA**	[6]

Table A2 (Continued)

Cultivars tested	**Explant**	**Explant Age (days) ***	**Auxin (mg/L) ***	**Cytokinin (mg/L) ***	**Ref**
All Year Round', 'Great Lakes', 'Greenfields', 'Green Velvet', 'Spring Salad', 'Summer Gem', 'Webb's Wonderful', 'Winter Triumph', 'Yatesdale', 'Bronze Mignonette', 'Buttercrunch', 'Green Mignonette', 'Sweet Butter', 'Tom Thumb', 'Red Oak Leaf', 'Red Regency', 'Red Sails', 'Salad Bowl', 'Cos', 'Green Cos', 'White Cos Signal'	cotyledon	5	**0.1 IAA**	**0.5 Kin**; 0.5 Kin; **0.05 zeatin**	[7]

[1] Ampomah-Dwamena et al., 1997. [2] Armas et al., 2017. [3] Brown et al., 1986. [4] Gómez-Montes et al., 2015. [5] Hunter and Burritt, 2002. [6] Mohebodini et al., 2011. [7] Zhang and Conner, 1992. Kin, Kinetin.